

Microtubule Integrity in Tauopathies: Exploring the Roles of TAU, Tubulin Tyrosine Ligase-Like Enzymes, and Tubulin Post-Translational Modifications



Inaugural-Dissertation
zur
Erlangung des Doktorgrades
der Mathematisch-Naturwissenschaftlichen Fakultät
der Universität zu Köln

vorgelegt von
Mhd Aghyad Al Kabbani
aus Damaskus, Syrien

November 2024

Tag der Disputation: 06.02.2025

Table of Contents

List of abbreviations	VI
List of figures	VIII
Data Availability Statement	VIII
Zusammenfassung	IX
Summary	XII
1. Introduction	14
1.1 TAU and Tauopathies	14
1.1.1 TAU structure, expression, and physiological role	14
1.1.2 Tauopathies	16
1.2 Microtubules: Structure, function, modifications, and disease association	18
1.2.1 Structure and function of microtubules	18
1.2.2 Post-translational modifications of microtubules	19
1.2.3 Microtubule-interacting proteins	21
1.2.4 Microtubules in AD and other tauopathies	22
1.3 Tubulin Tyrosine Ligase-Like enzymes	23
1.3.1 Family members	23
1.3.2 Physiological Roles of TTLs	24
1.3.3 Diseases Associated with TTL Dysfunction	24
2. Aims	26
3. Publications and preprints	27
3.1 Overview	27
3.2 Article 1: AAV-based gene therapy approaches for genetic forms of tauopathies and related neurogenetic disorders	28
3.2.1 Key message	28
3.2.2 Individual contribution	28

3.3	Article 2: Optimized Calcium-Phosphate-Based Co-transfection of TAU and tdTomato into Human iPSC-Derived Neurons for the Study of Intracellular Distribution of Wild-type and Mutant Human TAU.....	29
3.3.1	Key findings	29
3.3.2	Individual contribution	29
3.4	Article 3: Effects of P301L-TAU on post-translational modifications of microtubules in human iPSC-derived cortical neurons and TAU transgenic mice	30
3.4.1	Key findings	30
3.4.2	Individual contribution	30
3.5	Article 4: Knockdown of TTLL1 reduces A β -induced TAU pathology in human iPSC-derived cortical neurons	31
3.5.1	Key findings	31
3.5.2	Individual contribution	31
3.6	Article 5: Expression of recombinant human glutamylating TTLLs in human cells leads to differential tubulin glutamylation patterns, with only TTLL6 disrupting microtubule dynamics 32	
3.6.1	Key findings	32
3.6.2	Individual contribution	32
4.	Discussion	33
4.1	Establishing TAU missorting and microtubule loss in human neuronal models	34
4.2	Investigating TAU- and TTLL-mediated loss of microtubules and neuronal dysfunction, as well as the therapeutic potential of reducing TTLL expression in human neuronal models	35
4.3	Studying the expression and glutamylation activity of different recombinant TTLLs and their impact on microtubule dynamics in human cells	38
4.4	Significance, limitations, and outlook	39
5.	References	43
6.	Appendix.....	64
6.1	Article 1	64
6.2	Article 2	65

6.3	Article 3	66
6.4	Article 4	67
6.5	Article 5	68
	Acknowledgements.....	LXVIII
	Eidesstattliche Erklärung.....	LXX
	Curriculum Vitae	LXXII

List of abbreviations

AAV: Adeno-associated virus

A β : Amyloid-beta

AD: Alzheimer's disease

AIS: Axon initial segment

APP: Amyloid precursor protein

ATP: Adenosine triphosphate

CBD: Corticobasal degeneration

CCP: Cytosolic carboxypeptidase

CDK: Cyclin-dependent kinase

EB3: End-binding protein 3

FDA: Food and Drug Administration

FRET: Fluorescence resonance energy transfer

FTD: Frontotemporal Dementia

FTDP-17: Frontotemporal dementia with parkinsonism linked to chromosome 17

GDP: Guanosine diphosphate

GSK-3 β : Glycogen synthase kinase-3 β

GTP: Guanosine triphosphate

HDAC6: Histone deacetylase 6

HEK: Human embryonic kidney

hiPSC: Human induced pluripotent stem cell

HSP: Hereditary spastic paraplegia

ICV: Intracerebroventricular

iNeurons: hiPSC-derived neurons

KIF5B: Kinesin family member 5B

MAP: Microtubule-associated protein

MAPK: Mitogen-activated protein kinase

MATCAP: Microtubule-associated tyrosine carboxypeptidase

MEA: Microelectrode array

MTBD: Microtubule-binding domain
MTOC: Microtubule-organizing center
NAP: Nucleosome assembly protein
NF-L: Neurofilament-L
NFT: Neurofibrillary tangle
NMDA: N-methyl-D-aspartate
oA β : Oligomeric A β
PCD: Purkinje cell degeneration
PP2A: Protein phosphatase 2A
PSP: Progressive supranuclear palsy
PTM: Post-translational modification
shRNA: Short hairpin ribonucleic acid
SVBP: Small vasohibin binding protein
TAT: Tubulin acetyltransferase
TFP: Teal fluorescent protein
TTL: Tubulin tyrosine ligase
TTLL: Tubulin tyrosine ligase-like
TUBA4a: Tubulin alpha-4A chain
YFP: Yellow fluorescent protein

List of figures

Figure 1. TTLs and tubulin glutamylation.....	23
Figure 2. Proposed mechanism of TAU missorting and TTL1-mediated microtubule destabilization in response to A β insult.....	37
Figure 3. Schematic representation of the workflow of a preliminary experiment in mice to investigate AAV delivery to the brain.....	40

Data Availability Statement

The underlying data to support the findings of this thesis are available in the cited publications. Raw data is stored on the private servers of the research group Zempel, at the Institute of Human Genetics, University Hospital of Cologne and is available from the author(s) upon reasonable request.

Zusammenfassung

Tauopathien, zu denen auch die Alzheimer-Demenz (AD) gehört, stellen eine Klasse neurodegenerativer Erkrankungen dar, die durch die pathologische Aggregation des Mikrotubuli assoziierten Proteins TAU gekennzeichnet sind. Unter physiologischen Bedingungen stabilisiert TAU die Mikrotubuli, die für die neuronale Struktur, den intrazellulären Transport und die synaptische Funktion wesentlich sind. Bei Tauopathien löst sich TAU jedoch von den Mikrotubuli, wird hyperphosphoryliert, fehlsortiert und aggregiert, was in einer Destabilisierung der Mikrotubuli, einer synaptischen Dysfunktion und einer neuronalen Degeneration gipfelt. Neue Erkenntnisse unterstreichen die Rolle der posttranslationalen Modifikationen (PTM) des Tubulins, wie die Polyglutamylierung, bei der Regulierung der Mikrotubuli-Stabilität. Die Polyglutamylierung, die durch Tubulin-Tyrosin-Ligase-ähnliche (TTLL) Enzyme vermittelt wird, moduliert die Interaktionen zwischen Mikrotubuli, Motorproteinen und trennenden Enzymen. Eine dysregulierte Polyglutamylierung wurde jedoch mit Mikrotubuli-Instabilität und Neurodegeneration in Verbindung gebracht. In dieser Arbeit wird die Hypothese aufgestellt, dass TTLL-Enzyme zur Mikrotubuli-Dysfunktion bei Tauopathien beitragen und dass eine gezielte Beeinflussung dieser Enzyme die TAU-bedingte Neurodegeneration verhindern oder zumindest abschwächen kann.

Hierfür wurden in der Studie aus menschlichen induzierten pluripotenten Stammzellen (iPSC) abgeleitete kortikale Neuronen (iNeurons) und pR5-Mäuse, die das krankheitsassoziierte humanes P301L-TAU exprimieren, als Modelle für Tauopathien verwendet. iNeuronen wurden durch induzierbare genetische Differenzierung von iPSCs in kortikale glutamaterge Neuronen der Schicht 2/3 generiert, und die TAU-Pathologie wurde durch lentivirale Expression von P301L-TAU oder Behandlung mit oligomerem Amyloid-beta ($\text{oA}\beta$) induziert. Die Fehlsortierung von TAU, die Mikrotubuli-PTMs und die synaptische Integrität wurden mittels Immunofluoreszenzmikroskopie und Western Blotting untersucht. Der lentivirale Knockdown von TTLL-Enzymen wurde mit Hilfe von short hairpin RNA (shRNA)-Konstrukten durchgeführt, und die Auswirkungen auf die Mikrotubuli-Stabilität und die neuronale Funktion untersucht. Zur Charakterisierung der TTLL-Aktivität wurden rekombinante TTLL-Enzyme in HEK293T-Zellen exprimiert, um ihre Glutamylierungsprofile und die Mikrotubuli-Dynamik mittels Lebendzellbeobachtung zu analysieren, was durch Live-Zell-Bildgebung der Mikrotubuli plus endbindendem Protein EB3 beurteilt wurde. Außerdem wurde die Wirksamkeit eines neuartigen TTLL-Inhibitors auf seine Fähigkeit getestet, die pathologische Mikrotubuli-Destabilisierung umzukehren.

Die Ergebnisse zeigten, dass P301L-TAU in pR5-Mäusen pathologisch in die somatodendritischen Kompartimente fehlsortiert, begleitet von reduzierter Mikrotubuli-Acetylierung und erhöhter Polyglutamylierung in Hippocampus-Neuronen, was mit Mikrotubuli-Fragmentierung und beeinträchtigter dendritischer Morphologie in gealterten Mäusen korreliert. Die Expression von P301L-TAU in iNeuronen führte jedoch nicht zu einer Fehlsortierung oder Aggregation von TAU, aber durchaus zu einer weniger erhöhten Tubulinacetylierung und ausgeprägteren Polyglutamylierung als die wt-TAU Kontrolle. Andererseits führte oA β -Exposition von iNeuronen zu Fehlsortierung von TAU in Kombination mit erhöhter Tubulin-Polyglutamylierung, verringerter Acetylierung und Synapsen Verlust, gut vereinbar mit der menschlichen Pathologie. Der Knockdown der wichtigsten Hirnpolyglutamylase TTLL1, und in geringerem Maße auch der Knockdown von TTLL4, in iNeuronen führte zu einer signifikanten Verringerung der Tubulin-Polyglutamylierung, einer Abschwächung der TAU-Fehlverteilung und einer teilweisen schützten die synaptische Integrität. Fluoreszenz-Resonanz-Energie-Transfer (FRET)-basierte Interaktionsstudien in HEK293T-Zellen ergaben eine direkte Interaktion zwischen TTLL1 und TAU, was TTLL1 als Vermittler der TAU-bedingten Mikrotubuli-Dysfunktion erscheinen lässt. In ähnlicher Weise wurde gezeigt, dass TTLL6, eine weitere Polyglutamylase, in rekombinanten Proteinexpressionsversuchen in HEK293T-Zellen Mikrotubuli destabilisiert. Ein neuartiger TTLL-Inhibitor blockierte wirksam die Glutamylierungsaktivität mehrerer TTLLs, kehrte die TTLL6-induzierte Mikrotubuli-Destabilisierung um, und stellte die Mikrotubuli-Dynamik in HEK293T-Zellen wieder her.

Diese Ergebnisse belegen, dass TTLL-Enzyme, insbesondere TTLL1, TTLL4 und TTLL6, entscheidende Vermittler der Mikrotubuli-Dysfunktion bei Tauopathien sein und zu der pathologischen Kaskade beitragen könnten, die durch die Fehlsortierung und Aggregation von TAU ausgelöst oder zumindest begleitet wird. Die gezielte Beeinflussung von TTLLs stellt eine vielversprechende therapeutische Strategie für Tauopathien dar, die es durch Mikrotubuli- und Synapsenstabilisierung ermöglicht, frühzeitig in das Fortschreiten des Krankheitsprozesses einzugreifen. Die Verwendung menschlicher iPSC-Neuronen und TAU-humanisierter Mäuse in dieser Studie bieten physiologisch relevante Modelle zur Untersuchung der TAU-Pathologie und zur Bewertung des therapeutischen Potenzials der TTLL-Inhibition. Während diese Studie die Durchführbarkeit einer gezielten TTLL-Behandlung zeigt, werden künftige Arbeiten diese Ergebnisse auf In-vivo-Modelle, für die bereits wichtige Vorversuche wie AAV-Injektionen etabliert wurden, ausweiten, und die langfristige Wirksamkeit und Sicherheit einer TTLL-gerichteten Gentherapie untersuchen.

Zusammenfassend lässt sich sagen, dass diese Arbeit das Zusammenspiel zwischen der TAU-Pathologie und der Mikrotubuli-Dynamik beleuchtet und die TTL-Enzyme als zentrale Akteure bei der Neurodegeneration aufdeckt. Indem der Schwerpunkt von der möglicherweise eher symptomatischen und irreversiblen TAU-Aggregation auf die Mikrotubuli-Regulierung verlagert wird, werden neue, vielversprechende Ziele und therapeutische Ansätze identifiziert, um die verheerenden Auswirkungen von Tauopathien wie beispielsweise die Alzheimersche Erkrankung zu bekämpfen.

Summary

Tauopathies, including Alzheimer's disease (AD), represent a class of neurodegenerative disorders characterized by the pathological aggregation of the microtubule-associated protein TAU. Under physiological conditions, TAU stabilizes microtubules, which are essential for neuronal structure, intracellular transport, and synaptic function. However, in tauopathies, TAU detaches from microtubules, becomes hyperphosphorylated, missorted and aggregated, culminating in microtubule destabilization, synaptic dysfunction, and neuronal degeneration. Emerging evidence highlights the role of tubulin post-translational modifications (PTMs), such as polyglutamylation, in regulating microtubule stability. Polyglutamylation, mediated by Tubulin Tyrosine Ligase-Like (TTL) enzymes, modulates interactions between microtubules, motor proteins, and severing enzymes. However, dysregulated polyglutamylation has been implicated in microtubule instability and neurodegeneration. This thesis hypothesizes that TTL enzymes contribute to microtubule dysfunction in tauopathies and that targeting these enzymes can mitigate TAU-driven neurodegeneration.

To address this hypothesis, the study utilized human induced pluripotent stem cell (iPSC)-derived cortical neurons (iNeurons) and pR5 mice, transgenic for P301L-TAU, as models of tauopathies. iNeurons were generated by differentiating iPSCs into cortical layer 2/3 glutamatergic neurons, and TAU pathology was induced via lentiviral expression of P301L-TAU or treatment with oligomeric amyloid-beta ($\alpha\beta$). TAU missorting, microtubule PTMs, and synaptic integrity were assessed using immunocytochemistry, Western blotting, and fluorescence imaging. Lentiviral knockdown of TTL enzymes was achieved using short hairpin RNA (shRNA) constructs, and the effects on microtubule stability and neuronal health were evaluated. To further characterize TTL activity, recombinant TTL enzymes were expressed in HEK293T cells to analyze their glutamylation profiles and their effects on microtubule stability, which was assessed via live-cell imaging of the microtubule plus end-binding protein EB3. Additionally, the efficacy of a novel TTL inhibitor was tested for its ability to reverse pathological microtubule destabilization.

The results demonstrated that P301L-TAU in pR5 mice pathologically missorted into the somatodendritic compartments, accompanied by reduced microtubule acetylation and elevated polyglutamylation in hippocampal neurons, correlating with microtubule fragmentation and impaired dendritic morphology in aged mice. However, P301L-TAU expression in iNeurons did not result in TAU missorting or aggregation, but only in elevated tubulin acetylation and polyglutamylation. On the other hand, $\alpha\beta$ treatment of iNeurons led to TAU missorting, combined

with increased tubulin polyglutamylation, reduced acetylation, and synaptic loss, thus providing a suitable human tauopathy model. Knockdown of the major brain polyglutamylase TTLL1, and to a lesser extent TTLL4, in iNeurons significantly reduced tubulin polyglutamylation, mitigated TAU missorting, and partially protected synaptic integrity. Fluorescence resonance energy transfer (FRET)-based interaction studies in HEK293T cells revealed a direct interaction between TTLL1 and TAU, implicating TTLL1 as a mediator of TAU-driven microtubule dysfunction. Similarly, TTLL6, another polyglutamylase, was shown to destabilize microtubules in recombinant protein expression experiments in HEK293T cells. A novel TTLL inhibitor effectively blocked glutamylation activity across several TTLLs, reversed TTLL6-induced microtubule destabilization, and restored microtubule dynamics in HEK293T cells.

These findings establish TTLL enzymes, particularly TTLL1, TTLL4, and TTLL6, as critical mediators of microtubule dysfunction in tauopathies, and contributors to the pathological cascade initiated by TAU missorting and aggregation. Targeting TTLLs offers a promising therapeutic strategy for tauopathies, with the potential to intervene early in disease progression by stabilizing microtubules and preserving neuronal health. The use of human iPSC-derived neurons in this research provided a physiologically relevant model to study TAU pathology and evaluate the therapeutic potential of TTLL inhibition. While this study demonstrates the feasibility of targeting TTLLs, future work will extend these findings to in vivo models and investigate the long-term efficacy and safety of TTLL-targeting gene therapy.

In conclusion, this thesis highlights the interplay between TAU pathology and microtubule dynamics, uncovering TTLL enzymes as pivotal players in neurodegeneration. By shifting the focus from TAU aggregation to microtubule regulation, it identifies novel targets and therapeutic approaches that hold promise for mitigating the devastating effects of tauopathies such as AD.

1. Introduction

1.1 TAU and Tauopathies

1.1.1 TAU structure, expression, and physiological role

TAU is a microtubule-associated protein predominantly expressed in neurons, where it is traditionally suggested to play a pivotal role in stabilizing microtubules and promoting their assembly^{1,2}. TAU is encoded by the *MAPT* gene, located on chromosome 17q21, and is implicated in several neurodegenerative disorders collectively known as tauopathies, including Alzheimer's disease (AD), frontotemporal dementia (FTD), and Parkinsonism³⁻⁶.

The *MAPT* gene, consisting of 16 exons, undergoes complex alternative splicing to produce six main isoforms in the human brain. These isoforms differ in the number of microtubule-binding repeat domains (three or four repeats) and the presence of either zero, one, or two N-terminal inserts, resulting in six combinations: 0N3R, 1N3R, 2N3R, 0N4R, 1N4R, and 2N4R^{5,7}. The inclusion or exclusion of exon 10 is critical, as it determines the presence of the second microtubule-binding repeat, influencing TAU's binding affinity and regulatory properties^{8,9}. In the peripheral nervous system, a specific isoform, known as "big" TAU, that differs by 254 amino acids from the largest isoform (2N4R), is highly abundant¹⁰. TAU is also expressed in the enteric nervous system¹¹. Besides neuronal systems, TAU has been also found in the heart, kidney, skeletal muscles, among other tissues¹²⁻¹⁴.

The 3-repeat (3R) and 4-repeat (4R) isoforms are differentially expressed during development, with 3R TAU predominantly found in the fetal brain, while the adult human brain expresses a roughly equal ratio of 3R and 4R isoforms^{15,16}. Imbalances in this ratio are associated with various tauopathies, as seen in Pick's disease (3R) and progressive supranuclear palsy (4R)¹⁷⁻¹⁹. Mice express only up to four TAU isoforms. Similar to human, 0N3R is produced during murine neuronal development, but in adult mouse brains, the isoform composition shifts to exclusively 4R TAU isoforms²⁰⁻²². These differences may account for humans' susceptibility to splicing deficits in *MAPT* and the lack of TAU pathology in transgenic mouse models of Alzheimer's disease^{23,24}.

TAU is an intrinsically disordered protein, characterized by a lack of a stable tertiary structure under physiological conditions²⁵. Its primary structure consists of a N-terminal projection domain, a proline-rich region, a microtubule-binding domain (MTBD), and a C-terminal tail²⁶. The MTBD,

located towards the C-terminus, is responsible for interactions with microtubules and comprises either three or four repeats of approximately 31 amino acids ²⁷.

The disordered nature of TAU allows it to adopt multiple conformations, facilitating interactions with various proteins and other cellular components. This structural flexibility is essential for its physiological function but also predisposes TAU to pathological misfolding and aggregation under certain conditions, such as hyperphosphorylation, acetylation, contact with negatively charged molecules such as RNA, traumatic brain injury and oxidative stress ^{28–32}.

TAU is primarily localized in neurons, particularly in axons, where it supports microtubule stability and dynamics (see also 1.2.1 for microtubule dynamics) ^{33,34}. More than 80% of TAU is bound to microtubules, inducing their nucleation, elongation, and promoting their stability and rigidity ^{24,35,36}. It is also present, albeit at lower levels, in the somatodendritic compartment and in glial cells, along the length of microtubules, but also on ribosomes and in the nucleus ^{37,38}. This predominantly axonal sorting of TAU is thought to be controlled by a diffusion barrier located at the axon initial segment (AIS) that blocks the passage of TAU from the axon into the soma and dendrites ³⁹.

In pathological conditions, TAU's distribution is altered, with an abnormal accumulation in the somatodendritic compartment, leading to a loss of its normal function and the formation of insoluble aggregates called neurofibrillary tangles (NFTs), which are considered a hallmark of TAU pathology and are associated with neurodegeneration and cognitive impairment ^{40–43}.

TAU is subject to extensive post-translational modifications (PTMs), with phosphorylation being the most critical. Over 85 putative phosphorylation sites have been identified, over 50 of which have been validated experimentally, primarily at serine, threonine, and tyrosine residues. Most of these phosphorylation sites are present within the proline-rich and C-terminal regions, and to a lesser extent in the N-terminal domain, with fewer sites identified in the repeat domains ^{44–49}. These modifications are regulated by a balance between kinases (most notably: glycogen synthase kinase-3 β (GSK-3 β), cyclin-dependent kinase 5 (CDK5), and mitogen-activated protein kinase (MAPK)), and phosphatases (such as protein phosphatase 2A (PP2A)), which control TAU's affinity for microtubules and its susceptibility to aggregation ^{50–53}.

Physiologically, phosphorylation of TAU at specific sites, such as Ser262 and Ser356 within the MTBD, reduces its binding to microtubules, allowing dynamic reorganization of the cytoskeleton

^{44,54}. However, hyperphosphorylation at multiple sites, including Ser202, Thr212, Ser214, and Ser396/404, reduces microtubule binding affinity significantly, promoting TAU misfolding, aggregation, and toxicity ⁵⁵⁻⁵⁸. This pathological phosphorylation pattern is a hallmark of AD and other tauopathies, contributing to the formation of NFTs and neuronal dysfunction ⁵⁹⁻⁶¹.

TAU's primary physiological role is to stabilize microtubules, which are essential components of the cytoskeleton that facilitate intracellular transport, cell shape maintenance, and signaling ^{1,2}. By binding to microtubules, TAU promotes their polymerization and prevents depolymerization, particularly in axons, where microtubule stability is crucial for the transport of vesicles, organelles, and proteins necessary for synaptic function. By binding to axonal microtubules, TAU promotes axonal differentiation, morphogenesis, outgrowth, and neuronal plasticity. ^{9,62-65} Dendritic TAU functions include regulating synaptic plasticity via interactions with N-methyl-D-aspartate (NMDA) receptors and Fyn kinase ^{66,67}. While TAU knockout in mice does not result in severe phenotypes, likely due to the compensatory upregulation of other microtubule-associated proteins (MAPs) ⁶⁸, loss of TAU delays neuronal maturation and affects dendritic arborization in primary cultures ⁶⁹. These negative impacts could be age-related, as aged TAU knockout mice exhibit impaired long-term potentiation and depression, motor deficits resembling parkinsonism, and subtle memory deficits ⁷⁰⁻⁷².

1.1.2 Tauopathies

TAU protein plays a critical role in maintaining neuronal health through its regulation of microtubule dynamics and interactions with various cellular components. However, under pathological conditions, TAU undergoes missorting and hyperphosphorylation, leading to its dissociation from microtubules and aggregation into NFTs, which is the hallmark of a wide group of neurodegenerative diseases known collectively as tauopathies ⁷³⁻⁷⁵.

Tauopathies can be categorized into primary and secondary forms based on their etiology. Primary tauopathies are neurodegenerative diseases where TAU pathology is the predominant or sole hallmark ⁷⁶. These conditions include *MAPT*-associated-Frontotemporal Dementia (FTD), Progressive Supranuclear Palsy (PSP), and Corticobasal Degeneration (CBD), among others ⁷⁷.

Mutations in the TAU-coding *MAPT* gene plays a critical role in the pathogenesis of primary tauopathies. Such mutations can alter TAU's structure, function, its ability to bind microtubules, and interfere with alternative splicing ^{78,79}. One well-known mutation is the P301L mutation in exon 10 of the *MAPT* gene. This mutation reduces TAU ability to bind and assemble microtubules ^{18,80},

makes TAU more prone to hyperphosphorylation by increasing its accessibility to kinases⁸¹, and shifts the physiologically equal ratio of 3R and 4R isoforms⁸². The P301L mutation is mainly associated with Frontotemporal Dementia with Parkinsonism linked to chromosome 17 (FTDP-17), characterized by enhanced TAU aggregation, leading to early-onset dementia and motor dysfunction^{83,84}.

Secondary tauopathies are characterized by TAU pathology that occurs secondary to other primary pathologies, most notably AD²⁴. AD is the most common cause of dementia worldwide and features both amyloid-beta (A β) plaques and TAU NFTs⁸⁵. Amyloid pathology in AD is primarily characterized by the accumulation of A β peptides in the brain, forming extracellular plaques. A β peptides are produced through the sequential cleavage of the amyloid precursor protein (APP) by β -secretase and γ -secretase^{86,87}. Two major forms, A β 40 and A β 42, differ in length by two amino acids, with A β 42 being more prone to aggregation and more toxic⁸⁸. The imbalance between these two peptides, particularly the increased A β 42/A β 40 ratio, is a critical factor in AD pathogenesis, promoting plaque formation, neuronal toxicity, and ultimately leading to synaptic dysfunction and neurodegeneration⁸⁹⁻⁹¹. Additionally, A β accumulation is presumed to initiate a cascade of pathological events that eventually lead to TAU hyperphosphorylation and aggregation⁹². A β oligomers have been shown to activate kinases such as GSK-3 β , which hyperphosphorylates TAU⁹³. Once TAU is hyperphosphorylated, it detaches from microtubules, destabilizing the cytoskeleton and leading to synaptic dysfunction and neurodegeneration. On the other hand, TAU pathology is necessary for A β to exert its full neurotoxic effects. Transgenic mouse models expressing both human A β and TAU show more severe neurodegenerative phenotypes than those expressing either protein alone, indicating a synergistic relationship⁹⁴. Furthermore, TAU seems to be more tightly connected to cognitive impairment in AD, with reduction of TAU levels reverting behavioral and memory deficits in APP transgenic mice^{67,95,96}. Microtubules and synapses in primary neurons from TAU knockout mice show resistance against A β toxicity⁹⁷, while TAU knockout protects human neurons from A β -induced dampening of network activity⁹⁸.

While primary tauopathies often have a genetic basis, sporadic tauopathies like AD do not typically involve direct mutations in the *MAPT* gene, but arise due to a complex interplay of genetic and environmental factors, such as aging, traumatic brain injury, and lifestyle. These factors might influence TAU phosphorylation and aggregation indirectly through mechanisms involving oxidative stress, neuroinflammation, and altered cellular signaling pathways^{77,99}.

1.2 Microtubules: Structure, functions, modifications, and disease association

1.2.1 Structure and functions of microtubules

Microtubules are essential components of the cytoskeleton, playing a critical role in maintaining cell shape, intracellular transport, cell division, and various other cellular processes ¹⁰⁰. Microtubules are hollow, cylindrical structures composed of α - and β -tubulin protein subunits. These tubulin heterodimers polymerize head-to-tail to form protofilaments, and typically, 13 protofilaments arrange in parallel to create the cylindrical microtubule structure, with a diameter of approximately 25 nm ^{101,102}. Microtubules are highly dynamic, capable of rapid polymerization and depolymerization. This is driven by the binding and hydrolysis of guanosine triphosphate (GTP) in the tubulin subunits, where GTP-bound tubulin is more stable and supports microtubule growth, while guanosine diphosphate (GDP)-bound tubulin leads to depolymerization ^{103,104}.

Microtubules exhibit polarity, meaning they have distinct plus (+) and minus (-) ends ¹⁰⁵. The plus end, where polymerization occurs more rapidly, is typically oriented toward the cell periphery, while the minus end, which is more stable, is anchored near the microtubule-organizing center (MTOC) or centrosome ^{106,107}. This polarity is fundamental for the directionality of intracellular transport, as motor proteins interact with microtubules in a polarized manner ¹⁰⁸.

In neurons, microtubules are particularly vital, as they support the unique architecture and functions of these highly polarized cells, which have long axons and dendrites extending from the cell body. Their dynamic nature and specialized arrangement in neurons are crucial for synaptic function, intracellular transport, and overall neuronal health ^{109–111}. In mature neurons, the centrosome loses its function as the primary MTOC, with γ -tubulin and non-centrosomal MTOCs playing a crucial role in organizing complex microtubule network required for neuronal function. γ -tubulin can nucleate microtubules from sites like the Golgi apparatus and pre-existing microtubules ^{112–114}. Microtubules in axons and dendrites differ in their orientation and functional roles. Axonal microtubules are uniformly oriented, with their plus ends pointing away from the cell body and toward the axon terminal ^{115,116}. This orientation is essential for anterograde transport, where motor proteins like kinesin move cargo such as vesicles, organelles, and proteins from the soma to the synaptic terminals ¹¹⁷. Axonal microtubules are also responsible for retrograde transport, carried out by dynein, which moves cargo in the opposite direction, bringing back signaling molecules, damaged organelles, and waste products to the soma for degradation or processing ¹¹⁸. Dendritic microtubules, in contrast, exhibit mixed polarity, where microtubules can have either orientation ^{115,119}. This arrangement supports the bidirectional transport of cargo

required for maintaining dendritic spines and synaptic plasticity. The mixed polarity of dendritic microtubules facilitates the flow of materials both toward and away from the cell body, which is essential for the dynamic nature of synaptic communication and plasticity^{120–122}.

Besides their role in intracellular transport and maintaining polarity and shape, microtubules are also involved in processes like neuronal migration and axon guidance during neurodevelopment, ensuring that neurons reach their correct destinations in the developing brain^{123–125}. They are also essential for axonal growth and regeneration after injury, where they play a role in the reformation of the cytoskeleton, which is necessary for axonal regrowth and repair^{126,127}.

1.2.2 Post-translational modifications of microtubules

PTMs of tubulin play a critical role in modulating microtubule function, stability, and interactions with other cellular components. These modifications provide a versatile and dynamic regulatory mechanism that governs microtubule participation in diverse cellular activities. Essential PTMs of microtubules include acetylation, detyrosination, tyrosination, and glutamylation, among others.

Acetylation of tubulin primarily occurs on lysine 40 (K40) of α -tubulin^{128,129}, and it is most commonly associated with long-lived, stable microtubules^{130,131}. Acetylation is mediated by tubulin acetyltransferase (TAT) and is reversed by deacetylases like histone deacetylase 6 (HDAC6)^{132,133}. This modification enhances microtubule resilience to mechanical stress and promotes the interaction of motor proteins such as kinesin and dynein^{134–138}. Acetylated microtubules are often found in both axons and dendrites, where they support long-distance intracellular trafficking, neuronal polarity, and structural integrity¹³⁹.

Detyrosination involves the removal of the C-terminal tyrosine residue from α -tubulin by vasohibins, namely VASH1 and VASH2, and their co-factor small vasohibin binding protein (SVBP)^{140,141}, in addition to the recently identified microtubule-associated tyrosine carboxypeptidase (MATCAP)¹⁴², while re-adding tyrosine is catalyzed by tubulin tyrosine ligase (TTL)¹⁴³. Detyrosinated microtubules are more stable^{144,145}, and this modification is prominent in neurons and has important implications in neuronal activity and polarity. Stable detyrosinated microtubules are enriched in axons and thought to control neuronal polarization, as TTL depletion in cell culture leads to the emergence of neurons bearing multiple axons^{146,147}. On the other hand, dynamic tyrosinated microtubules are typically found in dendrites, supporting synaptic plasticity and function¹²¹, with decreased tyrosination in mice leading to reduced dendritic spine density, compromised synaptic plasticity, and memory deficits¹⁴⁸. Tyrosination cycles are critical for

regulating the interaction between microtubules and motor proteins. For example, experiments on purified recombinant tubulin demonstrated that tyrosination facilitates the initiation of dynein-tubulin encounter, while detyrosination enhanced kinesin-1's landing rate, with decreased binding affinity to tyrosinated microtubules ¹⁴⁹⁻¹⁵¹.

Polyglutamylation involves the addition of glutamate side chains to the γ -carboxyl group of glutamate residues in the C-terminal tails of both α - and β -tubulin ^{152,153}. This modification is catalyzed by a subset of tubulin tyrosine ligase-like (TTLL) enzymes ¹⁵⁴. Tubulin polyglutamylation is particularly enriched in the brain ¹⁵⁵, where it regulates the interaction of neuronal microtubules with MAPs, motor proteins, and severing enzymes. It has been shown that polyglutamylation recruits the microtubule-severing enzymes spastin and katanin ^{156,157}, slows the run length of motor proteins such as kinesin family member 5B (KIF5B) ¹⁵⁸, negatively regulate microtubule growth ¹⁵⁹, and increases the affinity of TAU for microtubules ¹⁵⁸. The length of the glutamate chain influences microtubule properties and regulates microtubule severing. Specifically, spastin activity increases as the number of glutamates in the side chain rises from one to eight, but it decreases once this glutamylation threshold is exceeded, with the severing activity of spastin shifting to a microtubule stabilizing function ¹⁶⁰. Interestingly, excessive glutamylation, due to the depletion of one or more of the deglutamylating enzymes cytosolic carboxypeptidases (CCPs), leads to microtubule destabilization, neurodegeneration, and perturbed axonal transport ¹⁶¹⁻¹⁶³.

Other tubulin PTMs include glycylation, which adds glycine residues to the C-terminal tails of tubulin in motile cilia and flagella ^{164,165}, and regulates their interactions with MAPs and motor proteins ¹⁶⁶, with depletion of the glycylation enzymes TTLL3 and TTLL8 resulting in the complete disintegration of motile cilia and reduced number of primary cilia in corneal endothelial cells and mouse embryonic fibroblasts ^{164,167}, potentially linking tubulin glycylation to ciliopathies. In addition, tubulin phosphorylation, although less understood than other PTMs, is mediated by kinases such as CDK1, and regulates microtubule polymerization during mitosis ¹⁶⁸, as mutations in the β -tubulin phosphorylation site Ser172 is associated with defects in microtubule stability and cell cycle in yeast, and abnormal cortical development in humans ^{169,170}. Furthermore, tubulin palmitoylation, a lipid modification that involves the addition of palmitic acid, is believed to enhance microtubule dynamics by promoting interactions with lipid membranes ^{171,172}, yet its impact on microtubule properties and functions remains largely unknown, with reports suggesting involvement in spindle abnormalities and cancer proliferation ^{173,174}.

Together, these modifications are hypothesized to provide a "tubulin code" that modulates microtubule behavior and fine-tune their structure and function in a highly regulated manner. This code could create a highly dynamic system, enabling microtubules to adapt to diverse functional demands placed upon them in various cellular environments ¹⁷⁵.

1.2.3 Microtubule-interacting proteins

In neurons, microtubules are regulated by MAPs that exert several functions, including regulating microtubule stability and dynamics, serving as linkers to other cytoskeletal elements, and controlling the activity of other microtubule-interacting proteins ¹⁷⁶. TAU is one of the most well-known MAPs, particularly in neurons, where it binds to microtubules and promotes their stabilization, especially in axons. However, TAU dysregulation, such as hyperphosphorylation, can lead to its detachment from microtubules and subsequent aggregation, as seen in tauopathies like AD. TAU hyperphosphorylation destabilizes the microtubule network, impairs intracellular transport, and contributes to neuronal dysfunction and degeneration ^{24,43}. Another notable MAP is MAP2, which is mainly found in dendrites. MAP2 stabilizes microtubules in these compartments, contributing to dendritic structure and function ^{177,178}.

Motor proteins, such as kinesin and dynein, are responsible for transporting cargo along microtubules. These proteins recognize the inherent polarity of microtubules, with kinesin moving toward the plus (+) end (anterograde transport) and dynein moving toward the minus (-) end (retrograde transport) ^{115,117,118}. This bidirectional transport is essential for neurons, where materials such as vesicles, proteins, and organelles need to be efficiently transported over long distances along axons and dendrites ^{105,119}. Motor proteins are crucial for maintaining neuronal function, and defects in motor protein activity can lead to neurodegenerative diseases due to impaired intracellular transport ^{179,180}.

Microtubule-severing proteins, like spastin and katanin, regulate microtubule turnover and remodeling by cutting microtubules into smaller fragments ^{181,182}. This severing activity is essential for various cellular processes, including cell division, axon branching, and neuronal plasticity ¹⁸³. Spastin, for example, plays a role in axonal growth and branching by severing microtubules to allow for their dynamic reorganization ^{184,185}. Mutations in spastin are linked to hereditary spastic paraplegia (HSP), a neurodegenerative disorder that affects motor neurons. These mutations often impair spastin's ability to sever microtubules, leading to microtubule stabilization defects and axonal degeneration ^{186,187}.

Microtubule-interacting proteins are essential for regulating the dynamic properties of microtubules, ensuring proper cell function and structural integrity. MAPs like TAU stabilize microtubules, while motor proteins like kinesin and dynein enable intracellular transport. Severing proteins such as spastin ensure microtubules can be efficiently remodeled. Disruptions in these proteins can lead to severe neurological and cellular dysfunction, underlying various neurodegenerative diseases. Understanding the roles of microtubule-interacting proteins is crucial for deciphering the molecular mechanisms that maintain cellular health and the development of therapies for diseases like AD and HSP.

1.2.4 Microtubules in AD and other tauopathies

Microtubule dysfunction is a hallmark of AD and other tauopathies. In AD patients' brains, there is a notable decrease in microtubule density^{188,189}. Hyperphosphorylated TAU from AD brains prevents microtubule assembly¹⁹⁰, while A β -treated primary hippocampal cultures exhibit microtubule disassembly and fragmentation¹⁹¹. Disruptions of microtubule dynamicity lead to interrupted axonal transport and synaptic dysfunction, contributing to neurodegeneration^{192,193}.

Several tubulin PTMs have been linked to neurodegeneration. Acetylation of microtubules, particularly in axons, is reduced in transgenic mice expressing human TAU, with NFT-bearing neurons exhibiting deacetylation of their microtubules^{194,195}. Microtubule deacetylation is associated with impaired axonal transport and neurodegeneration in mouse models of Parkinson's and Charcot-Marie-Tooth diseases, effects that are reversed with HDAC6 inhibition^{196,197}. Recently, significant accumulation of detyrosinated tubulin in the brains of advanced AD patients has been reported¹⁴⁸. Oligomeric A β (oA β) induces microtubule detyrosination in hippocampal neurons, and disruption in the tyrosination/detyrosination cycle contributes to synaptotoxicity and memory deficits^{198,199}.

On the other hand, post-mortem AD brains exhibit increased tubulin polyglutamylation^{189,200}. oA β -treated primary neurons show similar increase in tubulin polyglutamylation, inducing spastin-mediated microtubule severing⁹⁷, while mice deficient in CCP1, the major deglutamylating enzyme, suffer from neurodegeneration and impaired axonal transport¹⁶². Interestingly, loss of CCP1 is associated with infantile-onset neurodegeneration in humans²⁰¹. Therefore, targeting tubulin-modifying enzymes, such as HDAC6, vasohibins, and TTLLs, could be an alternative therapeutic strategy for tauopathies and related dementias.

1.3 Tubulin Tyrosine Ligase-Like enzymes

1.3.1 Family members

Tubulin Tyrosine Ligase-Like (TTLL) enzymes are a group of adenosine triphosphate (ATP)-dependent enzymes involved in microtubule PTMs. TTLLs are particularly known for their role in polyglutamylation and polyglycylation, two polymodifications in which glutamyl or glycyll chains are added to a glutamate residue on the C-terminal tail of either α - or β -tubulin^{153,165}. While polyglutamylation is highly enriched in neuronal microtubules²⁰², polyglycylation is largely restricted to cilia²⁰³.

The TTLL family consists of thirteen enzymes that share a conserved TTL homology domain containing an essential ATP binding site, but exhibit varying substrate and reaction specificities and tissue distributions¹⁵⁴. Only TTLL3, TTLL8, and TTLL10 exhibit glycyllating activities, while eight of the remaining TTLLs are primarily glutamylases²⁰⁴. Among glutamylating TTLLs, TTLL1, TTLL5, TTLL6, TTLL11, and TTLL13 have higher affinity to α -tubulin, while TTLL4 and TTLL7 modulate β -tubulin more efficiently. TTLL4, TTLL5, and TTLL7 exhibit preference for initiating the glutamate side chain, while TTLL1, TTLL6, TTLL11, and TTLL13 function as side chain elongators^{205,206}. Substrate and activity specificities of glutamylating TTLLs are depicted in Fig. 1.

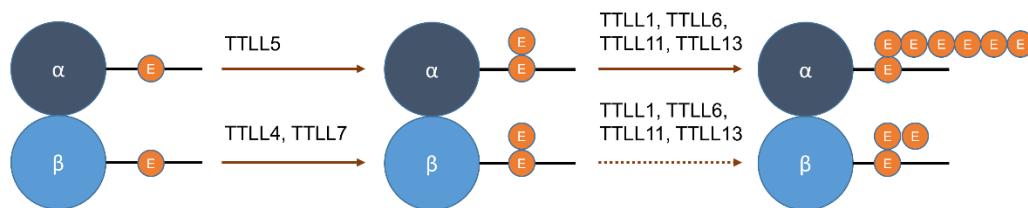


Figure 1. TTLLs and tubulin glutamylation. Schematic representation of the generation of glutamate side chains on C-terminal tails of tubulin by TTLLs, with tubulin isotype specificity (α - or β -tubulin) and reaction preference (initiation or elongation) delineated. Dashed lines indicate low preference.

These enzymes add varying lengths of glutamate chains to the γ -carboxyl group of glutamic acid residues in tubulin, which alters microtubule properties such as stability and interaction with motor proteins and severing enzymes^{158,207} (See also 1.3.2). The length and distribution of these glutamate chains are tightly regulated by a balance between the activity of TTLL enzymes (which add glutamates) and CCPs, the enzymes that remove them^{161,208}.

1.3.2 Physiological Roles of TTLLs

By adding glutamate chains to tubulin, TTLLs modulate the interaction of microtubules with motor proteins, MAPs, and severing enzymes. Most importantly, tubulin polyglutamylation enhances spastin's affinity for microtubules and influences its enzymatic activity. Spastin's severing activity rises as the length of the glutamate side chain increases. The highest severing efficiency occurs when microtubules have 8–9 glutamates per tubulin. However, longer glutamyl side chains diminish spastin's activity^{156,160}. Spastin-mediated microtubule fragmentation is essential for microtubule maintenance and reorganization, and increases the pool of free tubulin in the cell^{209,210}.

In the brain, tubulin polyglutamylation is essential for the development of healthy neurons and is mainly carried out by TTLL1 and TTLL7²¹¹. TTLL7-mediated polyglutamylation is required for the growth of MAP2-positive neurites²¹², while polyglutamylation by TTLL1 regulates molecular motors and synaptic vesicle transport²¹³. Polyglutamylation by TTLL1 and TTLL7 increases the affinity of TAU and the severing enzyme katanin to microtubules, while TTLL7-induced β -tubulin polyglutamylation reduces the run length of the motor protein KIF5B¹⁵⁸.

Besides neurons, TTLLs are essential for the proper functioning of cilia and flagella. In particular, polyglutamylation is required for proper ciliary assembly and motility and intraflagellar transport, regulating the functions of airway cilia and sperm flagella^{214–216}. Additionally, TTLL11-mediated polyglutamylation ensures the proper regulation of spindle microtubules during mitosis, thus playing a role in accurate chromosome segregation and the prevention of aneuploidy²¹⁷.

1.3.3 Diseases associated with TTLL dysfunction

Glutamylation is the predominant tubulin modification in brain tissue and it progressively increases throughout development²¹⁸. Dysregulation of tubulin glutamylation has been implicated in infantile-onset progressive neurodegeneration in humans, a condition caused by inactivating mutations in CCP1, leading to developmental delays, motor problems, and severe cognitive decline²⁰¹. Similarly, a spontaneous autosomal recessive mouse mutation in *Ccp1* gene causes severe degeneration of cerebellar Purkinje neurons, thalamic neurons, olfactory bulb, photoreceptors, in addition to male infertility²¹⁹. This mouse model, known as Purkinje cell degeneration (*pcd*) mouse, has served as a valuable tool in studying the link between glutamylation and neurodegeneration. Recent findings unveiled that *pcd* mice exhibit excessive polyglutamylation in their *CCP1*-deficient neurons¹⁶², and that knocking out TTLL1 and TTLL4,

but not other TTLLs, attenuated Purkinje cell loss and mitigated olfactory bulb and photoreceptor degeneration, but didn't rescue male infertility ²²⁰. In the past decade, more evidence of TTLL involvement in TAU-mediated neurodegeneration has accumulated: TTLL6 was shown to translocate with missorted TAU to the somatodendritic compartment of $\alpha\beta$ -treated rat neurons where it drove hyperglutamylation and spastin-mediated microtubule severing ⁹⁷. Mutation of all glutamylation sites in the C-terminal tail of tubulin alpha-4A chain (TUBA4A) reversed TAU hyperphosphorylation, TAU oligomerization, and increased microglial activation in brain tissue of a murine tauopathy model ²²¹. Hyperglutamylation can affect axonal transport and synaptic activity, evidenced by enhanced mitochondrial axonal motility and kinesin-microtubule binding interaction and run time in primary neurons from TTLL1 and TTLL7 knockout mice, respectively ^{158,207}.

Besides neurodegeneration, TTLLs have been associated with various ciliopathies, which are disorders that affect the structure or function of cellular cilia. Several case reports have linked mutations in TTLL5 to cone-rod dystrophies, azoospermia, and hearing loss ^{222–225}, while depletion of TTLL1 and TTLL9 leads to abnormal spermatogenesis ^{214,226}. More recently, some TTLLs have been implicated in cancer. TTLL11-induced microtubule polyglutamylation is required for chromosome segregation fidelity and the enzyme is downregulated in various human tumors ²¹⁷. In contrast, TTLL12 is upregulated in prostate and ovarian cancers, among others, and its oncogenic activity is thought to emanate from its suppression of tubulin nitrotyrosination, a cellular check-point induced by excessive oxidative stress ²²⁷.

Taken together, glutamylating TTLL enzymes play a crucial role in the spatial and temporal regulation of microtubules in various physiological processes. Disruption of polyglutamylation homeostasis is associated with a wide range of diseases, making these enzymes an emerging promising therapeutic target, most notably for tauopathies and related neurodegenerative disorders. However, the majority of research concerning TTLLs has been done in rodents, and their physiological functions and potential druggability in human disease-relevant models is critically understudied.

2. Aims

In tauopathy paradigms in rodent models, missorted TAU may recruit TTLL6 to the dendrites, where it induces microtubule polyglutamylation and spastin-mediated microtubule loss, hinting towards a TAU-triggered, TTLL- and spastin-driven degradation of microtubules following A β insult⁹⁷. Additionally, knockout of TTLL1 and TTLL4 mitigated neurodegeneration in *pcd* mice²²⁰. However, the role of TTLLs in human neurons and TAU-humanized mice remains unexplored. In this work, we aimed to establish human tauopathy-relevant models using human induced pluripotent stem cell (hiPSC)-derived cortical neurons, treated with oA β or transduced with FTDP-17-causing P301L mutation of TAU, along with brain sections from human P301L-TAU-transgenic pR5 mice.

Using these models, we investigated TAU-related effects on microtubule dynamics and stability, assessed primarily via their PTMs. We sought to identify the specific TTLL(s) involved in interacting with pathological TAU and mediating microtubule destabilization. Additionally, we examined whether reducing TTLL expression in human neurons could prevent AD-like pathology, microtubule loss, and synaptic dysfunction.

The aims of this study can be listed as follows:

Aim 1: Establishing TAU missorting and microtubule loss in human neuronal models.

Aim 2: Investigating TAU- and TTLL-mediated loss of microtubules and neuronal dysfunction, as well as the therapeutic potential of reducing TTLL expression in human neuronal models.

Aim 3: Studying the expression and glutamylation activity of different recombinant TTLLs and their impact on microtubule dynamics in human cells.

By addressing these questions, we hope to shed more light on the physiological roles of TTLLs and their pathological implications in TAU-related neurodegeneration, potentially revealing new therapeutic approaches for AD and related tauopathies.

3. Publications and preprints

3.1 Overview

The findings of this doctoral thesis have been summarized in three independent research articles, one of which was accepted and published in a peer-reviewed journal, while the other two articles were uploaded to a publicly available preprint repository. Additionally, one project-related viewpoint article and one protocol were published in peer-reviewed journals. In this chapter, the main findings from these articles and their contribution to the thesis aims will be described, and my individual contribution to the results and writing of the articles will be delineated.

Table 1. Overview of manuscripts included in this thesis.

Manuscript	Year	Type	Current status	Aim		
				1	2	3
Article 1	2022	Viewpoint	Published	-		
Article 2	2024	Protocol chapter	Published	-		
Article 3	2024	Research article	Published	x		
Article 4	2024	Research article	Preprint/Submitted	x	x	
Article 5	2024	Research article	Preprint			x

3.2 Article 1: AAV-based gene therapy approaches for genetic forms of tauopathies and related neurogenetic disorders

Authors	<u>Mohamed Aghyad Al Kabbani</u> , Gilbert Wunderlich, Christoph Köhler, Hans Zempel
Type	Viewpoint
Journal	Biocell
Date of publication	14.12.2021
DOI	10.32604/biocell.2022.018144

3.2.1 Key message

In this viewpoint, we explored the potential of gene therapy, specifically using adeno-associated virus (AAV) vectors, for treating tauopathies - neurodegenerative diseases primarily characterized by the abnormal accumulation of hyperphosphorylated TAU protein in neurons. These diseases, both genetic and sporadic, currently lack effective treatments.

We highlighted the promising potential of AAV-based gene therapy in treating difficult-to-treat genetic tauopathies, and emphasized that this approach could offer patient-specific therapeutic interventions, particularly in genetically defined cases. However, challenges remain, including technical and safety concerns, as well as the complexity of different tauopathy variants. The viewpoint calls for further research to optimize the use of AAV-based therapies and suggests that future clinical approaches could personalize treatments based on patient-specific genetic and epigenetic profiles.

In summary, while AAV-based gene therapy holds considerable promise for the treatment of tauopathies, further studies are needed to address its limitations and refine its application.

3.2.2 Individual contribution

As the first author of this viewpoint, I developed an existing idea and conceived and drafted the manuscript. All co-authors refined the concept and scientific context, especially Hans Zempel.

3.3 Article 2: Optimized Calcium-Phosphate-Based Co-transfection of TAU and tdTomato into Human iPSC-Derived Neurons for the Study of Intracellular Distribution of Wild-type and Mutant Human TAU

Authors	Panagiotis Lilis, <u>Mohamed Aghyad Al Kabbani</u> , Hans Zempel
Type	Protocol chapter
Journal	Tau Protein: Methods and Protocols, Methods in Molecular Biology
Date of publication	22.03.2024
DOI	10.1007/978-1-0716-3629-9_32

3.3.1 Key findings

In this protocol, we outlined a method for improving the transfection efficiency of iPSC-derived neurons. This approach uses calcium phosphate to introduce wild-type and mutant TAU proteins along with fluorescent markers like tdTomato. It achieves a higher efficiency (20-30%) compared to standard transfection methods, while maintaining neuron health. This optimized method is useful for studying intracellular TAU distribution in neurodegenerative diseases.

3.3.2 Individual contribution

As a second author of this protocol, I helped generating the data and creating the figures. The first author was an intern in our laboratory (Research Group Zempel, Institute of Human Genetics, University Hospital Cologne) at the time of conceiving this protocol and was methodologically supervised by me.

3.4 Article 3: Effects of P301L-TAU on post-translational modifications of microtubules in human iPSC-derived cortical neurons and TAU transgenic mice

Authors	<u>Mohamed Aghyad Al Kabbani</u> , Christoph Köhler, Hans Zempel
Type	Research article
Journal	Neural Regeneration Research
Date of publication	26.06.2024
DOI	10.4103/NRR.NRR-D-23-01742

3.4.1 Key findings

In this study, we investigated the effects of the P301L-TAU mutation, a known cause of tauopathies such as FTDP-17, on PTMs of microtubules in human iPSC-derived neurons and transgenic P301L-TAU mice. The findings indicate that the mutation leads to increased TAU phosphorylation and missorting into the somatodendritic compartments of neurons, and changes in microtubule stability-related PTMs, particularly acetylation and polyglutamylation.

In P301L-TAU transgenic mice, there was a significant reduction in microtubule acetylation, linked to reduced stability, and an increase in polyglutamylation, associated with microtubule fragmentation. In human iPSC-derived neurons, P301L-TAU expression led to increased microtubule polyglutamylation, further implicating microtubule instability in tauopathy progression.

These results suggest that microtubule destabilization, driven by specific PTMs, may contribute to the neurodegenerative process in tauopathies. Targeting these PTMs could offer potential therapeutic avenues for diseases like AD and FTD.

3.4.2 Individual contribution

As the first author of this study, I conceived, performed and analyzed the experiments, interpreted the data, and drafted the manuscript. All co-authors reviewed the manuscript and contributed to conception and data interpretation.

3.5 Article 4: Knockdown of TTLL1 reduces A β -induced TAU pathology in human iPSC-derived cortical neurons

Authors	<u>Mohamed Aghyad Al Kabbani</u> , Tamara Wied, Daniel Adam, Jennifer Klimek, Hans Zempel
Type	Research article
Preprint server	bioRxiv
Date of upload	19.11.2024
DOI	10.1101/2024.11.19.624324

3.5.1 Key findings

In this study, we explored the involvement of TTLL proteins in TAU pathology associated with AD, utilizing human iPSC-derived cortical neurons treated with oA β to simulate AD-like conditions. We focused on three TTLL proteins: TTLL1, TTLL4, and TTLL6.

The results demonstrated that oA β treatment led to TAU missorting, decreased tubulin acetylation, elevated tubulin polyglutamylation, and synaptic destabilization in the neurons. Knockdown of TTLL1 significantly diminished TAU missorting, tubulin polyglutamylation, and synaptic damage, whereas TTLL4 knockdown showed moderate effects and TTLL6 knockdown helped restore microtubule acetylation. Importantly, these knockdowns did not disrupt neuronal networks or impair neuronal activity, highlighting TTLL1 as a promising therapeutic target.

Further analysis through fluorescence resonance energy transfer (FRET) microscopy indicated a direct interaction between TTLL1 and TAU, emphasizing TTLL1's crucial role in oA β -induced TAU pathology. Overall, the findings suggest that targeting TTLL1 could potentially alleviate microtubule dysfunction and synaptic loss in AD, presenting a novel therapeutic strategy for tauopathies.

3.5.2 Individual contribution

As the first author of this preprint, I co-designed the study alongside Hans Zempel, performed the experimental work, and analyzed and interpreted the data. All co-authors offered technical support and reviewed the manuscript.

3.6 Article 5: Expression of recombinant human glutamylating TTLLs in human cells leads to differential tubulin glutamylation patterns, with only TTLL6 disrupting microtubule dynamics

Authors	<u>Mohamed Aghyad Al Kabbani</u> , Pragma Jatoo, Kathrin Klebl, Bert M Klebl, Hans Zempel
Type	Research article
Preprint server	bioRxiv
Date of upload	27.11.2024
DOI	10.1101/2024.11.25.624814

3.6.1 Key findings

In this study, we investigated the effects of several glutamylating TTLLs on tubulin glutamylation patterns and microtubule stability in human HEK293T cells. We found that expression of different TTLLs led to distinct patterns of tubulin glutamylation, validating their varied roles in initiating or elongating glutamate chains. TTLL4, for instance, mainly initiated glutamylation, while TTLL6 and TTLL11 were primarily involved in elongating these chains. Among the TTLLs examined, TTLL6 had a unique impact on microtubule dynamics, significantly reducing microtubule stability, as shown through live-cell imaging. This destabilization was associated with an unexpected increase in microtubule growth rate, suggesting that TTLL6 may facilitate a dynamic restructuring of the microtubule network.

The study also explored the therapeutic potential of LDC10, a novel TTLL inhibitor, and demonstrated its ability to block glutamylation activity across all TTLL enzymes tested. Importantly, LDC10 was able to counteract the microtubule-destabilizing effects induced by TTLL6, restoring microtubule stability and growth rate. These findings suggest that TTLL6 could play a pathogenic role in disorders related to microtubule destabilization and that LDC10 could be a promising pharmacological tool for mitigating the effects of TTLL-induced microtubule instability.

3.6.2 Individual contribution

As the first author of this preprint, I carried out the experiments, analyzed and interpreted the data, and drafted the manuscript. The study was conceived by me and Hans Zempel, who also reviewed the manuscript.

4. Discussion

Neurodegeneration and cognitive decline associated with AD and other tauopathies represent a significant challenge for the ageing population. Despite extensive research, effective therapies remain elusive, with most interventions focusing on targeting aggregated TAU or A β showing only modest efficacy. Challenges of achieving effective brain concentrations of aggregate-targeting antibodies, limited cognitive improvement, and concerning side effects such as brain swelling, bleeding, and seizures, still persist²²⁸. Microtubule loss is a major hallmark of tauopathies^{188,229}, prompting exploration of microtubule-stabilizing drugs like paclitaxel. However, limited brain penetration and significant toxicities have hindered their therapeutic application^{230,231}. These challenges emphasize the need to investigate alternative molecular targets and delivery routes that may offer more substantial benefits with reduced side effects.

Gene therapy is a cutting-edge approach that involves delivering genetic material into patients' cells to treat a disease. This technique has shown potential in addressing genetic diseases by either silencing faulty genes or introducing functional ones. The delivery method of therapeutic genetic materials is usually viral-based, with adeno-associated virus (AAV) being the vehicle of choice due to their safety and efficacy²³². There are currently six AAV-based gene therapies approved by the Food and Drug Administration (FDA) for the treatment of retinal dystrophy, hemophilia, Duchenne muscular dystrophy, and spinal muscular atrophy. Therefore, neurodegenerative diseases where the genetic cause is clearly identified, such as genetic tauopathies or CCP1-associated infantile-onset neurodegeneration, are optimal targets for AAV-based gene therapy²³³.

In this work, we explored alternative microtubule-targeting strategies in the paradigm of AD and tauopathies from a gene therapy-focused angle. Microtubules exhibit a complex code of PTMs that regulate their stability, dynamics, and protein interactions. The most abundant neuronal tubulin PTM, polyglutamylation, has been linked to microtubule severing and neurodegeneration in animal models^{162,163,202}. Therefore, we decided to target several of the TTL enzymes that catalyze tubulin glutamylation in human tauopathy-relevant models to assess how reduced TTL expression affects TAU sorting, microtubule stability, and neuronal morphology and function. We identified stability-decreasing alterations in microtubule PTMs in pR5 mice transgenic for P301L-TAU, shedding the light on the effects of this disease-causing mutation. In addition, by treating hiPSC-derived neurons (iNeurons) with oA β and lentivirally knocking down specific TTLs, we established AD-like pathology in these human neurons and identified TTL1 as a major

contributor to TAU-mediated pathology and a potential therapeutic target. Lastly, recombinant protein expression and pharmacological treatment experiments in human cells demonstrated the efficacy of a novel TLL inhibitor in reducing glutamylation and reversing TLL6-induced microtubule instability.

4.1 Establishing TAU missorting and microtubule loss in human neuronal models

TAU missorting and microtubule loss are two events that occur early in the course of tauopathies, including AD^{41,234}. Studies on TLLs in rodent models link these tubulin-modifying enzymes to neurodegenerative processes, including spastin- and katanin-mediated microtubule severing, interaction with missorted TAU, and synaptic dysfunction^{97,162,220}. However, insights on TLLs and their potential pathological roles in human tauopathy models remain limited. To address this gap, we aimed to establish a human model of tauopathy to explore the effects of TAU pathology on microtubules and their PTMs, particularly polyglutamylation.

Our first approach (Article 3) utilized the well-established pR5 mouse strain, which expresses the longest human TAU isoform (2N4R) with the P301L mutation under the murine neuronal-specific Thy1.2 promoter²³⁵. pR5 mice exhibit TAU hyperphosphorylation and NFT assembly across various brain regions by approximately eight months of age^{235–237}, and develop tauopathy-like spatial reference memory deficits^{238,239}. Additionally, we expressed the same mutant TAU construct in iNeurons via lentiviral transduction on a *MAPT* knockout background⁹⁸. iNeurons are engineered from human iPSCs and differentiated into cortical layer 2/3 glutamatergic neurons through doxycycline-induced expression of the transcription factor neurogenin 2, resulting in highly pure cultures of polarized, active cortical neurons²⁴⁰.

In immunolabelled paraffin sections of pR5 mouse brains, we observed significant TAU aggregation, hyperphosphorylation, and missorting. These pathological features were associated with decreased acetylated tubulin in NFT-bearing neurons compared to adjacent tangle-free neurons, indicating decreased microtubule stability in these neurons. Interestingly, the number of hippocampal long dendrites positive for polyglutamylated tubulin was significantly decreased in 24-month-old pR5 mice compared to age-matched non-transgenic littermates, replaced with short, stubby dendrites, with increased polyglutamylation levels in the remaining long dendrites. These findings suggest that polyglutamylation may drive microtubule loss, with spastin-recruiting signaling potentially happening earlier, as indicated by increased polyglutamylated tubulin levels in immunoblotted hippocampal lysates of 9-month-old pR5 mice. However, P301L-TAU-expressing iNeurons did not exhibit TAU missorting or aggregation when compared to wildtype

TAU-expressing iNeurons. This could be due to the young age of these neurons compared to the aged mice, or because the exposure to mutant TAU in iNeurons was not as long as in the mice. While mutant TAU expression led to slightly increased tubulin polyglutamylation, acetylated tubulin levels were actually elevated rather than reduced, suggesting microtubule stabilization via TAU binding. This outcome indicates that lentiviral expression of P301L-TAU in iNeurons may not be a suitable model for studying TAU pathology and the associated TTLL/microtubule axis.

As an alternative, we employed α A β to induce TAU pathology. Although A β 42 are more aggregation-prone and more neurotoxic than A β 40^{241,242}, oligomers of A β 40 and A β 42 together in a 7:3 ratio exhibit stronger neurotoxicity, better synaptic colocalization, enhanced stability, and are more physiologically relevant compared to aggregates from isolated peptides²⁴³. In rodent-derived primary neurons, α A β induces tau missorting, microtubule loss, and synaptic declustering^{97,244}. Following 3 hours of α A β exposure, our day 21 iNeurons showed increased tau localization in somatic compartments, indicating TAU missorting, alongside decreased tubulin acetylation and increased polyglutamylation. These changes mirror early tauopathy-like conditions, suggesting impaired microtubule stability and possible spastin recruitment. In addition, the size of synaptic clusters, identified through Homer1 and synaptophysin co-staining, was significantly reduced. In sum, day 21 α A β -treated iNeurons recapitulated some AD-like conditions, such as TAU missorting, reduced microtubule stability, and synaptic loss, thus providing a suitable human tauopathy model for subsequent studies discussed in the following sections.

4.2 Investigating TAU- and TTLL-mediated loss of microtubules and neuronal dysfunction, as well as the therapeutic potential of reducing TTLL expression in human neuronal models

TTLL-induced hyperglutamylation has been linked to neurodegeneration due to CCP1 loss and the resulting imbalance between glutamate chain addition and removal^{162,201}. We examined whether TTLLs contribute to TAU pathology in our α A β -treated iNeurons by knocking down one initiator (TTLL4) and two elongators (TTLL1 and TTLL6) (Article 4). Prior studies have implicated TTLL6 in α A β -induced, TAU-driven dendritic microtubule loss through interaction with missorted TAU and subsequent spastin-mediated microtubule severing⁹⁷, while TTLL1 and TTLL4 have been identified as the key drivers of neurodegeneration in *pcd* mice²²⁰.

In our study, we successfully reduced the expression of all three TTLLs in iNeurons by 20-50% using lentiviral transduction with target-specific short hairpin ribonucleic acid (shRNA) constructs.

When assessing readouts of AD-like pathology established in Aim1, we found that TTLL1 knockdown, and to a lesser extent TTLL4 knockdown, reduced TAU missorting, decreased microtubule polyglutamylation, and partially protected synaptic clusters from the detrimental effects of $\alpha\beta$ insult. Interestingly, only TTLL6 knockdown restored tubulin acetylation, though it did not affect TAU missorting or tubulin polyglutamylation levels, suggesting a potential TAU-independent pathway of microtubule stabilization. Previous studies in human embryonic kidney (HEK) 293 cells have proposed a potential direct interaction between recombinant TAU and TTLL6⁹⁷. Therefore, we asked whether a similar interaction between TAU and any of the TTLLs studied here could be the underlying mechanism behind the mitigation of $\alpha\beta$ -induced TAU pathology following TTLL knockdown. To this end, we used fluorescence resonance energy transfer (FRET) microscopy to assess potential interactions between teal fluorescent protein (TFP)-TAU and yellow fluorescent protein (YFP)-tagged TTLL1, TTLL4, and TTLL6. Notably, we observed a significant increase in FRET efficiency only in HEK293T cells co-expressing TFP-TAU and YFP-TTLL1, compared to negative controls and cells co-expressing TFP-TAU with YFP-TTLL4 or YFP-TTLL6. This result suggests a potential direct interaction between TAU and TTLL1, potentially explaining the mitigating effects of TTLL1 knockdown on TAU pathology, microtubule stability, and synaptic structure.

Our findings suggest that TTLL1 may translocate with missorted TAU to the somatodendritic compartments of affected neurons, leading to microtubule hyperglutamylation, spastin recruitment, and subsequent dendritic microtubule and synaptic loss (Fig. 2). However, our experiments did not reveal direct interactions between TAU and TTLL4 or TTLL6. Another possible explanation for the pathological roles of these TTLLs could be the creation of repulsive forces between negatively charged hyperphosphorylated TAU and the similarly negatively charged glutamate residues on the microtubule surface. This repulsion could lead to TAU detachment from microtubules, promoting TAU aggregation and microtubule disassembly²⁴⁵.

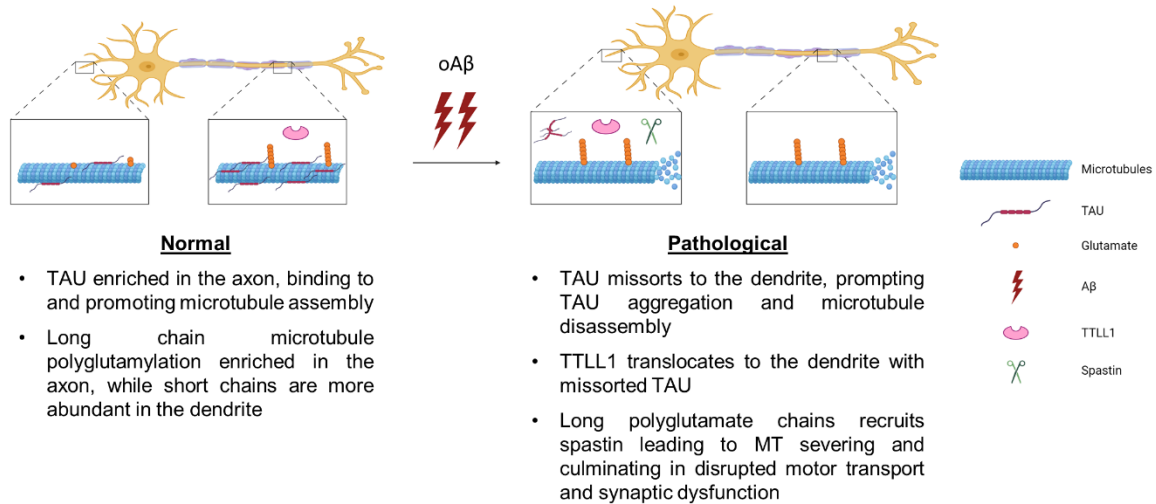


Figure 2. Proposed mechanism of TAU missorting and TTLL1-mediated microtubule destabilization in response to Aβ insult. Under normal conditions, TAU is localized predominantly in axons, where it stabilizes microtubules. Upon exposure to Aβ, TAU becomes missorted to the somatodendritic compartments. Concurrently, TTLL1, potentially directly interacting with TAU, translocates to the dendrites, where its activity promotes excessive microtubule polyglutamylation. This polyglutamylation destabilizes the microtubule network, leading to microtubule loss and subsequent synaptic dysfunction, contributing to neuronal impairment and tauopathy progression.

Polyglutamylation plays a crucial role in spatial and temporal regulation of microtubule dynamics and interactions with other proteins^{157–159}, and it is the most abundant tubulin PTM in the brain²⁰². Therefore, manipulating the expression of glutamylating TTLLs could have significant effects on neuronal morphology and function, especially given that TTLL1, our primary target, is the major glutamylase in the brain^{211,220}. To address this issue, we carried out Sholl analysis to assess dendritic arborization and complexity in TTLL-knockdown iNeurons, and performed immunostainings of neurofilament-L (NF-L) and MAP2 to examine axonal and dendritic networks, respectively. Neither analysis revealed significant changes in neurite structure following TTLL knockdowns. Moreover, microelectrode array (MEA) recordings showed no erratic changes in neuronal activity.

Taken together, our results position TTLL1, and potentially other TTLLs, as promising therapeutic targets for AD and tauopathies by targeting microtubule PTMs rather than protein aggregation. This is especially important since subtle changes in TAU localization and microtubule code likely occur earlier in the pathological cascade than TAU aggregation and Aβ plaque formation. Thus,

targeting TLLs and similar microtubule modifying enzymes could serve as an early intervention strategy to prevent subsequent neuronal death and cognitive impairment.

4.3 Studying the expression and glutamylation activity of different recombinant TLLs and their impact on microtubule dynamics in human cells

At least eight TLLs are known to have glutamylating activity, with distinct functions based on their substrate specificity -either α - or β -tubulin- and their preference for initiating or elongating glutamate side chain ^{204,205}. Understanding these differences is essential to distinguish the unique glutamylation patterns carried out by individual TLLs, and their specific roles in microtubule dynamics. This knowledge is critical for selectively targeting specific TLLs without affecting broader cellular processes. HEK293T cells express low endogenous levels of glutamylating TLLs ²⁴⁶, making these cells a suitable controlled model for studying the function and impact of exogenously expressed recombinant TLLs.

Following expression in HEK293T cells (Article 5), initiator TLL4 exhibited the strongest monoglutamylation activity, followed by moderate activity from another initiator, TLL7. On the other hand, the elongator TLL11 showed the highest polyglutamylation activity, though initiators TLL4 and TLL7 also displayed some elongation activity. TLL6, another elongator, had remarkably lower polyglutamylation activity but was the only expressed TLL to significantly destabilize microtubules, as observed through live-cell imaging of EB3 comets. Substrate and activity preferences of TLLs are not strictly exclusive, with initiators still exhibiting minor elongation activity and vice versa ^{205,247}. Polyglutamylation, rather than monoglutamylation, is expected to exert the strongest influence on microtubule dynamics since longer chains recruit the severing enzyme spastin. However, excessively long glutamate chains (over eight residues) shift the function of spastin from severing to stabilizing microtubules ¹⁶⁰. This might explain why modest polyglutamylation by TLL6 could be enough to trigger the microtubule severing activity of spastin or katanin, while excessive polyglutamylation by TLL11 could stabilize rather than destabilize microtubules.

Given the role of TLLs in various diseases, including neurodegenerative disorders, ciliopathies, and cancer, developing selective TLL inhibitors holds significant therapeutic potential. Therefore, we tested a novel compound, LDC10, with a potential TLL inhibitory activity. LDC10 effectively inhibited the glutamylating activities of recombinant TLL4, TLL6, and TLL11 in HEK293T cells, with only modest activity against TLL7. Notably, LDC10 counteracted TLL6

effects on microtubule dynamics, restoring microtubule stability and growth rate to control values. While these results are promising, further investigation into the potential side effects of manipulating tubulin glutamylation is necessary. In addition, because other proteins, such as nucleosome assembly proteins (NAPs) and certain histones, also undergo polyglutamylation^{248,249}, further studies are warranted to assess possible off-target effects of pharmacological TLL inhibition.

4.4 Significance, limitations, and outlook

This doctoral thesis explores understudied aspects of tauopathies and their underlying molecular mechanisms, contributing to the field of neurodegenerative disease research. Tauopathies, such as AD and FTD, represent a class of neurodegenerative disorders marked by the pathological accumulation of hyperphosphorylated TAU protein, which disrupts neuronal function and leads to cognitive decline. Despite significant advances, effective therapeutic strategies for tauopathies remain limited. The studies presented here shed light on novel mechanisms that may offer new avenues for therapeutic intervention.

The major significance of this thesis lies in its approach to addressing TAU pathology from a microtubule-centric perspective, particularly through the investigation of PTMs of tubulin and their influence on TAU pathology. By focusing on the role of TLLs in microtubule dynamics, this research explores a new and underexplored area of tauopathies. The findings suggest that targeting specific TLLs, such as TLL1, could offer an innovative therapeutic strategy by modulating the microtubule code rather than directly targeting TAU aggregation. This is particularly significant because microtubule dysfunction is an early event in tauopathies^{250,251}, potentially offering an opportunity for early intervention, before the onset of widespread TAU aggregation, neuronal death, and cognitive decline.

Additionally, the usage of human-based models such as iPSC-derived neurons in this research enhances the relevance and translational potential of the findings. The use of these models allows for a more accurate depiction of human tauopathies, as opposed to rodent models, which often do not fully recapitulate the complexity of human neurodegenerative diseases^{252,253}. By employing lentiviral-based knockdowns of several TLLs in cell culture and identifying novel potential therapeutic targets, this thesis lays the groundwork for genetic targeting of TLL1 and other TLLs in animal models using AAVs carrying murine shRNAs. We have in fact successfully established intracerebroventricular (ICV) injections to administer AAVs into mouse brains.

Additionally, we have obtained the necessary regulatory approvals to conduct experiments in mice, which involves AAV-based expression of mutant APP to establish an AD-like phenotype and AAV-based knockdown of TTLs to evaluate their protective potential as well as possible detrimental effects on neuronal function and viability. These effects will be assessed through biochemical analyses such as Western blotting and immunostaining of mouse brain lysates for TAU, tubulin PTMs, and synaptic markers, as well as through behavioral, motor, and cognitive tests, as represented in Fig. 3. By bridging the gap between basic molecular biology and clinical relevance, we hope to make a significant contribution to the ongoing search for effective treatments for tauopathies.

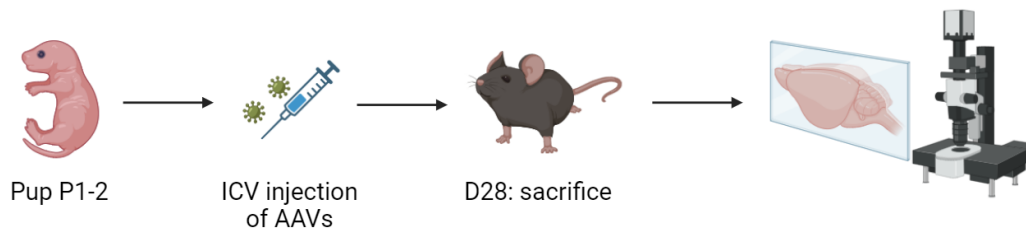


Figure 3. Schematic representation of the workflow of a preliminary experiment in mice to investigate AAV delivery to the brain. Mouse pups at the postnatal age of 1-2 days will undergo ICV injections to deliver mock AAVs, followed by animal sacrifice after four weeks and subsequent brain sectioning and microscopic analysis.

While this thesis provides novel insights into targeting microtubule modifying enzymes as a therapeutic strategy for AD and tauopathies, it is not without limitations. A significant limitation is the reliance on cellular models, particularly iPSC-derived neurons, to study TAU pathology. While iNeurons are proving to be an invaluable tool for investigating human-specific disease mechanisms, they also have inherent limitations. iNeurons are not perfect representations of the complex neuronal networks found in the human brain. Their limited maturity, homogeneity, and the lack of fully developed dendritic spines may lead to incomplete representation of tauopathy features, especially those related to advanced stages of disease progression^{254,255}. One potential solution is co-culturing iNeurons with primary or iPSC-derived glial cells, such as astrocytes, to provide mechanical support and promote neuronal maturation^{256,257}. In addition, the 3-hour $\text{oA}\beta$ treatment used in our model to mimic certain AD-like features represents an acute insult that does not fully capture the complexity of a chronic, progressive disorder like AD. Future strategies

should explore approaches that induce more robust and long-term pathological changes, such as overexpression of mutant APP.

Moreover, the studies presented here primarily focused on specific tubulin PTMs and TTLLs, but other molecular pathways and cellular mechanisms contributing to tauopathies, such as neuroinflammation or the role of glial cells, were not explored. Co-cultures of iNeurons with glia could also address this limitation by enabling the assessment of glial structure and function under different tauopathy-inducing stressors. Additionally, such co-culture models could facilitate the investigation of neuroinflammatory markers, providing a more comprehensive understanding of the contributions of glial cells and inflammation to tauopathies²⁵⁸.

Another limitation is the relatively narrow focus on specific TTLLs, particularly TTLL1, TTLL4, and TTLL6. While the results are promising, it remains unclear whether targeting TTLL1 alone would be sufficient for therapeutic success, or if other TTLLs or tubulin-modifying enzymes could play significant roles in the disease process. The complexity of PTMs, the potential redundancy of some enzymes, and the variability across different tauopathies mean that a more comprehensive understanding of the entire tubulin code is necessary to create robust therapeutic strategies. TTLL1-immunoprecipitation coupled with mass spectrometry could be a valuable approach to identify novel TTLL1 interactors involved in microtubule regulation or dysregulation under both naïve and pathological conditions. These findings could reveal new independent or synergistic therapeutic targets. In addition, investigating the role of other TTLLs, such as brain-enriched TTLL7 and disease-associated TTLL5, is crucial to gaining a more complete understanding of the functions, redundancies, and pathological relevance of the full spectrum of glutamylating TTLLs.

Despite these limitations, the findings of this thesis open up several exciting avenues for future research and therapeutic development. One promising direction is the continued investigation into the role of TTLLs and other microtubule modifying enzymes in tauopathies. Future studies should aim to identify additional PTMs that contribute to TAU pathology and microtubule destabilization, potentially revealing other novel therapeutic targets. Future research should also focus on validating the therapeutic potential of TTLL depletion in animal models. Our successful lentiviral-based knockdown of different TTLLs in cell culture paves the way for establishing AAV-based vectors targeting murine TTLLs in vivo. This approach will enable the investigation of the long-term effects of TTLL manipulation on both disease progression and neuronal health in complex living organisms, which is essential for translating this research into viable clinical therapies. Beyond gene therapy approaches, our data highlight the promising potential of a novel TTLL

inhibitor in reducing TTLL6-mediated polyglutamylation and microtubule destabilization. Further studies should focus on elucidating the inhibitor's brain permeability and specificity, identifying potential off-target effects, and conducting pharmacokinetics and pharmacodynamics studies to optimize its pharmacological properties. Furthermore, it is important to evaluate potential compensatory mechanisms activated by the depletion or inhibition of specific TTLLs. Differential mass spectrometry or transcriptomics could be employed to identify genes and proteins that are upregulated or downregulated in response to such interventions, providing insights into adaptive cellular response and uncovering additional therapeutic targets.

Another exciting direction for future research is the application of the aforementioned multi-omics approaches to identify other molecular pathways involved in tauopathy, as well as potential interactors of TTLLs that may influence their function or act downstream of them. The potential TAU and TTLL1 direct interaction that we observed with recombinant proteins in HEK293T cells using FRET microscopy should be validated in neuronal models with endogenous proteins under healthy and pathological conditions, such as $\alpha\text{A}\beta$ insult or APP overexpression, using techniques like co-immunoprecipitation or proximity ligation.

Finally, the development of more sophisticated and human-relevant disease models, including 3D neuronal cultures and brain organoids, could further enhance the understanding of tauopathies and facilitate the testing of therapeutic interventions. While these models would better mimic the human brain's architecture, they are not without limitations, as they exhibit high heterogeneity and culture-dependent alterations, lack proper vascularization and blood brain barrier, and are deficient in myelination ²⁵⁹.

In conclusion, this thesis identifies TTLLs, especially TTLL1, as novel potential therapeutic targets for AD and related tauopathies, offering new insights into the molecular mechanisms underlying these diseases. The novel approach of targeting microtubule PTMs, particularly via TTLLs, provides a fresh perspective on how to address TAU-related neurodegeneration. Future work should continue exploring these pathways and validate our findings in more advanced disease models, including mouse models, paving the way for more effective, gene therapy-based treatments for tauopathies in the future.

5. References

1. Weingarten, M. D., Lockwood, A. H., Hwo, S. Y. & Kirschner, M. W. A protein factor essential for microtubule assembly. *Proc. Natl. Acad. Sci. U. S. A.* **72**, 1858–1862 (1975).
2. Witman, G. B., Cleveland, D. O. N. W., Weingarten, M. D. & Kirschner, M. W. Tubulin requires tau for growth onto. **73**, 4070–4074 (1976).
3. Grundke-Iqbal, I., Iqbal, K. & Tung, Y. C. Abnormal phosphorylation of the microtubule-associated protein τ (tau) in Alzheimer cytoskeletal pathology. *Proc. Natl. Acad. Sci. U. S. A.* **83**, 44913–44917 (1986).
4. Pollock, N. J., Mirra, S. S., Binder, L. I., Hansen, L. A. & Wood, J. G. Filamentous Aggregates in Pick's Disease, Progressive Supranuclear Palsy, and Alzheimer's Disease Share Antigenic Determinants With Microtubule-Associated Protein, Tau. *Lancet* **328**, 1211 (1986).
5. Goedert, M., Spillantini, M. G., Jakes, R., Rutherford, D. & Crowther, R. A. Multiple isoforms of human microtubule-associated protein tau: sequences and localization in neurofibrillary tangles of Alzheimer's disease. *Neuron* **3**, 519–526 (1989).
6. Arima, K. *et al.* NACP/ α -synuclein and tau constitute two distinctive subsets of filaments in the same neuronal inclusions in brains from a family of parkinsonism and dementia with Lewy bodies: double-immunolabeling fluorescence and electron microscopic studies. *Acta Neuropathol.* **100**, 115–121 (2000).
7. Himmler, A., Drechsel, D., Kirschner, M. W. & Martin, D. W. Tau consists of a set of proteins with repeated C-terminal microtubule-binding domains and variable N-terminal domains. *Mol. Cell. Biol.* **9**, 1381–1388 (1989).
8. Andreadis, A., Brown, W. M. & Kosik, K. S. Structure and Novel Exons of the Human τ Gene. *Biochemistry* **31**, 10626–10633 (1992).
9. Hutton, M. *et al.* Association of missense and 5'-splice-site mutations in tau with the inherited dementia FTDP-17. *Nature* **393**, 702–705 (1998).
10. Goedert, M., Spillantini, M. G. & Crowther, R. A. Cloning of a big tau microtubule-associated protein characteristic of the peripheral nervous system. *Proc. Natl. Acad. Sci.* **89**, 1983–1987 (1992).
11. Tam, P. K. H. An immunohistological study of the human enteric nervous system with microtubule-associated proteins. *Gastroenterology* **99**, 1841–1844 (1990).

12. Vallés-Saiz, L., Peinado-Cahuchola, R., Ávila, J. & Hernández, F. Microtubule-associated protein tau in murine kidney: role in podocyte architecture. *Cell. Mol. Life Sci.* **79**, 1–12 (2022).
13. Gu, Y., Oyama, F. & Ihara, Y. τ Is widely expressed in rat tissues. *J. Neurochem.* **67**, 1235–1244 (1996).
14. Ashman, J. B., Hall, E. S., Eveleth, J. & Boekelheide, K. Tau, the neuronal heat-stable microtubule-associated protein, is also present in the cross-linked microtubule network of the testicular spermatid manchette. *Biol. Reprod.* **46**, 120–129 (1992).
15. Goedert, M., Spillantini, M. G., Potier, M. C., Ulrich, J. & Crowther, R. A. Cloning and sequencing of the cDNA encoding an isoform of microtubule-associated protein tau containing four tandem repeats: differential expression of tau protein mRNAs in human brain. *EMBO J.* **8**, 393–399 (1989).
16. Hefti, M. M. *et al.* High-resolution temporal and regional mapping of MAPT expression and splicing in human brain development. *PLoS One* **13**, 1–14 (2018).
17. Grover, A., Deurel, M., Yen, S. H. & Hutton, M. Effects on splicing and protein function of three mutations in codon N296 of tau in vitro. *Neurosci. Lett.* **323**, 33–36 (2002).
18. D'Souza, I. *et al.* Missense and silent tau gene mutations cause frontotemporal dementia with parkinsonism-chromosome 17 type, by affecting multiple alternative RNA splicing regulatory elements. *Proc. Natl. Acad. Sci. U. S. A.* **96**, 5598–5603 (1999).
19. Andorfer, C. *et al.* Hyperphosphorylation and aggregation of tau in mice expressing normal human tau isoforms. *J. Neurochem.* **86**, 582–590 (2003).
20. Takuma, H., Arawaka, S. & Mori, H. Isoforms changes of tau protein during development in various species. *Dev. Brain Res.* **142**, 121–127 (2003).
21. Bullmann, T., Holzer, M., Mori, H. & Arendt, T. Pattern of tau isoforms expression during development in vivo. *Int. J. Dev. Neurosci.* **27**, 591–597 (2009).
22. McMillan, P. *et al.* Tau isoform regulation is region- and cell-specific in mouse brain. *J. Comp. Neurol.* **511**, 788–803 (2008).
23. Götz, J. Tau and transgenic animal models. *Brain Res. Rev.* **35**, 266–286 (2001).
24. Arendt, T., Stieler, J. T. & Holzer, M. Tau and tauopathies. *Brain Res. Bull.* **126**, 238–292 (2016).
25. Skrabana, R., Sevcik, J. & Novak, M. Intrinsically disordered proteins in the

- neurodegenerative processes: Formation of tau protein paired helical filaments and their analysis. *Cell. Mol. Neurobiol.* **26**, 1085–1097 (2006).
26. Barbier, P. *et al.* Role of tau as a microtubule-associated protein: Structural and functional aspects. *Front. Aging Neurosci.* **10**, 1–14 (2019).
 27. Xie, C. *et al.* The homologous carboxyl-terminal domains of microtubule-associated protein 2 and Tau induce neuronal dysfunction and have differential fates in the evolution of neurofibrillary tangles. *PLoS One* **9**, (2014).
 28. Mengham, K. *et al.* Shapeshifting tau: From intrinsically disordered to paired-helical filaments. *Essays Biochem.* **66**, 1001–1011 (2022).
 29. Skrabana, R., Skrabanova-Khuebachova, M., Kontsek, P. & Novak, M. Alzheimer's-disease-associated conformation of intrinsically disordered tau protein studied by intrinsically disordered protein liquid-phase competitive enzyme-linked immunosorbent assay. *Anal. Biochem.* **359**, 230–237 (2006).
 30. Caballero, B. *et al.* Acetylated tau inhibits chaperone-mediated autophagy and promotes tau pathology propagation in mice. *Nat. Commun.* **12**, 1–18 (2021).
 31. Edwards, G., Zhao, J., Dash, P. K., Soto, C. & Moreno-Gonzalez, I. Traumatic brain injury induces tau aggregation and spreading. *J. Neurotrauma* **37**, 80–92 (2020).
 32. Kampers, T., Friedhoff, P., Biernat, J., Mandelkow, E. M. & Mandelkow, E. RNA stimulates aggregation of microtubule-associated protein tau into Alzheimer-like paired helical filaments. *FEBS Lett.* **399**, 344–349 (1996).
 33. Brion, J. P., Guilleminot, J., Couchie, D., Flament-Durand, J. & Nunzf, J. Both adult and juvenile tau microtubule-associated proteins are axon specific in the developing and adult rat cerebellum. *Neuroscience* **25**, 139–146 (1988).
 34. Binder, L. I., Frankfurter, A. & Rebhun, L. I. The distribution of tau in the mammalian central nervous central nervous. *J. Cell Biol.* **101**, 1371–1378 (1985).
 35. Kanai, Y., Chen, J. & Hirokawa, N. Microtubule bundling by tau proteins in vivo: analysis of functional domains. *EMBO J.* **11**, 3953–3961 (1992).
 36. Drechsel, D. N., Hyman, A. A., Cobb, M. H. & Kirschner, M. W. Modulation of the dynamic instability of tubulin assembly by the microtubule-associated protein tau. *Mol. Biol. Cell* **3**, 1141–1154 (1992).
 37. Loomis, P. A., Howard, T. H., Castleberry, R. P. & Binder, L. I. Identification of nuclear T

- isoforms in human neuLoomis, P. A., Howard, T. H., Castleberry, R. P., & Binder, L. I. (1990). Identification of nuclear T isoforms in human neuroblastoma cells. *Proceedings of the National Academy of Sciences of the United Sta. Proc. Natl. Acad. Sci. U. S. A.* **87**, 8422–8426 (1990).
38. Papasozomenos, S. C. & Binder, L. I. Phosphorylation determines two distinct species of Tau in the central nervous system. *Cell Motil. Cytoskeleton* **8**, 210–226 (1987).
 39. Li, X. *et al.* Novel diffusion barrier for axonal retention of Tau in neurons and its failure in neurodegeneration. *EMBO J.* **30**, 4825–4837 (2011).
 40. Kowall, N. W. & Kosik, K. S. Axonal disruption and aberrant localization of tau protein characterize the neuropil pathology of Alzheimer's disease. *Ann. Neurol.* **22**, 639–643 (1987).
 41. Thies, E. & Mandelkow, E. M. Missorting of tau in neurons causes degeneration of synapses that can be rescued by the kinase MARK2/Par-1. *J. Neurosci.* **27**, 2896–2907 (2007).
 42. Hoover, B. R. *et al.* Tau Mislocalization to Dendritic Spines Mediates Synaptic Dysfunction Independently of Neurodegeneration. *Neuron* **68**, 1067–1081 (2010).
 43. Zempel, H. & Mandelkow, E. Lost after translation: missorting of Tau protein and consequences for Alzheimer disease. *Trends Neurosci.* **37**, 721–732 (2014).
 44. Biernat, J., Gustke, N., Drewes, G., Mandelkow, E. & Mandelkow, E. Phosphorylation of Ser262 strongly reduces binding of tau to microtubules: Distinction between PHF-like immunoreactivity and microtubule binding. *Neuron* **11**, 153–163 (1993).
 45. Usardi, A. *et al.* Tyrosine phosphorylation of tau regulates its interactions with Fyn SH2 domains, but not SH3 domains, altering the cellular localization of tau. *FEBS J.* **278**, 2927–2937 (2011).
 46. Noble, W., Hanger, D. P., Miller, C. C. J. & Lovestone, S. The importance of tau phosphorylation for neurodegenerative diseases. *Front. Neurol.* **4 JUL**, 1–11 (2013).
 47. Hanger, D. P., Anderton, B. H. & Noble, W. Tau phosphorylation: the therapeutic challenge for neurodegenerative disease. *Trends Mol. Med.* **15**, 112–119 (2009).
 48. Buchholz, S. & Zempel, H. The six brain-specific TAU isoforms and their role in Alzheimer's disease and related neurodegenerative dementia syndromes. *Alzheimer's Dement.* **20**, 3606–3628 (2024).

49. Wegmann, S., Biernat, J. & Mandelkow, E. A current view on Tau protein phosphorylation in Alzheimer's disease. *Curr. Opin. Neurobiol.* **69**, 131–138 (2021).
50. Drewes, G. *et al.* Mitogen activated protein (MAP) kinase transforms tau protein into an Alzheimer-like state. *EMBO J.* **11**, 2131–2138 (1992).
51. Mandelkow, E. M. *et al.* Glycogen synthase kinase-3 and the Alzheimer-like state of microtubule-associated protein tau. *FEBS Lett.* **314**, 315–321 (1992).
52. Baumann, K., Mandelkow, E. M., Biernat, J., Piwnica-Worms, H. & Mandelkow, E. Abnormal Alzheimer-like phosphorylation of tau-protein by cyclin-dependent kinases cdk2 and cdk5. *FEBS Lett.* **336**, 417–424 (1993).
53. Liu, F., Grundke-Iqbal, I., Iqbal, K. & Gong, C. X. Contributions of protein phosphatases PP1, PP2A, PP2B and PP5 to the regulation of tau phosphorylation. *Eur. J. Neurosci.* **22**, 1942–1950 (2005).
54. Oba, T. *et al.* Microtubule affinity-regulating kinase 4 with an Alzheimer's disease-related mutation promotes tau accumulation and exacerbates neurodegeneration. *J. Biol. Chem.* **295**, 17138–17147 (2020).
55. Bancher, C. *et al.* Accumulation of abnormally phosphorylated τ precedes the formation of neurofibrillary tangles in Alzheimer's disease. *Brain Res.* **477**, 90–99 (1989).
56. Evans, D. B. *et al.* Tau phosphorylation at serine 396 and serine 404 by human recombinant tau protein kinase II inhibits tau's ability to promote microtubule assembly. *J. Biol. Chem.* **275**, 24977–24983 (2000).
57. Allen, B. *et al.* Abundant tau filaments and neurodegeneration in mice transgenic for human P301S tau. *J. Neuropathol. Exp. Neurol.* **22**, 9340–9351 (2002).
58. Zheng-Fischhöfer, Q. *et al.* Sequential phosphorylation of Tau by glycogen synthase kinase-3 β and protein kinase A at Thr212 and Ser214 generates the Alzheimer-specific epitope of antibody AT100 and requires a paired-helical-filament-like conformation. *Eur. J. Biochem.* **252**, 542–552 (1998).
59. Šimić, G. *et al.* Tau protein hyperphosphorylation and aggregation in Alzheimer's disease and other tauopathies, and possible neuroprotective strategies. *Biomolecules* **6**, 2–28 (2016).
60. Köpke, E. *et al.* Microtubule-associated protein tau: Abnormal phosphorylation of a non-paired helical filament pool in Alzheimer disease. *J. Biol. Chem.* **268**, 24374–24384

- (1993).
61. Billingsley, M. L. & Kincaid, R. L. Regulated phosphorylation and dephosphorylation of tau protein: Effects on microtubule interaction, intracellular trafficking and neurodegeneration. *Biochem. J.* **323**, 577–591 (1997).
 62. Esmaeli-Azad, B., McCarty, J. H. & Feinstein, S. C. Sense and antisense transfection analysis of tau function: Tau influences net microtubule assembly, neurite outgrowth and neuritic stability. *J. Cell Sci.* **107**, 869–879 (1994).
 63. Hirokawa, N., Shiomura, Y. & Okabe, S. Tau proteins: the molecular structure and mode of binding on microtubules. *J. Cell Biol.* **107**, 1449–1459 (1988).
 64. Kempf, M., Clement, A., Faissner, A., Lee, G. & Brandt, R. Tau binds to the distal axon early in development of polarity in a microtubule- and microfilament-dependent manner. *J. Neurosci.* **16**, 5583–5592 (1996).
 65. Dixit, R., Ross, J. L., Goldman, Y. E. & Holzbaur, E. L. F. Differential Regulation of Dynein and. *Science (80-.)*. **319**, 1086–1089 (2008).
 66. Mondragón-Rodríguez, S. *et al.* Interaction of endogenous tau protein with synaptic proteins is regulated by N-methyl-D-aspartate receptor-dependent tau phosphorylation. *J. Biol. Chem.* **287**, 32040–32053 (2012).
 67. Ittner, L. M. *et al.* Dendritic Function of Tau Mediates Amyloid- β Toxicity in Alzheimer's Disease Mouse Models. *Cell* **142**, 387–397 (2010).
 68. A. Harada *et al.* Altered microtubule organization in small-calibre axons of mice lacking tau protein. *Nature* **369**, 488–490 (1994).
 69. Dawson, H. N. *et al.* Inhibition of neuronal maturation in primary hippocampal neurons from tau deficient mice. *J. Cell Sci.* **114**, 1179–1187 (2001).
 70. Ahmed, T. *et al.* Cognition and hippocampal synaptic plasticity in mice with a homozygous tau deletion. *Neurobiol. Aging* **35**, 2474–2478 (2014).
 71. Kimura, T. *et al.* Microtubule-associated protein tau is essential for long-term depression in the hippocampus. *Philos. Trans. R. Soc. B Biol. Sci.* **369**, (2014).
 72. Lopes, S. *et al.* Absence of Tau triggers age-dependent sciatic nerve morphofunctional deficits and motor impairment. *Aging Cell* **15**, 208–216 (2016).
 73. Spillantini, M. G. *et al.* Familial multiple system tauopathy with presenile dementia: A disease with abundant neuronal and glial tau filaments. *Proc. Natl. Acad. Sci. U. S. A.* **94**,

- 4113–4118 (1997).
74. Ferrer, I. *et al.* Glial and neuronal tau pathology in tauopathies: Characterization of disease-specific phenotypes and tau pathology progression. *J. Neuropathol. Exp. Neurol.* **73**, 81–97 (2014).
 75. Samudra, N., Lane-Donovan, C., VandeVrede, L. & Boxer, A. L. Tau pathology in neurodegenerative disease: disease mechanisms and therapeutic avenues. *J. Clin. Invest.* **133**, 1–10 (2023).
 76. Kovacs, G. G., Ghetti, B. & Goedert, M. Classification of diseases with accumulation of Tau protein. *Neuropathol. Appl. Neurobiol.* **48**, 1–10 (2022).
 77. Langerscheidt, F. *et al.* Genetic forms of tauopathies: inherited causes and implications of Alzheimer's disease-like TAU pathology in primary and secondary tauopathies. *J. Neurol.* **271**, 2992–3018 (2024).
 78. Goedert, M., Falcon, B., Zhang, W., Ghetti, B. & Scheres, S. H. W. Distinct conformers of assembled tau in Alzheimer's and Pick's diseases. *Cold Spring Harb. Symp. Quant. Biol.* **83**, 163–171 (2018).
 79. Caroppo, P., Prioni, S., Maderna, E., Grisoli, M. & Rossi, G. New MAPT variant in a FTD patient with Alzheimer's disease phenotype at onset. *Neurol. Sci.* **42**, 2111–2114 (2021).
 80. Hong, M. *et al.* Mutation-Specific Functional Impairments in Distinct Tau Isoforms of Hereditary FTDP-17. *Science (80-.)*. **282**, 1914–1917 (1998).
 81. Alonso, A. del C., Mederlyova, A., Novak, M., Grundke-Iqbal, I. & Iqbal, K. Promotion of Hyperphosphorylation by Frontotemporal Dementia Tau Mutations. *J. Biol. Chem.* **279**, 34873–34881 (2004).
 82. Rizzu, P. *et al.* High prevalence of mutations in the microtubule-associated protein tau in a population study of frontotemporal dementia in the Netherlands. *Am. J. Hum. Genet.* **64**, 414–421 (1999).
 83. Olszewska, D. A. *et al.* A clinical, molecular genetics and pathological study of a FTDP-17 family with a heterozygous splicing variant c.823-10G>T at the intron 9/exon 10 of the MAPT gene. *Neurobiol. Aging* **106**, 343.e1-343.e8 (2021).
 84. Tacik, P. *et al.* Clinicopathologic heterogeneity in frontotemporal dementia and parkinsonism linked to chromosome 17 (FTDP-17) due to microtubule-associated protein tau (MAPT) p.P301L mutation, including a patient with globular glial tauopathy.

- Neuropathol. Appl. Neurobiol.* **43**, 200–214 (2017).
85. Braak, H. & Braak, E. Neuropathological staging of Alzheimer-related changes. *Acta Neuropathol* 82239 - 259cta *Neuropathol* 82239 - 259 1–4 (1991)
doi:10.1109/ICINIS.2015.10.
 86. Haass, C., Kaether, C., Thinakaran, G. & Sisodia, S. Trafficking and proteolytic processing of APP. *Cold Spring Harb. Perspect. Med.* **2**, 1–25 (2012).
 87. Thinakaran, G. & Koo, E. H. Amyloid precursor protein trafficking, processing, and function. *J. Biol. Chem.* **283**, 29615–29619 (2008).
 88. Barrow, C. J., Yasuda, A., Kenny, P. T. M. & Zagorski, M. Solution conformations and aggregational properties of synthetic amyloid b-peptides of Alzheimer's disease. *J. Mol. Biol.* **225**, 1075–1093 (1992).
 89. Spires-Jones, T. L. & Hyman, B. T. The Intersection of Amyloid Beta and Tau at Synapses in Alzheimer's Disease. *Neuron* **82**, 756–771 (2014).
 90. Hellström-Lindahl, E., Viitanen, M. & Marutle, A. Comparison of A β levels in the brain of familial and sporadic Alzheimer's disease. *Neurochem. Int.* **55**, 243–252 (2009).
 91. Selkoe, dennis j & Hardy, J. The amyloid hypothesis of Alzheimer's disease at 25 years. *EMBO Mol. Med.* **8**, 595–608 (2016).
 92. Hardy, J. & Allsop, D. Amyloid deposition as the central event in the aetiology of Alzheimer's disease. *Trends Pharmacol. Sci.* **12**, 383–388 (1991).
 93. Hernández, F., Gómez de Barreda, E., Fuster-Matanzo, A., Lucas, J. J. & Avila, J. GSK3: A possible link between beta amyloid peptide and tau protein. *Exp. Neurol.* **223**, 322–325 (2010).
 94. Sahara, N. & Lewis, J. Amyloid precursor protein and tau transgenic models of Alzheimer's disease: Insights from the past and directions for the future. *Future Neurol.* **5**, 411–420 (2010).
 95. Bejanin, A. *et al.* Tau pathology and neurodegeneration contribute to cognitive impairment in Alzheimer's disease. *Brain* **140**, 3286–3300 (2017).
 96. Roberson, E. D. *et al.* Reducing endogenous tau ameliorates amyloid β -induced deficits in an Alzheimer's disease mouse model. *Science (80-.)*. **316**, 750–754 (2007).
 97. Zempel, H. *et al.* Amyloid- β oligomers induce synaptic damage via Tau-dependent microtubule severing by TTL6 and spastin. *EMBO J.* **32**, 2920–2937 (2013).

98. Bachmann, S. *et al.* Tau deficiency protects human neurons from Abeta-induced reduction of network activity. *Alzheimer's Dement.* **19**, 63601 (2023).
99. Zhang, Y., Wu, K.-M., Yang, L., Dong, Q. & Yu, J.-T. Tauopathies: new perspectives and challenges. *Mol. Neurodegener.* **17**, 28 (2022).
100. Logan, C. M. & Menko, A. S. Microtubules: Evolving roles and critical cellular interactions. *Exp. Biol. Med.* **244**, 1240–1254 (2019).
101. Mandelkow, E. & Mandelkow, E. M. Microtubule structure. *Curr. Opin. Struct. Biol.* **4**, 171–179 (1994).
102. Ledbetter, M. C. & Porter, K. R. A 'microtubule' in plant cell fine structure. *J. Cell Biol.* **19**, 239–250 (1963).
103. Desai, A. & Mitchison, T. J. Microtubule polymerization dynamics. *Annu. Rev. Cell Dev. Biol.* **13**, 83–117 (1997).
104. Hyman, A. A., Salser, S., Drechsel, D. N., Unwin, N. & Mitchison, T. J. Role of GTP hydrolysis in microtubule dynamics: Information from a slowly hydrolyzable analogue, GMPCPP. *Mol. Biol. Cell* **3**, 1155–1167 (1992).
105. Baas, P. W. & Lin, S. Orientation in the Neuron. *Dev Neurobiol.* **71**, 403–418 (2011).
106. Akhmanova, A. & Steinmetz, M. O. Control of microtubule organization and dynamics: Two ends in the limelight. *Nat. Rev. Mol. Cell Biol.* **16**, 711–726 (2015).
107. Sanchez, A. D. & Feldman, J. L. Microtubule-organizing centers: from the centrosome to non-centrosomal sites. *Curr. Opin. Cell Biol.* **44**, 93–101 (2017).
108. Vale, R. D. The molecular motor toolbox for intracellular transport. *Cell* **112**, 467–480 (2003).
109. Kelliher, M. T., Saunders, H. A. & Wildonger, J. Microtubule control of functional architecture in neurons. *Curr. Opin. Neurobiol.* **57**, 39–45 (2019).
110. Merriam, E. B. *et al.* Dynamic microtubules promote synaptic NMDA receptor-dependent spine enlargement. *PLoS One* **6**, 1–7 (2011).
111. Conde, C. & Cáceres, A. Microtubule assembly, organization and dynamics in axons and dendrites. *Nat. Rev. Neurosci.* **10**, 319–332 (2009).
112. Wilkes, O. R. & Moore, A. W. Distinct Microtubule Organizing Center Mechanisms Combine to Generate Neuron Polarity and Arbor Complexity. *Front. Cell. Neurosci.* **14**, 1–

- 11 (2020).
113. Sulimenko, V., Dráberová, E. & Dráber, P. γ -Tubulin in microtubule nucleation and beyond. *Front. Cell Dev. Biol.* **10**, 1–14 (2022).
 114. Sánchez-Huertas, C. *et al.* Non-centrosomal nucleation mediated by augmin organizes microtubules in post-mitotic neurons and controls axonal microtubule polarity. *Nat. Commun.* **7**, (2016).
 115. Baas, P. W., Deitch, J. S., Black, M. M. & Banker, G. A. Polarity orientation of microtubules in hippocampal neurons: Uniformity in the axon and nonuniformity in the dendrite. *Proc. Natl. Acad. Sci. U. S. A.* **85**, 8335–8339 (1988).
 116. Rolls, M. M. & Jegla, T. J. Neuronal polarity: An evolutionary perspective. *J. Exp. Biol.* **218**, 572–580 (2015).
 117. Hirokawa, N. *et al.* Kinesin associates with anterogradely transported membranous organelles in vivo. *J. Cell Biol.* **114**, 295–302 (1991).
 118. Hirokawa, N., Sato-Yoshitake, R., Yoshida, T. & Kawashima, T. Brain dynein (MAP1C) localizes on both anterogradely and retrogradely transported membranous organelles in vivo. *J. Cell Biol.* **111**, 1027–1037 (1990).
 119. Yau, K. W. *et al.* Dendrites In vitro and In vivo contain microtubules of opposite polarity and axon formation correlates with uniform plus-end-out microtubule orientation. *J. Neurosci.* **36**, 1071–1085 (2016).
 120. Jaworski, J. *et al.* Dynamic Microtubules Regulate Dendritic Spine Morphology and Synaptic Plasticity. *Neuron* **61**, 85–100 (2009).
 121. Hu, X., Viesselmann, C., Nam, S., Merriam, E. & Dent, E. W. Activity-dependent dynamic microtubule invasion of dendritic spines. *J. Neurosci.* **28**, 13094–13105 (2008).
 122. Dent, E. W. Of microtubules and memory: Implications for microtubule dynamics in dendrites and spines. *Mol. Biol. Cell* **28**, 1–8 (2017).
 123. Kuijpers, M. & Hoogenraad, C. C. Centrosomes, microtubules and neuronal development. *Mol. Cell. Neurosci.* **48**, 349–358 (2011).
 124. Marín, O., Valiente, M., Ge, X. & Tsai, L. Marín *t al.*, 2010.pdf. 1–20 (2010).
 125. Reiner, O. & Sapiro, T. Polarity regulation in migrating neurons in the cortex. *Mol. Neurobiol.* **40**, 1–14 (2009).

126. Murillo, B. & Mendes Sousa, M. Neuronal Intrinsic Regenerative Capacity: The Impact of Microtubule Organization and Axonal Transport. *Dev. Neurobiol.* **78**, 952–959 (2018).
127. Blanquie, O. & Bradke, F. Cytoskeleton dynamics in axon regeneration. *Curr. Opin. Neurobiol.* **51**, 60–69 (2018).
128. Fukushige, T., Hendzel, M. J., Bazett-Jones, D. P. & McGhee, J. D. Direct visualization of the elt-2 gut-specific GATA factor binding to a target promoter inside the living *Caenorhabditis elegans* embryo. *Proc. Natl. Acad. Sci. U. S. A.* **96**, 11883–11888 (1999).
129. L'Hernault, S. W. & Rosenbaum, J. L. Chlamydomonas α -tubulin is posttranslationally modified in the flagella during flagellar assembly. *J. Cell Biol.* **97**, 258–263 (1983).
130. Portran, D., Schaedel, L., Xu, Z., Théry, M. & Nachury, M. V. Tubulin acetylation protects long-lived microtubules against mechanical ageing. *Nat. Cell Biol.* **19**, 391–398 (2017).
131. Maruta, H., Greer, K. & Rosenbaum, J. L. The acetylation of alpha-tubulin and its relationship to the assembly and disassembly of microtubules. *J. Cell Biol.* **103**, 571–579 (1986).
132. Shida, T., Cueva, J. G., Xu, Z., Goodman, M. B. & Nachury, M. V. The major α -tubulin K40 acetyltransferase α TAT1 promotes rapid ciliogenesis and efficient mechanosensation. *Proc. Natl. Acad. Sci. U. S. A.* **107**, 21517–21522 (2010).
133. Hubbert, C. *et al.* HDAC6 is a microtubule-associated deacetylase. *Nature* **417**, 456–458 (2002).
134. Xu, Z. *et al.* Microtubules acquire resistance from mechanical breakage through intraluminal acetylation. *Science (80-.).* **356**, 328–332 (2017).
135. Balabanian, L., Berger, C. L. & Hendricks, A. G. Acetylated Microtubules Are Preferentially Bundled Leading to Enhanced Kinesin-1 Motility. *Biophys. J.* **113**, 1551–1560 (2017).
136. Reed, N. A. *et al.* Microtubule Acetylation Promotes Kinesin-1 Binding and Transport. *Curr. Biol.* **16**, 2166–2172 (2006).
137. Eshun-Wilson, L. *et al.* Effects of α -tubulin acetylation on microtubule structure and stability. *Proc. Natl. Acad. Sci. U. S. A.* **116**, 10366–10371 (2019).
138. Alper, J. D., Decker, F., Agana, B. & Howard, J. The Motility of Axonemal Dynein Is Regulated by the Tubulin Code. *Biophys. J.* **107**, 2872–2880 (2014).
139. Park, J. H. & Roll-Mecak, A. The tubulin code in neuronal polarity. *Curr. Opin. Neurobiol.*

- 51**, 95–102 (2018).
140. Aillaud, C. *et al.* Regulate Neuron Differentiation. *Science (80-.)*. **1453**, 1448–1453 (2017).
 141. Nieuwenhuis, J. *et al.* Vasohibins encode tubulin detyrosinating activity. *Science (80-.)*. **358**, 1453–1456 (2017).
 142. Landskron, L. *et al.* Posttranslational modification of microtubules by the MATCAP detyrosinase. *Science (80-.)*. **376**, (2022).
 143. Raybin, D. & Flavin, M. Enzyme Which Specifically Adds Tyrosine to the α Chain of Tubulin. *Biochemistry* **16**, 2189–2194 (1977).
 144. Kreis, T. E. Microtubules containing detyrosinated tubulin are less dynamic. *EMBO J.* **6**, 2597–2606 (1987).
 145. Bre, M. H., Kreis, T. E. & Karsenti, E. Control of microtubule nucleation and stability in Madin-Darby canine kidney cells: The occurrence of noncentrosomal, stable detyrosinated microtubules. *J. Cell Biol.* **105**, 1283–1296 (1987).
 146. Erck, C. *et al.* A vital role of tubulin-tyrosine-ligase for neuronal organization. *Proc. Natl. Acad. Sci. U. S. A.* **102**, 7853–7858 (2005).
 147. Marcos, S. *et al.* Tubulin tyrosination is required for the proper organization and pathfinding of the growth cone. *PLoS One* **4**, (2009).
 148. Peris, L. *et al.* Tubulin tyrosination regulates synaptic function and is disrupted in Alzheimer's disease. *Brain* **145**, 2486–2506 (2022).
 149. McKenney, R. J., Huynh, W., Vale, R. D. & Sirajuddin, M. Tyrosination of α -tubulin controls the initiation of processive dynein–dynactin motility. *EMBO J.* **35**, 1175–1185 (2016).
 150. Kaul, N., Soppina, V. & Verhey, K. J. Effects of α -tubulin K40 acetylation and detyrosination on kinesin-1 motility in a purified system. *Biophys. J.* **106**, 2636–2643 (2014).
 151. Liao, G. & Gundersen, G. G. Kinesin is a candidate for cross-bridging microtubules and intermediate filaments: Selective binding of kinesin to detyrosinated tubulin and vimentin. *J. Biol. Chem.* **273**, 9797–9803 (1998).
 152. Janke, C., Rogowski, K. & van Dijk, J. Polyglutamylolation: A fine-regulator of protein function? 'Protein Modifications: Beyond the Usual Suspects' Review Series. *EMBO Rep.*

- 9, 636–641 (2008).
153. Eddé, B. *et al.* Posttranslational Glutamylation of α -tubulin. *Science (80-.)*. **247**, 83–85 (1990).
 154. Janke, C. *et al.* Biochemistry: Tubulin polyglutamylase enzymes are members of the TTL domain protein family. *Science (80-.)*. **308**, 1758–1762 (2005).
 155. Wolff, A. *et al.* Distribution of glutamylated α and β -tubulin in mouse tissues using a specific monoclonal antibody, GT335. *Eur. J. Cell Biol.* **59**, 425–432 (1992).
 156. Lacroix, B. *et al.* Tubulin polyglutamylation stimulates spastin-mediated microtubule severing. *J. Cell Biol.* **189**, 945–954 (2010).
 157. Szczesna, E. *et al.* Combinatorial and antagonistic effects of tubulin glutamylation and glycylation on katanin microtubule severing. *Dev. Cell* **57**, 2497-2513.e6 (2022).
 158. Genova, M. *et al.* Tubulin polyglutamylation differentially regulates microtubule-interacting proteins. *EMBO J.* **42**, 1–17 (2023).
 159. Chen, J. & Roll-Mecak, A. Glutamylation is a negative regulator of microtubule growth. *Mol. Biol. Cell* **34**, 1–13 (2023).
 160. Valenstein, M. L. & Roll-Mecak, A. Graded Control of Microtubule Severing by Tubulin Glutamylation. *Cell* **164**, 911–921 (2016).
 161. Rogowski, K. *et al.* A family of protein-deglutamylating enzymes associated with neurodegeneration. *Cell* **143**, 564–578 (2010).
 162. Magiera, M. M. *et al.* Excessive tubulin polyglutamylation causes neurodegeneration and perturbs neuronal transport. *EMBO J.* **37**, 1–14 (2018).
 163. Bodakuntla, S., Janke, C. & Magiera, M. M. Tubulin polyglutamylation, a regulator of microtubule functions, can cause neurodegeneration. *Neurosci. Lett.* **746**, 135656 (2021).
 164. Grau, M. B. *et al.* Tubulin glycylation and glutamylases have distinct functions in stabilization and motility of ependymal cilia. *J. Cell Biol.* **202**, 441–451 (2013).
 165. Redeker, V. *et al.* Polyglycylation of Tubulin: a Posttranslational Modification in Axonemal Microtubules. *Science (80-.)*. **266**, 1688–1691 (1994).
 166. Kubo, T., Sasaki, R. & Oda, T. Tubulin glycylation controls ciliary motility through modulation of outer-arm dyneins. *Mol. Biol. Cell* **35**, 1–13 (2024).
 167. Rocha, C. *et al.* Tubulin glycylation is required for primary cilia, control of cell

- proliferation and tumor development in colon. *EMBO J.* **33**, 2247–2260 (2014).
168. Fourest-Lieuvin, A. *et al.* Microtubule Regulation in Mitosis: Tubulin Phosphorylation by the Cyclin-dependent Kinase Cdk1. *Mol. Biol. Cell* **17**, 1041–1050 (2006).
169. Jaglin, X. H. *et al.* Mutations in the B-tubulin gene TUBB2B result in asymmetrical polymicrogyria. *Nat. Genet.* **41**, 746–752 (2009).
170. Caudron, F. *et al.* Mutation of ser172 in yeast β tubulin induces defects in microtubule dynamics and cell division. *PLoS One* **5**, (2010).
171. Zambito, A. M. & Wolff, J. Palmitoylation of tubulin. *Biochem. Biophys. Res. Commun.* **239**, 650–654 (1997).
172. Caron, J. M. Posttranslational modification of tubulin by palmitoylation: I. In vivo and cell-free studies. *Mol. Biol. Cell* **8**, 621–636 (1997).
173. Fang, C. T. *et al.* Inhibition of acetyl-CoA carboxylase impaired tubulin palmitoylation and induced spindle abnormalities. *Cell Death Discov.* **9**, (2023).
174. Wenqing, L. I. *et al.* Palmitoylome profiling indicates that androgens regulate the palmitoylation of α -tubulin in prostate cancer-derived LNCaP cells and supernatants. *Oncol. Rep.* **42**, 2788–2796 (2019).
175. Janke, C. & Magiera, M. M. The tubulin code and its role in controlling microtubule properties and functions. *Nat. Rev. Mol. Cell Biol.* **21**, 307–326 (2020).
176. Bodakuntla, S., Jijumon, A. S., Villablanca, C., Gonzalez-Billault, C. & Janke, C. Microtubule-Associated Proteins: Structuring the Cytoskeleton. *Trends Cell Biol.* **29**, 804–819 (2019).
177. Caceres, A., Banker, G., Steward, O., Binder, L. & Payne, M. MAP2 is localized to the dendrites of hippocampal neurons which develop in culture. *Dev. Brain Res.* **13**, 314–318 (1984).
178. Harada, A., Teng, J., Takei, Y., Oguchi, K. & Hirokawa, N. MAP2 is required for dendrite elongation, PKA anchoring in dendrites, and proper PKA signal transduction. *J. Cell Biol.* **158**, 541–549 (2002).
179. Brady, S. T. & Morfini, G. A. Regulation of motor proteins, axonal transport deficits and adult-onset neurodegenerative diseases. *Neurobiol. Dis.* **105**, 273–282 (2017).
180. Hirokawa, N. & Takemura, R. Biochemical and molecular characterization of diseases linked to motor proteins. *Trends Biochem. Sci.* **28**, 558–565 (2003).

181. Vale, R. D. Severing of stable microtubules by a mitotically activated protein in xenopus egg extracts. *Cell* **64**, 827–839 (1991).
182. Roll-Mecak, A. & Vale, R. D. Structural basis of microtubule severing by the hereditary spastic paraplegia protein spastin. *Nature* **451**, 363–367 (2008).
183. Sharp, D. J. & Ross, J. L. Microtubule-severing enzymes at the cutting edge. *J. Cell Sci.* **125**, 2561–2569 (2012).
184. Trotta, N., Orso, G., Rossetto, M. G., Daga, A. & Broadie, K. The Hereditary Spastic Paraplegia Gene, spastin, Regulates Microtubule Stability to Modulate Synaptic Structure and Function. *Curr. Biol.* **14**, 1135–1147 (2004).
185. Errico, A., Ballabio, A. & Rugarli, E. I. Spastin, the protein mutated in autosomal dominant hereditary spastic paraplegia, is involved in microtubule dynamics. *Hum. Mol. Genet.* **11**, 153–163 (2002).
186. Solowska, J. M. *et al.* Pathogenic mutation of spastin has gain-of-function effects on microtubule dynamics. *J. Neurosci.* **34**, 1856–1867 (2014).
187. Ferreirinha, F. *et al.* Axonal degeneration in paraplegin-deficient mice is associated with abnormal mitochondria and impairment of axonal transport. *J. Clin. Invest.* **113**, 231–242 (2004).
188. Cash, A. D. *et al.* Microtubule reduction in Alzheimer's disease and aging is independent of τ filament formation. *Am. J. Pathol.* **162**, 1623–1627 (2003).
189. Zhang, F. *et al.* Posttranslational modifications of α -tubulin in alzheimer disease. *Transl. Neurodegener.* **4**, 1–9 (2015).
190. Alonso, A. D. C., Grundke-Iqbal, I., Barra, H. S. & Iqbal, K. Abnormal phosphorylation of tau and the mechanism of Alzheimer neurofibrillary degeneration: Sequestration of microtubule-associated proteins 1 and 2 and the disassembly of microtubules by the abnormal tau. *Proc. Natl. Acad. Sci. U. S. A.* **94**, 298–303 (1997).
191. I. Mota, S., L. Ferreira, I., Pereira, C., R. Oliveira, C. & Cristina Rego, A. Amyloid-Beta Peptide 1-42 Causes Microtubule Deregulation through N-methyl-D-aspartate Receptors in Mature Hippocampal Cultures. *Curr. Alzheimer Res.* **9**, 844–856 (2012).
192. Brandt, R. & Bakota, L. Microtubule dynamics and the neurodegenerative triad of Alzheimer's disease: The hidden connection. *J. Neurochem.* **143**, 409–417 (2017).
193. Zempel, H., Thies, E., Mandelkow, E. & Mandelkow, E. M. A β oligomers cause localized

- Ca²⁺ elevation, missorting of endogenous Tau into dendrites, Tau phosphorylation, and destruction of microtubules and spines. *J. Neurosci.* **30**, 11938–11950 (2010).
194. Al Kabbani, M. A., Köhler, C. & Zempel, H. Effects of P301L-TAU on post-translational modifications of microtubules in human iPSC-derived cortical neurons and TAU transgenic mice. *Neural Regen. Res.* **20**, 2348–2360 (2024).
195. Brion, J. P. *et al.* Neurofibrillary tangles and tau phosphorylation. *Biochem. Soc. Symp.* **67**, 81–88 (2001).
196. Godena, V. K. *et al.* Increasing microtubule acetylation rescues axonal transport and locomotor deficits caused by LRRK2 Roc-COR domain mutations. *Nat. Commun.* **5**, (2014).
197. D'Ydewalle, C. *et al.* HDAC6 inhibitors reverse axonal loss in a mouse model of mutant HSPB1-induced Charcot-Marie-Tooth disease. *Nat. Med.* **17**, 968–974 (2011).
198. Uchida, S. *et al.* Learning-induced and stathmin-dependent changes in microtubule stability are critical for memory and disrupted in ageing. *Nat. Commun.* **5**, (2014).
199. Qu, X. *et al.* Stabilization of dynamic microtubules by mDia1 drives Tau-dependent A β 1-42 synaptotoxicity. *J. Cell Biol.* **216**, 3161–3178 (2017).
200. Vu, H. T., Akatsu, H., Hashizume, Y., Setou, M. & Ikegami, K. Increase in α -tubulin modifications in the neuronal processes of hippocampal neurons in both kainic acid-induced epileptic seizure and Alzheimer's disease. *Sci. Rep.* **7**, 1–14 (2017).
201. Shashi, V. *et al.* Loss of tubulin deglutamylase CCP 1 causes infantile-onset neurodegeneration. *EMBO J.* **37**, 1–12 (2018).
202. Janke, C. & Bulinski, J. C. Post-translational regulation of the microtubule cytoskeleton: Mechanisms and functions. *Nat. Rev. Mol. Cell Biol.* **12**, 773–786 (2011).
203. Rogowski, K. *et al.* Evolutionary Divergence of Enzymatic Mechanisms for Posttranslational Polyglycylation. *Cell* **137**, 1076–1087 (2009).
204. Wloga, D., Joachimiak, E. & Fabczak, H. Tubulin post-translational modifications and microtubule dynamics. *Int. J. Mol. Sci.* **18**, (2017).
205. van Dijk, J. *et al.* A Targeted Multienzyme Mechanism for Selective Microtubule Polyglutamylation. *Mol. Cell* **26**, 437–448 (2007).
206. Regnard, C., Desbruyères, E., Denoulet, P. & Eddé, B. Tubulin polyglutamylase: Isozymic variants and regulation during the cell cycle in HeLa cells. *J. Cell Sci.* **112**,

- 4281–4289 (1999).
207. Bodakuntla, S. *et al.* Distinct roles of α - and β -tubulin polyglutamylation in controlling axonal transport and in neurodegeneration. *EMBO J.* **40**, 1–15 (2021).
208. Berezniuk, I. *et al.* Cytosolic carboxypeptidase 1 is involved in processing α - and β -tubulin. *J. Biol. Chem.* **287**, 6503–6517 (2012).
209. Aiken, J. & Holzbaur, E. L. F. Spastin locally amplifies microtubule dynamics to pattern the axon for presynaptic cargo delivery. *Curr. Biol.* **34**, 1687-1704.e8 (2024).
210. Kuo, Y. W., Trottier, O., Mahamdeh, M. & Howard, J. Spastin is a dual-function enzyme that severs microtubules and promotes their regrowth to increase the number and mass of microtubules. *Proc. Natl. Acad. Sci. U. S. A.* **116**, 5533–5541 (2019).
211. Ping, Y. *et al.* Tubulin Polyglutamylation by TTLL1 and TTLL7 Regulate Glutamate Concentration in the Mice Brain. *Biomolecules* **13**, 1–20 (2023).
212. Ikegami, K. *et al.* TTLL7 is a mammalian β -tubulin polyglutamylase required for growth of MAP2-positive neurites. *J. Biol. Chem.* **281**, 30707–30716 (2006).
213. Ikegami, K. *et al.* Loss of α -tubulin polyglutamylation in ROSA22 mice is associated with abnormal targeting of KIF1A and modulated synaptic function. *Proc. Natl. Acad. Sci. U. S. A.* **104**, 3213–3218 (2007).
214. Vogel, P., Hansen, G., Fontenot, G. & Read, R. Tubulin tyrosine ligase-like 1 deficiency results in chronic rhinosinusitis and abnormal development of spermatid flagella in mice. *Vet. Pathol.* **47**, 703–712 (2010).
215. Ikegami, K., Sato, S., Nakamura, K., Ostrowski, L. E. & Setou, M. Tubulin polyglutamylation is essential for airway ciliary function through the regulation of beating asymmetry. *Proc. Natl. Acad. Sci. U. S. A.* **107**, 10490–10495 (2010).
216. Suryavanshi, S. *et al.* Tubulin Glutamylation Regulates Ciliary Motility by Altering Inner Dynein Arm Activity. *Curr. Biol.* **20**, 435–440 (2010).
217. Zadra, I. *et al.* Chromosome segregation fidelity requires microtubule polyglutamylation by the cancer downregulated enzyme TTLL11. *Nat. Commun.* **13**, (2022).
218. Audebert, S. *et al.* Developmental regulation of polyglutamylated α - and β -tubulin in mouse brain neurons. *J. Cell Sci.* **107**, 2313–2322 (1994).
219. Wang, T. & Morgan, J. I. The Purkinje cell degeneration (pcd) mouse: An unexpected molecular link between neuronal degeneration and regeneration. *Brain Res.* **1140**, 26–40

- (2007).
220. Wu, H. Y. *et al.* TTLL1 and TTLL4 polyglutamylases are required for the neurodegenerative phenotypes in pcd mice. *PLoS Genet.* **18**, 1–25 (2022).
 221. Hausrat, T. J. *et al.* Disruption of tubulin-alpha4a polyglutamylation prevents aggregation of hyper-phosphorylated tau and microglia activation in mice. *Nat. Commun.* **13**, 1–18 (2022).
 222. Bedoni, N. *et al.* Mutations in the polyglutamylase gene TTLL5, expressed in photoreceptor cells and spermatozoa, are associated with cone-rod degeneration and reduced male fertility. *Hum. Mol. Genet.* **25**, 4546–4555 (2016).
 223. Oh, J. K. *et al.* Expanding the phenotype of TTLL5-associated retinal dystrophy: a case series. *Orphanet J. Rare Dis.* **17**, 1–10 (2022).
 224. Wagenaar, M. *et al.* Hearing impairment related to age in Usher syndrome types 1B and 2A. *Arch. Otolaryngol. - Head Neck Surg.* **125**, 441–445 (1999).
 225. Sergouniotis, P. I. *et al.* Biallelic variants in TTLL5, encoding a tubulin glutamylase, cause retinal dystrophy. *Am. J. Hum. Genet.* **94**, 760–769 (2014).
 226. Konno, A. *et al.* Ttll9^{-/-} mice sperm flagella show shortening of doublet 7, reduction of doublet 5 polyglutamylation and a stall in beating. *J. Cell Sci.* **129**, 2757–2766 (2016).
 227. Deshpande, A. *et al.* TTLL12 has a potential oncogenic activity, suppression of ligation of nitrotyrosine to the C-terminus of detyrosinated α -tubulin, that can be overcome by molecules identified by screening a compound library. *PLoS One* **19**, 1–21 (2024).
 228. Zhang, Y., Chen, H., Li, R., Sterling, K. & Song, W. Amyloid β -based therapy for Alzheimer's disease: challenges, successes and future. *Signal Transduct. Target. Ther.* **8**, 248 (2023).
 229. Jean, D. C. & Baas, P. W. It cuts two ways: Microtubule loss during Alzheimer disease. *EMBO J.* **32**, 2900–2902 (2013).
 230. Ballatore, C. *et al.* Microtubule stabilizing agents as potential treatment for alzheimer's disease and related neurodegenerative tauopathies. *J. Med. Chem.* **55**, 8979–8996 (2012).
 231. Varidaki, A., Hong, Y. & Coffey, E. T. Repositioning microtubule stabilizing drugs for brain disorders. *Front. Cell. Neurosci.* **12**, 1–15 (2018).
 232. Wang, D., Tai, P. W. L. & Gao, G. Adeno-associated virus vector as a platform for gene

- therapy delivery. *Nat. Rev. Drug Discov.* **18**, 358–378 (2019).
233. Al Kabbani, M. A., Wunderlich, G., Köhler, C. & Zempel, H. AAV-based gene therapy approaches for genetic forms of tauopathies and related neurogenetic disorders. *Biocell* **46**, 847–853 (2022).
234. Dubey, J., Ratnakaran, N. & Koushika, S. P. Neurodegeneration and microtubule dynamics: Death by a thousand cuts. *Front. Cell. Neurosci.* **9**, 1–15 (2015).
235. Götz, J., Chen, F., Barmettler, R. & Nitsch, R. M. Tau filament formation in transgenic mice expressing P301L tau. *J. Biol. Chem.* **276**, 529–534 (2001).
236. Köhler, C., Dinekov, M. & Götz, J. Active glycogen synthase kinase-3 and tau pathology-related tyrosine phosphorylation in pR5 human tau transgenic mice. *Neurobiol. Aging* **34**, 1369–1379 (2013).
237. Deters, N., Ittner, L. M. & Götz, J. Divergent phosphorylation pattern of tau in P301L tau transgenic mice. *Eur. J. Neurosci.* **28**, 137–147 (2008).
238. Pennanen, L., Wolfer, D. P., Nitsch, R. M. & Götz, J. Impaired spatial reference memory and increased exploratory behavior in P301L tau transgenic mice. *Genes, Brain Behav.* **5**, 369–379 (2006).
239. Pennanen, L., Welzl, H., D’Adamo, P., Nitsch, R. M. & Götz, J. Accelerated extinction of conditioned taste aversion in P301L tau transgenic mice. *Neurobiol. Dis.* **15**, 500–509 (2004).
240. Wang, C. *et al.* Scalable Production of iPSC-Derived Human Neurons to Identify Tau-Lowering Compounds by High-Content Screening. *Stem Cell Reports* **9**, 1221–1233 (2017).
241. El-Agnaf, O. M. A., Mahil, D. S., Patel, B. P. & Austen, B. M. Oligomerization and toxicity of β -amyloid-42 implicated in Alzheimer’s disease. *Biochem. Biophys. Res. Commun.* **273**, 1003–1007 (2000).
242. Zhang, Y., McLaughlin, R., Goodyer, C. & LeBlanc, A. Selective cytotoxicity of intracellular amyloid β peptide1-42 through p53 and Bax in cultured primary human neurons. *J. Cell Biol.* **156**, 519–529 (2002).
243. Kuperstein, I. *et al.* Neurotoxicity of Alzheimer’s disease A β peptides is induced by small changes in the A β 42 to A β 40 ratio. *EMBO J.* **29**, 3408–3420 (2010).
244. Roselli, F., Hutzler, P., Wegerich, Y., Livrea, P. & Almeida, O. F. X. Disassembly of shank

- and homer synaptic clusters is driven by soluble b-amyloid 1-40 through divergent NMDAR-dependent signalling pathways. *PLoS One* **4**, 1–12 (2009).
245. Rogowski, K., Hached, K., Crozet, C. & van der Laan, S. Tubulin modifying enzymes as target for the treatment ofttau-related diseases. *Pharmacol. Ther.* **218**, 107681 (2021).
 246. Rodriguez-Calado, S. *et al.* Proximity Mapping of CCP6 Reveals Its Association with Centrosome Organization and Cilium Assembly. *Int. J. Mol. Sci.* **24**, (2023).
 247. Mahalingan, K. K. *et al.* Structural basis for polyglutamate chain initiation and elongation by TTL family enzymes. *Nat. Struct. Mol. Biol.* **27**, 802–813 (2020).
 248. Warren, C. *et al.* Dynamic intramolecular regulation of the histone chaperone nucleoplamin controls histone binding and release. *Nat. Commun.* **8**, (2017).
 249. Regnard, C. *et al.* Polyglutamylation of nucleosome assembly proteins. *J. Biol. Chem.* **275**, 15969–15976 (2000).
 250. Praprotnik, D., Smith, M. A., Richey, P. L., Vinters, H. V. & Perry, G. Filament heterogeneity within the dystrophic neurites of senile plaques suggests blockage of fast axonal transport in Alzheimer's disease. *Acta Neuropathol.* **91**, 226–235 (1996).
 251. Stokin, G. B. *et al.* Axonopathy and transport deficits early in the pathogenesis of Alzheimer's diseases. *Science (80-.)*. **307**, 1282–1288 (2005).
 252. Sahara, N. & Yanai, R. Limitations of human tau-expressing mouse models and novel approaches of mouse modeling for tauopathy. *Front. Neurosci.* **17**, (2023).
 253. Wenger, K. *et al.* Common mouse models of tauopathy reflect early but not late human disease. *Mol. Neurodegener.* **18**, 1–15 (2023).
 254. De Leeuw, S. & Tackenberg, C. Alzheimer's in a dish - Induced pluripotent stem cell-based disease modeling. *Transl. Neurodegener.* **8**, 1–13 (2019).
 255. Lin, W. *et al.* Dendritic spine formation and synapse maturation in transcription factor-induced human iPSC-derived neurons. *iScience* **26**, 106285 (2023).
 256. Hedegaard, A. *et al.* Pro-maturational Effects of Human iPSC-Derived Cortical Astrocytes upon iPSC-Derived Cortical Neurons. *Stem Cell Reports* **15**, 38–51 (2020).
 257. Batenburg, K. L. *et al.* A Human Neuron/Astrocyte Co-culture to Model Seeded and Spontaneous Intraneuronal Tau Aggregation. *Curr. Protoc.* **3**, 1–29 (2023).
 258. Stöberl, N., Maguire, E., Salis, E., Shaw, B. & Hall-Roberts, H. Human iPSC-derived glia

- models for the study of neuroinflammation. *J. Neuroinflammation* **20**, 1–20 (2023).
259. Urrestizala-Arenaza, N., Cerchio, S., Cavaliere, F. & Magliaro, C. Limitations of human brain organoids to study neurodegenerative diseases: a manual to survive. *Front. Cell. Neurosci.* **18**, (2024).

6. Appendix

6.1 Article 1

Al Kabbani, M. A., Wunderlich, G., Köhler, C. & Zempel, H. (2022) AAV-based gene therapy approaches for genetic forms of tauopathies and related neurogenetic disorders. *Biocell*. 46: 847–853. doi: 10.32604/biocell.2022.018144.

AAV-based gene therapy approaches for genetic forms of tauopathies and related neurogenetic disorders

MOHAMED AGHYAD AL KABBANI^{1,2}; GILBERT WUNDERLICH^{3,4}; CHRISTOPH KÖHLER⁵; HANS ZEMPEL^{1,2,*}

¹ Faculty of Medicine and University Hospital Cologne, Institute of Human Genetics, University of Cologne, Cologne, 50931, Germany

² Faculty of Medicine and University Hospital Cologne, Center for Molecular Medicine Cologne (CMMC), University of Cologne, Cologne, 50931, Germany

³ Faculty of Medicine and University Hospital Cologne, Department of Neurology, University of Cologne, Cologne, 50937, Germany

⁴ Faculty of Medicine and University Hospital Cologne, Center for Rare Diseases, University of Cologne, Cologne, 50937, Germany

⁵ Faculty of Medicine and University Hospital Cologne, Center Anatomy, Department of Molecular and Translational Neuroscience, University of Cologne, Cologne, 50931, Germany

Key words: Tauopathies, Neurogenetic diseases, AAV-based gene therapy, Neurodegeneration, Alzheimer disease, TAU

Abstract: Tauopathies comprise a spectrum of genetic and sporadic neurodegenerative diseases mainly characterized by the presence of hyperphosphorylated TAU protein aggregations in neurons or glia. Gene therapy, in particular adeno-associated virus (AAV)-based, is an effective medical approach for difficult-to-treat genetic diseases for which there are no convincing traditional therapies, such as tauopathies. Employing AAV-based gene therapy to treat, in particular, genetic tauopathies has many potential therapeutic benefits, but also drawbacks which need to be addressed in order to successfully and efficiently adapt this still unconventional therapy for the various types of tauopathies. In this Viewpoint, we briefly introduce some potentially treatable tauopathies, classify them according to their etiology, and discuss the potential advantages and possible problems of AAV-based gene therapy. Finally, we outline a future vision for the application of this promising therapeutic approach for genetic and sporadic tauopathies.

Abbreviations

AAV:	Adeno-associated virus
AD:	Alzheimer's Disease
AGD:	Argyrophilic Grain Disease
ASO:	Antisense oligonucleotide
CBD:	Corticobasal Degeneration
CDK5:	Cyclin-dependent kinase 5
CNS:	Central nervous system
DM:	Myotonic Dystrophy
ELISA:	Enzyme-linked Immunosorbent Assay
FDA:	US Food and Drug Administration
FTLD-TAU:	Frontotemporal Lobar Degeneration with Tauopathy
GoF:	Gain-of-function
iPSCs:	Induced Pluripotent Stem Cells
ITR:	Inverted terminal repeats
LoF:	Loss-of-function

MAP:	Microtubule-associated proteins
PiD:	Pick's Disease
PSP:	Progressive Supranuclear Palsy
rAAV:	Recombinant adeno-associated virus
RNAi:	RNA interference
RPE65:	Retinal-pigment epithelium-specific-65-kDa-protein
scAAV:	Self-complementary AAV
shRNA:	Short hairpin RNA
siRNA:	Small interfering RNA
VUS:	Variant of unknown significance

Introduction

TAU is a microtubule binding protein encoded in humans by the gene MAPT, which is alternatively spliced to produce eight isoforms, six of which are expressed in the human central nervous system (CNS). Under normal conditions, TAU is sorted into the axons likely due to several sorting mechanisms (Zempel and Mandelkow, 2019), where it promotes microtubule assembly and stability. However, in disease conditions (e.g., Alzheimer's Disease (AD), pathological TAU

*Address correspondence to: Hans Zempel, hans.zempel@uk-koeln.de; hzempel@uni-koeln.de

Received: 02 July 2021; Accepted: 03 September 2021



mutations, etc.) these sorting mechanisms malfunction, which leads to mislocalization of TAU into the soma and dendrites. Under pathological conditions, TAU missorting is associated with TAU hyperphosphorylation and subsequent dissociation from microtubules. Hyperphosphorylated TAU can form insoluble aggregates called neurofibrillary tangles, the hallmark of several neurodegenerative diseases known collectively as tauopathies, the most frequent of which is AD (Zempel and Mandelkow, 2014).

Tauopathies encompass a spectrum of neurodegenerative diseases whose main feature is the presence of aggregated deposits of TAU protein in the form of neurofibrillary or gliofibrillary tangles (Goedert and Spillantini, 2017). Most tauopathies present clinically as syndromes of cognitive deterioration or movement disorders, or both (Murley et al., 2020). Several systems to classify tauopathies have been proposed, but the diversity of their etiologies, pathomechanisms and phenotypes leads to overlapping classifications. The distinction between primary and secondary tauopathies is often blurry, as in the case of AD, which is traditionally classified as a secondary tauopathy, but mounting evidence suggests a central role of TAU pathology in driving the pathomechanisms of the disease. Only 1–2% of AD cases are familial, presenting a clear genetic inheritance, and while the causes of the rest of AD cases are poorly understood, the disease starts almost universally with the accumulation of A β plaques and TAU tangles in the brain, leading to neurodegeneration and loss of cognitive function (Long and Holtzman, 2019). Moreover, imbalanced or altered isoform expression alone of TAU can be causative for an AD-like form of Frontotemporal Dementia (FTD), Frontotemporal Lobar Degeneration with tauopathy (FTLD-TAU), and is observed in several FTD-associated tauopathies, i.a. Progressive Supranuclear Palsy (PSP), Corticobasal Degeneration (CBD), Pick's Disease (PiD), Argyrophilic Grain Disease (AGD) (Park et al., 2016). Here, we subdivide major tauopathies into either *genetic* diseases, in which proven inherited genetic mutations are the cause of the disease, or *sporadic* or *idiopathic* diseases, in which clear genetic causes are absent (Table 1) (For a more extensive list see Zimmer-Bensch and Zempel, 2021), and outline potential AAV-based gene therapy approaches.

Gene therapy aims to correct a genetic problem at its roots, and focuses on gene modification to treat genetic diseases by repairing or suppressing defective genes or reintroducing functional ones (Kaji and Leiden, 2001). The delivery of the therapeutic genetic material is usually achieved via vectors, the majority of which are of viral origin, although other non-viral methods do exist (e.g., naked DNA, electroporation, lipoplexes, etc.), albeit with reduced levels of transfection and therapeutic efficiency (Ramamoorth and Narvekar, 2015).

As of 2021, over 3,180 gene therapy clinical trials were conducted, with more than half of them in phase I. In 263 of these trials (approximately 8.3% of the total number of gene therapy clinical trials), AAV has been used as the vector of choice for gene transfer, with 24 trials relevant to neurogenetic diseases (Gene Therapy Clinical Trials Worldwide Database. The Journal of Gene Medicine. Wiley 2021). Following the approval of Spark Therapeutics' Luxturna (for the treatment of Retinal-pigment epithelium-specific-65-kDa-protein(RPE65)-mutation-induced blindness/retinitis pigmentosa) by the U.S.

Food and Drug Administration (FDA) in 2017 as the first AAV vector-based gene therapy, several gene therapies have also received FDA approval, with Novartis' Zolgensma (to treat spinal muscular atrophy) being the second FDA-approved AAV-based gene therapy.

The recombinant adeno-associated virus (rAAV) is the standard vehicle of choice when it comes to AAV-based gene therapy, renowned for its safety and efficacy. It is a 4.8 kb single-stranded DNA virus that comprises two inverted terminal repeats (ITR) framing the expression cassette, which contains either a constitutive or a tissue-specific promoter that drives the transgene expression, and a polyA sequence (Le Bec and Douar, 2006).

The current line of treatment for tauopathies is generally supportive, aiming at symptom alleviation. A variety of efforts have been made to develop drugs that manipulate TAU post translational modifications or aggregation, or target TAU immunologically via antibodies, but most of these trials have shown varying, and sometimes disappointing, levels of success (Coughlin and Irwin, 2017). The promise of gene therapy is to cure the disease, improve symptoms, and stop disease progression. Several studies have demonstrated that TAU knockout mice have no obvious phenotype, with Microtubule-associated proteins (MAP)/microtubule functions being preserved probably via compensation by upregulation of other MAPs (van Hummel et al., 2016). Therapeutically, reducing TAU levels or its toxic gain-of-function can be achieved by inhibiting TAU translation or even by inducing alternative splicing in favor of one isoform or the other, *via* the use of small interfering RNA fragments (siRNA) or antisense oligonucleotides (ASOs) (DeVos et al., 2017; Sud et al., 2014; Xu et al., 2014). While potentially promising, delivery of siRNA and ASOs remains challenging, and effects are limited to a few weeks or months, requiring several administrations per year. Viral vectors, such as AAV, can present an optimal medium to deliver not only RNAi (RNA interference), but also serve as a vector for gene replacement therapy with long lasting expression.

Viewpoint

With approximately 150 clinical trials completed (~50% with met clinical safety and endpoints), more than 3000 treated patients, only 9 serious adverse events and no related deaths (Kuzmin et al., 2021), AAVs are the best choice for difficult-to-treat neurological disorders, like genetic forms of tauopathy. AAVs are not pathogenic, and some of their serotypes have a natural tropism for the CNS (Serotypes 4, 5, 8, 9). Also, AAV expression can persist for decades in neurons and other long lasting cells like cardiomyocytes (which is relevant for tauopathies that also affect the heart, e.g., Myotonic Dystrophy (DM) type 1 and 2), unlike mitotically active cells in which AAV expression is lost overtime (Sun and Roy, 2021). Tauopathies with clear genetic causes would be prime targets for AAV-based gene therapy; similar approaches have been tested in animal models of other neurodegenerative diseases like Huntington's disease (Franich et al., 2008), and AAV2/8 have already been used to deliver anti-TAU antibodies into the brain of P301S-tg-mice, a model of frontotemporal dementia (Ising et al., 2017).

TABLE 1

List of noteworthy examples of tauopathies with (epi)genetic etiologies or risk factors (Adapted from Zimmer-Bensch and Zempel (2021))

Disease entity	Clinical description	Etiology	Potential Gene therapy approaches	Tested species/Major findings
Familial FTLT-TAU	Very heterogeneous group of age-related tauopathies, including formerly FTDP17(t) and patients diagnosed with PSP	Genetic: MAPT	AAV-based silencing of MAPT (Wegmann <i>et al.</i> , 2021)	Mouse: TAU reduction rescues neuronal damage
Other forms of FTLT-TAU (like tauopathies)	Heterogenous group of age-related tauopathies, like CBD, PiD, AGD and others, most of which are further subclassified	Sporadic, (epi)genetic causes unclear	Antisense-mediated exon skipping (Sud <i>et al.</i> , 2014)	Human neuroblastoma cell lines, Mouse: Reduced TAU protein levels up to 80%, reduced susceptibility to seizures
Progressive supranuclear palsy (PSP)	Rare neurodegenerative disorder, but a common atypical Parkinson's syndrome with cognitive, motor, behavior and language abnormalities, often misdiagnosed as AD	Epigenetic: Hypomethylation of MAPT Genetic: MAPT Sporadic: GWAS with loci close to MAPT, STX6, EIF2AK3, MOBP, DUSP, SLCO1A2, RUNX2, i.a.	AAV-mediated silencing of MAPT (Wegmann <i>et al.</i> , 2021)	Mouse: TAU reduction rescues neuronal damage
Myotonic Dystrophy (DM)	Muscular dystrophy, often accompanied by intellectual disability, cardiac arrhythmia, endocrine disorders, and cataracts	Genetic: Type 1: DMPK Type 2: CNBP Mutations leading to repeat expansions	AAV-delivered RNAi-targeting of mRNA containing the expanded repeat (Bisset <i>et al.</i> , 2015)	Mouse: Reduced disease pathology in muscles
Familial Alzheimer Disease	Age of onset usually between 40 and 70 years, fast progression	Genetic: APP, PSEN1, PSEN2, up to ~75 risk modifying genes	AAV-delivered CRISPR/Cas9 mediated disruption of mutated APP (György <i>et al.</i> , 2018), AAV-delivered antibodies targeting A β (Kou <i>et al.</i> , 2011), AAV-based expression of APP _{sA} (Fol <i>et al.</i> , 2016)	Mouse: Decreased pathogenic A β and plaque load, restored synaptic plasticity and rescued spine density deficits, enhanced memory
Niemann Pick Disease Type C	Lysosomal storage disease with hepatosplenomegaly, progressive dementia, ataxia, spasticity, and premature death ranging from infancy to late adulthood	Genetic: NPC1, NPC2	AAV delivery of NPC1 or 2 gene (Chandler <i>et al.</i> , 2017)	Mouse: Increased lifespan, diminished motor decline, reduced cholesterol accumulation

These AAV-mediated gene transfer methods can be employed to deliver shRNAs (short hairpin RNA) based on siRNAs that suppressed the expression of P301S-mutated human TAU in mouse primary neurons, leading to amelioration of behavioural deficits in this mouse model of tauopathies (Xu *et al.*, 2014).

The potential therapeutic benefits of AAV-based therapy are not exclusive to genetic tauopathies, but may be extended to sporadic forms of those diseases, if pathomechanistic workup reveals clear targets. AAV-delivered RNAi interference (RNAi), e.g., targeting of Cyclin-dependent kinase 5 (CDK5), a major TAU kinase that contributes to pathological TAU hyperphosphorylation, decreased the numbers of neurofibrillary tangles in the brains of AD mice (Piedrahita *et al.*, 2010).

Naturally, there are limitations (For notable advantages and limitations of AAV-based gene therapy, see Box 1): Although AAVs are considered non pathogenic, activation of

the host immune response can occur. Neutralizing antibodies or other forms of immunity against certain serotypes (AAV1, AAV2) are present in up to 70% of the population (Mingozzi and High, 2013). Although very young children are naive to AAV exposure, maternal antibodies may restrict the use of peripherally delivered AAVs to the age of approximately 7–11 months (Calcedo *et al.*, 2011). However, hardly any severe adverse effects have been noticed in AAV-based gene therapy clinical trials, with transient, and usually asymptomatic, hepatitis being the most severe side effect (Kuzmin *et al.*, 2021; Büning and Schmidt, 2015). Another issue is diseases that require a high proportion of transduced cells in the body, and for which much higher virus doses are needed to achieve beneficial results. Such high doses can be toxic and lead to liver failure and shock (Hinderer *et al.*, 2018).

The diagnosis of pediatric forms of tauopathies and neurogenetic diseases is usually based on unclear genetic

evidence, which makes pinpointing a specific target for gene therapy an exhausting task. On the other hand, in age-associated tauopathies, brain damage that has already happened at the disease onset is unlikely to be reversed with AAV-based gene therapy. Yet, given the probable ability of atrophic neurons to regenerate their normal function (Huang *et al.*, 2014), the timing of initiation of the treatment would be a crucial factor in its success, with patients with known familial tauopathies treated in the presymptomatic phase having the highest chance of benefiting from treatment (Martier and Konstantinova, 2020). This complicates clinical studies due to necessary long-term follow up.

Vision of the Future

Several issues must be addressed for AAV-based gene therapy to become useful for genetic forms of tauopathy and related disorders.

Host immunity: One way to overcome host immunity when using AAVs is to focus on recombinant viruses derived from AAV-serotypes that i) are not serotype 1/2, and ii) already have a natural tropism for the CNS (i.e., serotypes 4,5,8,9, and for certain neuromuscular diseases with muscle involvement also skeletal/cardiac muscle, i.e., serotypes 6,7,8,9), and unconventional/novel AAVs already in clinical use/trials (e.g., AAVrh10, AAVrh74, LK200, AAVHSC15, SPK100, AAVhu37). To further reduce the danger of neutralizing antibodies/immunity, in case of pre-existing immunity against certain serotypes, standard Enzyme-linked Immunosorbent Assay (ELISA)-based serotyping or antibody titration of patients for existing antibodies against the specified AAV-serotypes could be used to identify the therapeutic serotype window on a patient-by-patient basis, where adequate.

Toxicity and tropism: To further reduce the (already low) risk of peripheral immune response or other possible peripheral side effects (such as hepatic toxicity), and to reduce the necessary amount of virus (also reducing production cost/time), intrathecal delivery should be the preferred route of administration for CNS specific disease. Other points to

consider in order to avoid administering very high doses of AAV can include designing new promoters and capsids that enhance respectively the transgene expression and target tissue specificity, dose adjustment based on patient-specific factors and genetic predispositions, and the calculated administration of immunosuppressive agents to eliminate neutralizing antibodies (He *et al.*, 2021). Further, modifying cap-proteins could constitute an approach to set up a library of viruses redundantly targeting CNS cells: Cap gene of AAV encodes three capsid proteins, which interact to form the capsid. These capsid proteins contain 12 hypervariable regions, and their serotype determines the tropism of the AAV virus (Gao *et al.*, 2003). Consequently, hybrid AAV particles, in which the capsid is provided by one strain and the genome by another or the capsid itself is the result of hybridized capsids from different strains, can achieve more controlled and higher specific tissue targeting (Burger *et al.*, 2004). This will provide a redundant battery of viruses from all specified serotypes with different (CNS)-tropisms, with up to a 1000-fold higher delivery capacity for specific cells compared to native AAVs (Ravindra Kumar *et al.*, 2020), dramatically reducing titer necessity, potential toxicity and production cost/time.

Delivery: Interestingly, the tropism of different AAV serotypes is not solely controlled by the capsid proteins, but can also be influenced by the conditions of administration. Different serotypes tend to show different tropism depending on the route of delivery. For example, AAV9 showed higher transduction efficiency of cardiomyocytes when injected *via* the mouse tail vein, but this efficiency was reduced in comparison to AAV6 when both were injected into the left ventricle of the heart (Zincarelli *et al.*, 2010). Moreover, age of the host at the time of AAV administration can affect the biodistribution of AAV particles; changing the time of injection from the day of birth to later stages of development shifted the tropism of several AAV serotypes from neuronal to non-neuronal, respectively (Chakrabarty *et al.*, 2013). These factors should be considered carefully when designing clinical trials for AAV-based gene therapy.

Human specific disease-relevant neuronal assay systems: In case of necessity for a patient-specific genetic intervention

BOX 1

Notable advantages, limitations, and examples of possible technical solutions of AAV-based gene therapy

Advantages:

- Not pathogenic, unusual low rate of side- and adverse effects.
- Efficient entry and transduction of target cells, tunable tropism biotechnologically possible.
- AAV expression persists for decades in non-dividing cells (e.g., neurons, cardiomyocytes).

Limitations & Possible Solutions:

- Neutralizing antibodies (in particular against serotypes 1/2) are expressed in the population after childhood age for certain serotypes.
 - Solution: The use of novel AAV viruses that are not derived from AAV 1/2, and measuring neutralizing antibody titers to identify patient-specific immunity gaps.
- Limited genome capacity (4.8 kb), limiting the expression to smaller genes proteins.
 - Solution: Use of trans-splicing AAV vectors, in which two AAV genomes form head-to-tail concatemers, increasing the packaging capacity (Yan *et al.*, 2000).
- Conversion of the single-stranded vector DNA into double-stranded DNA by the host cell is rate-limiting.
 - Solution: Use of self-complementary AAV (scAAV) to circumvent the need for second DNA strand synthesis (McCarty *et al.*, 2001).

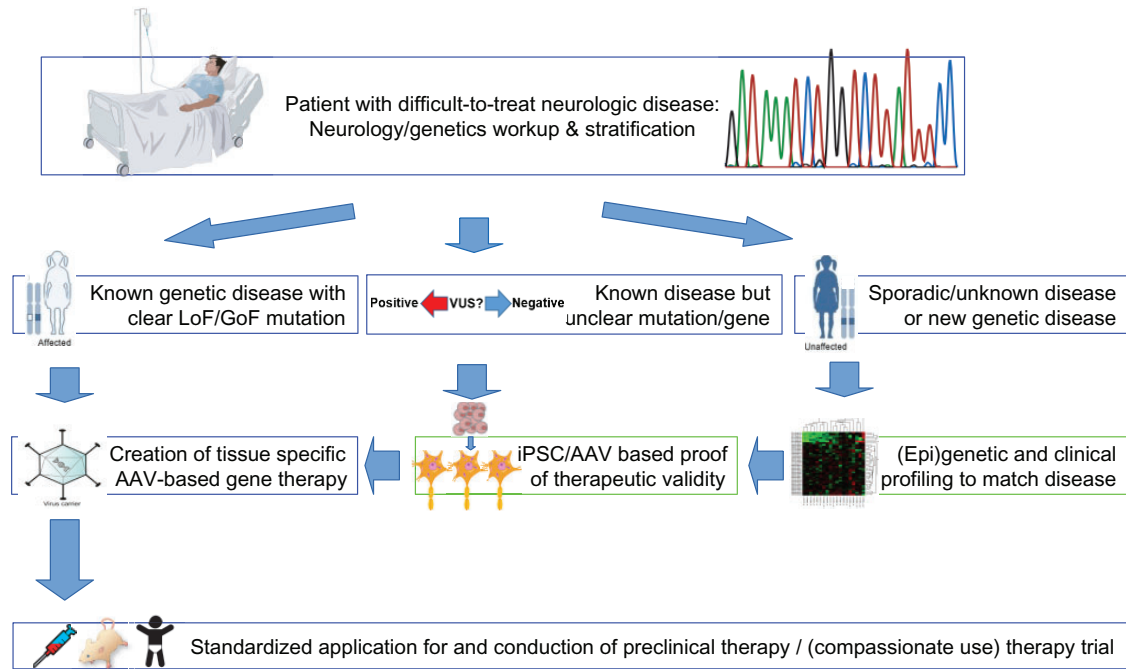


FIGURE 1. Scheme for envisioned gene therapy approach for tauopathies and neurogenetic diseases (Abbreviations: LoF, loss of function; GoF, gain of function; VUS, variant of unknown significance; iPSC, induced pluripotent stem cells; AAV, adeno-associated virus).

(e.g., diseases with gain-of-function (GoF) mutations where silencing of the single nucleotide-mutated allele is necessary), the use of induced Pluripotent Stem Cells (iPSC)-derived CNS-cells expressing the mutated transgene could help to validate patient-tailored knockdown efficiency and functional consequences. Functional tests in iPSC-derived CNS-cells (e.g., allele specific knockdown) could also resolve candidate genetic alterations in case of a clear disease entity but unclear genetic pathogenic cause, and also serve as the functional readout for the genetic intervention (for scheme see Fig. 1). The arguments raised above, the current methodologies that allow testing AAVs on human cells of specific lineages, and the potentially patient specific shRNA design or gene replacement strategies all speak against the notion of routinely using non-human primates to test the safety of the developed viruses. With cell-type specific tropism of engineered AAVs, and human specific RNAi/gene expression paradigms, experiments in primates appear to us unnecessary and unhelpful due to unpredictable side/off-target effects simply due to interspecies differences. We strongly discourage the routine testing of all AAV-based gene therapy approaches in primates.

In conclusion, AAV-based gene therapy is a potentially powerful tool to cure hereditary diseases. Genetic tauopathies and related neurogenetic diseases are prime targets for this kind of therapy, especially since there is no traditional therapy in sight, and promising data have been obtained from a number of clinical trials for other neurogenetic and neurodegenerative diseases. Nonetheless, strategies to adapt current AAV-based gene therapy approaches to target the heterogeneous group of genetic or sporadic, pediatric or age-related tauopathies need to be developed and implemented in order to establish a safe, effective and personalized AAV-based gene therapy for specific tauopathies.

Authors' Contribution: The authors confirm contribution to the paper as follows: Concept and initial drafting of the manuscript: MAAK, HZ; Refinement of conceptualization, proofreading, scientific and clinical context: MAAK, CK, GW and HZ. All authors reviewed the results and approved the final version of the manuscript.

Funding Statement: This work was supported by funding from Else-Kröner-Fresenius-Stiftung and by the Köln Fortune Program/ Faculty of Medicine, University of Cologne.

Conflicts of Interest: The authors declare that they have no conflicts of interest to report regarding the present viewpoint.

References

- Bisset DR, Stepniak-Konieczna EA, Zavaljevski M, Wei J, Carter GT, Weiss MD, Chamberlain JR (2015). Therapeutic impact of systemic AAV-mediated RNA interference in a mouse model of myotonic dystrophy. *Human Molecular Genetics* **24**: 4971–4983. DOI 10.1093/hmg/ddv219.
- Büning H, Schmidt M (2015). Adeno-associated vector toxicity—To be or not to be? *Molecular Therapy* **23**: 1673–1675. DOI 10.1038/mt.2015.182.
- Burger C, Gorbatyuk OS, Velardo MJ, Peden CS, Williams P, Zolotuchin S, Reier PJ, Mandel RJ, Muzyczka N (2004). Recombinant AAV viral vectors pseudotyped with viral capsids from serotypes 1, 2, and 5 display differential efficiency and cell tropism after delivery to different regions of the central nervous system. *Molecular Therapy* **10**: 302–317. DOI 10.1016/j.ymthe.2004.05.024.
- Calcedo R, Morizono H, Wang L, McCarter R, He J, Jones D, Batshaw ML, Wilson JM (2011). Adeno-associated virus antibody profiles in newborns, children, and adolescents. *Clinical and Vaccine Immunology* **18**: 1586–1588. DOI 10.1128/CVI.05107-11.
- Chakrabarty P, Rosario A, Cruz P, Siemiński Z, Ceballos-Diaz C et al. (2013). Capsid serotype and timing of injection

- determines AAV transduction in the neonatal mice brain. *PLOS ONE* **8**: e67680. DOI 10.1371/journal.pone.0067680.
- Chandler RJ, Williams IM, Gibson AL, Davidson CD, Incao AA, Hubbard BT, Porter FD, Pavan WJ, Venditti CP (2017). Systemic AAV9 gene therapy improves the lifespan of mice with Niemann-Pick disease, type C1. *Human Molecular Genetics* **26**: 52–64. DOI 10.1093/hmg/ddw367.
- Coughlin D, Irwin DJ (2017). Emerging diagnostic and therapeutic strategies for tauopathies. *Current Neurology and Neuroscience Reports* **17**: 72. DOI 10.1007/s11910-017-0779-1.
- DeVos SL, Miller RL, Schoch KM, Holmes BB, Kebodeaux S et al. (2017). Tau reduction prevents neuronal loss and reverses pathological tau deposition and seeding in mice with tauopathy. *Science Translational Medicine* **9**: 1–30. DOI 10.1126/scitranslmed.aag0481.Tau.
- Fol R, Braudeau J, Ludewig S, Abel T, Weyer SW et al. (2016). Viral gene transfer of APP^{sa} rescues synaptic failure in an Alzheimer's disease mouse model. *Acta Neuropathologica* **131**: 247–266. DOI 10.1007/s00401-015-1498-9.
- Franich NR, Fitzsimons HL, Fong DM, Klugmann M, Doring MJ, Young D (2008). AAV vector-mediated RNAi of mutant Huntingtin expression is neuroprotective in a novel genetic rat model of Huntington's disease. *Molecular Therapy* **16**: 947–956. DOI 10.1038/mt.2008.50.
- Gao G, Alvira MR, Somanathan S, Lu Y, Vandenberghe LH, Rux JJ, Calcedo R, Sanmiguel J, Abbas Z, Wilson JM (2003). Adeno-associated viruses undergo substantial evolution in primates during natural infections. *Proceedings of the National Academy of Sciences of the United States of America* **100**: 6081–6086. DOI 10.1073/pnas.0937739100.
- Goedert M, Spillantini MG (2017). Propagation of Tau aggregates. *Molecular Brain* **10**: 1–9. DOI 10.1186/s13041-017-0298-7.
- György B, Lööv C, Zaborowski MP, Takeda S, Kleinstiver BP et al. (2018). CRISPR/Cas9 mediated disruption of the Swedish APP allele as a therapeutic approach for early-onset Alzheimer's Disease. *Molecular Therapy—Nucleic Acids* **11**: 429–440. DOI 10.1016/j.omtn.2018.03.007.
- He X, Urip BA, Zhang Z, Ngan CC, Feng B (2021). Evolving AAV-delivered therapeutics towards ultimate cures. *Journal of Molecular Medicine* **99**: 593–617. DOI 10.1007/s00109-020-02034-2.
- Hinderer C, Katz N, Buza EL, Dyer C, Goode T, Bell P, Richman LK, Wilson JM (2018). Severe toxicity in nonhuman primates and piglets following high-dose intravenous administration of an adeno-associated virus vector expressing human SMN. *Human Gene Therapy* **29**: 285–298. DOI 10.1089/hum.2018.015.
- Huang Z, Ha GK, Petitto JM, Petitto J (2014). Reversal of neuronal atrophy: Role of cellular immunity in neuroplasticity and aging the neuroprotective effects of cellular immunity. *Journal of Neurological Disorders* **2**: 1000170. DOI 10.4172/2329-6895.1000170.
- Ising C, Gallardo G, Leyns CEG, Wong CH, Jiang H et al. (2017). Correction: AAV-mediated expression of anti-tau scFvs decreases tau accumulation in a mouse model of tauopathy. *Journal of Experimental Medicine* **214**: 2163–2163. DOI 10.1084/jem.2016212505192017c.
- Kaji EH, Leiden JM (2001). Gene and stem cell therapies. *Journal of the American Medical Association* **285**: 545–550. DOI 10.1001/jama.285.5.545.
- Kou J, Kim H, Pattanayak A, Song M, Lim JE, Taguchi H, Paul S, Cirrito JR, Ponnazhagan S, Fukuchi KI (2011). Anti-amyloid- β single-chain antibody brain delivery via AAV reduces amyloid load but may increase cerebral hemorrhages in an Alzheimer's disease mouse model. *Journal of Alzheimer's Disease* **27**: 23–28. DOI 10.3233/JAD-2011-110230.
- Kuzmin DA, Shutova MV, Johnston NR, Smith OP, Fedorin VV et al. (2021). The clinical landscape for AAV gene therapies. *Nature Reviews. Drug Discovery* **20**: 173–174. DOI 10.1038/d41573-021-00017-7.
- Le Bec C, Douar AM (2006). Gene therapy progress and prospects—Vectorology: Design and production of expression cassettes in AAV vectors. *Gene Therapy* **13**: 805–813. DOI 10.1038/sj.gt.3302724.
- Long JM, Holtzman DM (2019). Alzheimer disease: An update on pathobiology and treatment strategies. *Cell* **179**: 312–339. DOI 10.1016/j.cell.2019.09.001.
- Martier R, Konstantinova P (2020). Gene therapy for neurodegenerative diseases: Slowing down the ticking clock. *Frontiers in Neuroscience* **14**: 580179. DOI 10.3389/fnins.2020.580179.
- McCarty DM, Monahan PE, Samulski RJ (2001). Self-complementary recombinant adeno-associated virus (scAAV) vectors promote efficient transduction independently of DNA synthesis. *Gene Therapy* **8**: 1248–1254. DOI 10.1038/sj.gt.3301514.
- Mingozzi F, High KA (2013). Immune responses to AAV vectors: Overcoming barriers to successful gene therapy. *Blood* **122**: 23–36. DOI 10.1182/blood-2013-01-306647.
- Murley AG, Coyle-Gilchrist I, Rouse MA, Simon Jones P, Li W et al. (2020). Redefining the multidimensional clinical phenotypes of frontotemporal lobar degeneration syndromes. *Brain* **143**: 1555–1571. DOI 10.1093/brain/awaa097.
- Park SA, Il Ahn S, Gallo JM (2016). Tau mis-splicing in the pathogenesis of neurodegenerative disorders. *BMB Reports* **49**: 405–413. DOI 10.5483/BMBRep.2016.49.8.084.
- Piedrahita D, Hernández I, López-Tobón A, Fedorov D, Obara B et al. (2010). Silencing of CDK5 reduces neurofibrillary tangles in transgenic Alzheimer's mice. *Journal of Neuroscience* **30**: 13966–13976. DOI 10.1523/JNEUROSCI.3637-10.2010.
- Ramamoorth M, Narvekar A (2015). Non viral vectors in gene therapy—An overview. *Journal of Clinical and Diagnostic Research* **9**: GE01–GE06. DOI 10.7860/JCDR/2015/10443.5394.
- Ravindra Kumar S, Miles TF, Chen X, Brown D, Dobrev T et al. (2020). Multiplexed Cre-dependent selection yields systemic AAVs for targeting distinct brain cell types. *Nature Methods* **17**: 541–550. DOI 10.1038/s41592-020-0799-7.
- Sud R, Geller ET, Schellenberg GD (2014). Antisense-mediated exon skipping decreases Tau protein expression: A potential therapy for tauopathies. *Molecular Therapy—Nucleic Acids* **3**: 1–11. DOI 10.1038/mtna.2014.30.
- Sun J, Roy S (2021). Gene-based therapies for neurodegenerative diseases. *Nature Neuroscience* **24**: 297–311. DOI 10.1038/s41593-020-00778-1.
- van Hummel A, Bi M, Ippati S, Van Der Hoven J, Volkerling A et al. (2016). No overt deficits in aged tau-deficient C57Bl/6. Mapttm1(EGFP)kit GFP knockin mice. *PLoS One* **11**: 1–14. DOI 10.1371/journal.pone.0163236.
- Wegmann S, DeVos SL, Zeitler B, Marlen K, Bennett RE et al. (2021). Persistent repression of tau in the brain using engineered zinc finger protein transcription factors. *Science Advances* **7**: 1–20. DOI 10.1126/sciadv.abe1611.
- Xu H, Rösler TW, Carlsson T, de Andrade A, Fiala O, Hollerhage M, Oertel WH, Goedert M, Aigner A, Höglinger GU (2014). Tau silencing by siRNA in the P301S mouse model of tauopathy. *Current Gene Therapy* **14**: 343–351. DOI 10.2174/156652321405140926160602.

- Yan Z, Zhang Y, Duan D, Engelhardt JF (2000). Trans-splicing vectors expand the utility of adeno-associated virus for gene therapy. *Proceedings of the National Academy of Sciences of the United States of America* **97**: 6716–6721. DOI 10.1073/pnas.97.12.6716.
- Zempel H, Mandelkow E (2014). Lost after translation: Missorting of Tau protein and consequences for Alzheimer disease. *Trends in Neurosciences* **37**: 721–732. DOI 10.1016/j.tins.2014.08.004.
- Zempel H, Mandelkow E (2019). Mechanisms of axonal sorting of tau and influence of the axon initial segment on tau cell polarity. *Advances in Experimental Medicine and Biology* **1184**: 69–77. DOI 10.1007/978-981-32-9358-8_6.
- Zimmer-Bensch G, Zempel H (2021). DNA methylation in genetic and sporadic forms of neurodegeneration: Lessons from Alzheimer's, related tauopathies and genetic tauopathies. Preprints: 2021050717. DOI 10.20944/preprints202105.0717.v1.
- Zincarelli C, Soltys S, Rengo G, Koch WJ, Rabinowitz JE (2010). Comparative cardiac gene delivery of adeno-associated virus serotypes 1–9 reveals that AAV6 mediates the most efficient transduction in mouse heart. *Clinical and Translational Science* **3**: 81–89. DOI 10.1111/j.1752-8062.2010.00190.x.

© 2022. This work is licensed under <https://creativecommons.org/licenses/by/4.0/> (the “License”). Notwithstanding the ProQuest Terms and Conditions, you may use this content in accordance with the terms of the License.

6.2 Article 2

Lilis, P., Al Kabbani, M. A., Zempel, H. (2024) Optimized Calcium-Phosphate-Based Co-transfection of Tau and tdTomato into Human iPSC-Derived Neurons for the Study of Intracellular Distribution of Wild-type and Mutant Human Tau. *Methods Mol Biol.* 2754: 551-560. doi: 10.1007/978-1-0716-3629-9_32.



Optimized Calcium-Phosphate-Based Co-transfection of Tau and tdTomato into Human iPSC-Derived Neurons for the Study of Intracellular Distribution of Wild-type and Mutant Human Tau

Panagiotis Lilis, Mohamed Aghyad Al Kabbani, and Hans Zempel

Abstract

The study of Tau protein in disease-relevant neuronal cells in culture requires efficient delivery systems for transfection of exogenous Tau and also modulators and interactors of Tau. Transfection of cultivated cells using calcium phosphate precipitation is a simple and cost-effective approach, also for difficult-to-transfect and sensitive cells such as primary neurons. Because of its low cell toxicity and ease of use, the Ca^{2+} -phosphate transfection method is one of the most widely used gene transfer procedures in neuroscience. However, Ca^{2+} -phosphate transfection efficacy in neurons is poor, often in the range of 1–5%, limiting its use in functional investigations. Here, we outline our improved Ca^{2+} -phosphate transfection methodology for human iPSC-derived neurons that yields a reasonable efficiency (20–30% for bright volume markers) without apparent effects on cell health. We have used it to introduce wild-type and mutant human Tau with and without co-transfection of a volume marker (used here: tdTomato). In sum, our procedure can deliver neuronal genes (e.g., *MAPT*) using typical eukaryotic expression vectors (e.g., using CMV promoter) and is optimized for transfection of human iPSC-derived neurons.

Key words Tau, Co-transfection, tdTomato, iPSC-derived neurons, Calcium-phosphate transfection, Transfection efficiency

1 Introduction

Because primary neurons are postmitotic and sensitive to microenvironmental alterations, they are among the most difficult cell types to transfect [1–4]. In comparison to viral vectors, the Ca^{2+} -phosphate transfection approach permits transfection of plasmid DNA regardless of its size and is labor- and cost-effective [2, 3, 5]. Graham and Van Der Eb (1973) were the first to employ this approach to transport adenovirus DNA into mammalian cells [6]. Transfection with Ca^{2+} -phosphate causes the formation of DNA crystals that are complexed with the calcium ions in the phosphate buffer

[2, 3]. This permits DNA/ Ca^{2+} -phosphate precipitates to develop, which attach to the cell surface (when gradually deposited over a monolayer of cells), are taken up by endocytosis, and eventually reach the nucleus [7]. Ca^{2+} -phosphate transfection efficiency typically ranges from 0.5% to 5% [1, 3–5]. It is feasible though to achieve a transfection efficiency of about 30–40% with thorough tuning and consistent execution of the experimental methodology [3]. The formation of optimally sized precipitate particles and the subsequent dissolution of the Ca^{2+} -phosphate precipitate are crucial components in obtaining this high rate [3, 5]. The development of homogenous and tiny Ca^{2+} -phosphate precipitates, as well as their removal following transfection, was crucial in the prior work [3, 8].

Here, we have improved the former approach [3] by using completely defined components and no commercial kits. For consistent tiny precipitates, we optimized the quantity of DNA and calcium chloride concentration. Moreover, we developed a washing buffer that dissolves all Ca^{2+} -phosphate precipitates after transfection. The approach presented here may be used to transfect neurons at practically any stage of differentiation in culture, with the exception of extremely early stages and with decreasing efficiency when neurons become more mature.

In sum, our procedure can (i) deliver neuronal genes (e.g., *MAPT*) using typical eukaryotic expression vectors (e.g., using CMV promoter), (ii) be used for co-transfection, (iii) be adapted for efficiency and expression duration, and (iv) is optimized for transfection of human iPSC-derived neurons.

Neuronal gene delivery can be achieved using typical eukaryotic expression vectors [4]. A number of genes and gene combinations (i.e., co-transfection) have previously been carried out using Ca^{2+} -phosphate transfection [9]. Here we use *MAPT*/*TAU* knock-out human iPSC-derived neurons to introduce wild-type (wt) and mutant human Tau, co-transfected with a volume marker (tdTomato), 10 days after seeding. The WT and mutant Tau (used here: P301L- Tau) plasmids make use of the CMV promoter and are both fused with a green fluorescent protein (here: Dendra2c, a particularly dim fluorescent protein). They are thus easily distinguishable from the co-transfected volume marker (here, tdTomato, red fluorescence). To summarize, using the procedure outlined below, we were able to transfect notoriously difficult-to-transfect human iPSC-derived neurons with decent efficiency using both Tau fused to Dendra2c and tdTomato (Figs. 1 and 2).

We also used single gene transfection (tdTomato only) to study the correlation between transfection efficiency and DNA concentration. We demonstrate that different DNA concentrations can be used to change the time course and quantities of protein expression [10, 11]. Low amount of DNA equals low efficiency, while after a certain threshold of DNA concentration, the efficiency plateaued

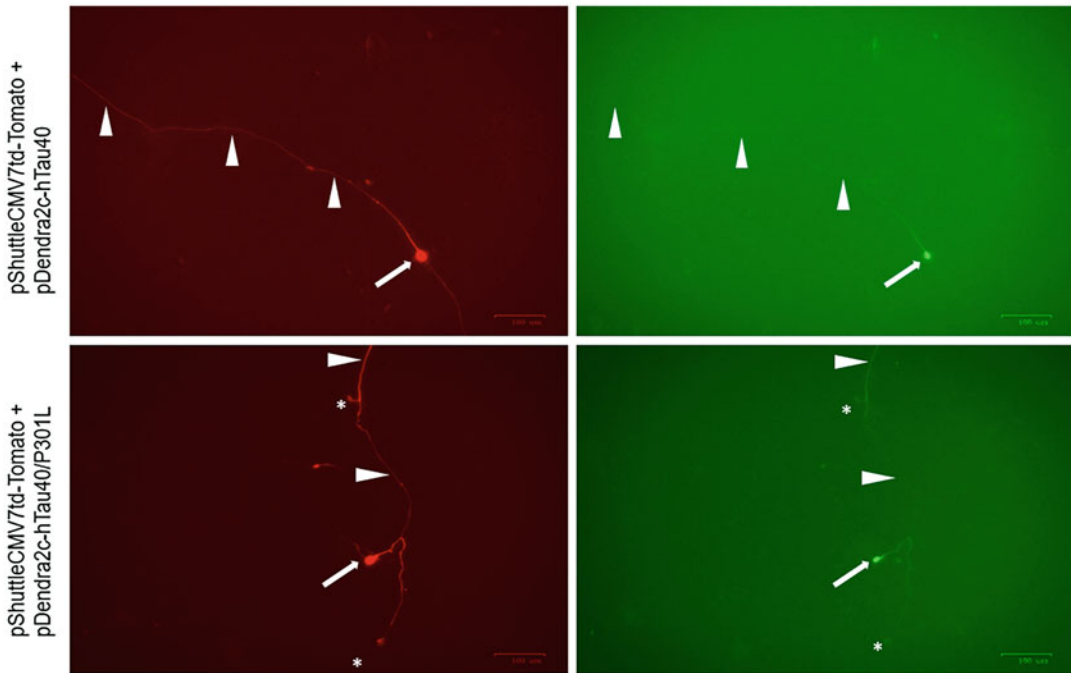


Fig. 1 Representative Ca^{2+} -phosphate-based co-transfection of 0.2 μg tdTomato with either 0.8 μg hTau (upper panel) or 1.6 μg hTau-P301L (lower panel), respectively. iPSC-derived neurons were transfected with the corresponding plasmids at D10 of differentiation for 4 days and then imaged in live conditions using a standard cell culture microscope. Note that even with one-eighth or one-fifth of optimal DNA/plasmid content (in case of tdTomato, left panels), and with the very dim protein Dendra2c, (co-)transfected neurons can be identified and imaged in standard cell culture place, in conditioned and phenol-red containing medium, in low magnification (shown here: 10x). (Scale bars: 100 μm)

with gradual increase in cell death. We identified a range of 1.0–1.5 μg of DNA to be the optimal one for transfection efficiency in a well of a 24-well plate (Chart 1).

Last, we examined the duration of protein expression after transfection, by recording the expression levels under an epifluorescence microscope on each day up to day 10 after transfection. Daily monitoring of protein expression levels under the epifluorescence microscope concludes that protein expression (tdTomato) is visible even after a few (3–6) hours after transfection, reaching its peak between day 4 and day 6 after transfection. One week after transfection, the protein expression levels begin to drop, correlating with increasing death of transfected cells (Chart 2).

2 Materials

2.1 Equipment

1. Standard laminar flow hood
2. 5% CO_2 incubator at 37 $^\circ\text{C}$

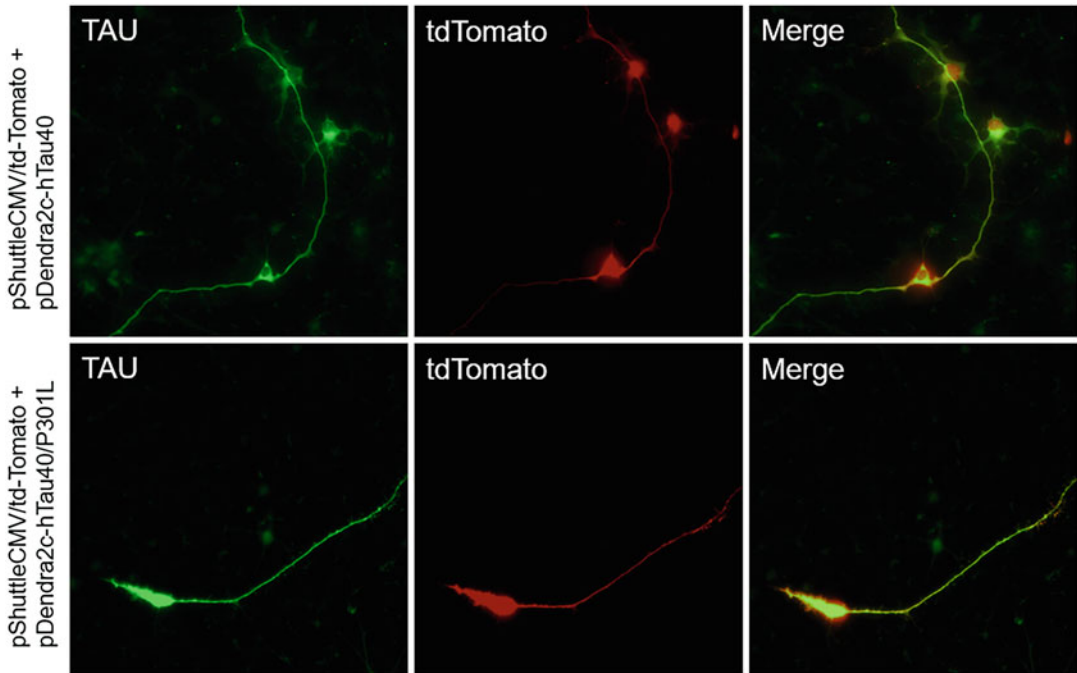


Fig. 2 Representative CaP-based co-transfection of 0.1 or 0.5 μg tdTomato with either 0.8 μg hTau (upper panel) or 1.5 μg hTau-P301L (lower panel), respectively. Briefly, iPSC-derived neurons were transfected with the corresponding plasmids at D10 of differentiation for 6 days and then fixed and stained with a specific anti-Tau antibody (K9JA)

3. 10% CO_2 incubator at 37 $^\circ\text{C}$
4. Vortex machine
5. Centrifuge
6. Water bath (37 $^\circ\text{C}$)
7. pH meter
8. Sterile 24-well tissue culture plates

2.2 Buffers and Reagents

1. Tissue culture sterile water (nuclease-free water).
2. Cell culture media (500 mL MEM, 5% FBS, 10 mL B27 supplement, 100 mg NaHCO_3 , 20 mM D-glucose, 0.5 mM L-glutamine) [4, 5].
3. Transfection medium: Dulbecco's Modified Eagle Medium/Nutrient Mixture F-12 (DMEM/F-12), without supplements.
4. 2X HEPES-buffered saline (HBS), pH = 7.05–7.12 [6]: 16.4 g NaCl (0.28 M final), 11.9 g HEPES (N-2-hydroxyethylpiperazine-N'-2-ethanesulfonic acid; 0.05 M final), 0.21 g Na_2HPO_4 (1.5 M final), and 800 mL H_2O ; titrate to pH 7.05–7.12 with NaOH or HCl; add H_2O to 1 L; filter-sterilize through a 0.45- μm nitrocellulose filter. Check for

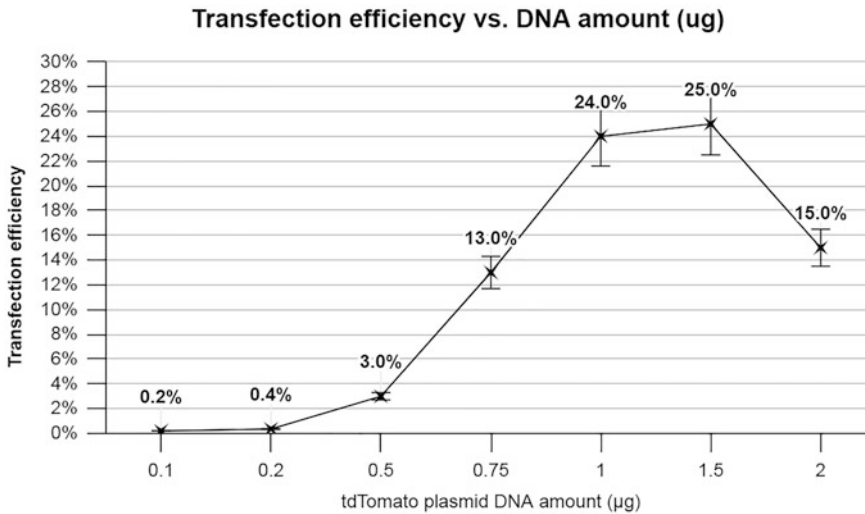


Chart 1 Correlation of introduced DNA concentration on Ca^{2+} -phosphate transfection efficiency. Human iPSC-derived neurons were transfected with tdTomato plasmid in a 24-well plate (see protocol for details) and observed 5 days post-transfection. Different concentrations of the plasmid were used in order to study the correlation between protein expression levels and plasmid DNA concentration [6, 12]. When a small amount of DNA (0.1–0.2 ug per well in a 24-well plate) is introduced into the iPSC-derived neurons, the transfection efficiency is low (below 1%). However, the number of transfected neurons increases dramatically when we introduce >0.5 ug of plasmid DNA and levels off after the threshold of 1 ug of DNA. Concentrations higher than 1 ug per well show imperceptible changes in transfection efficiency indicating a saturation point for the cells. Further increase of DNA amount appears to be toxic to the cells reducing the transfection efficiency alongside. Error bars: SEM from $n = 3$ experiments

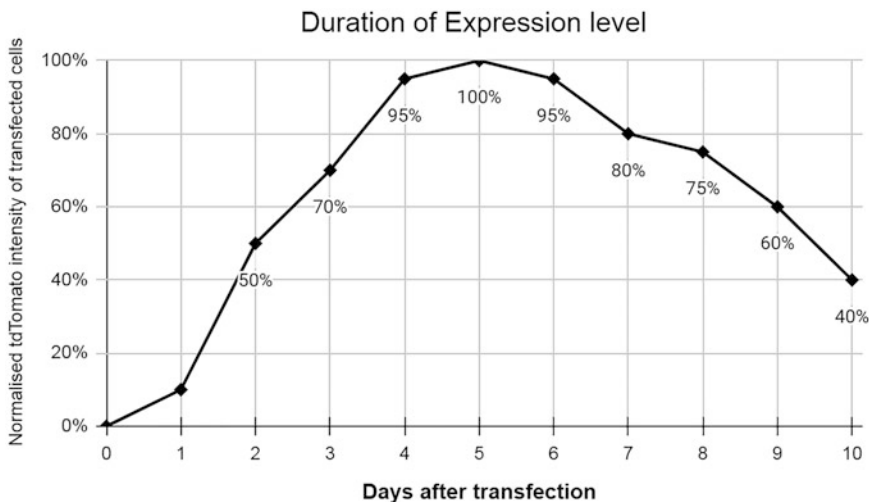


Chart 2 Correlation between level of protein expression and time (days) after Ca^{2+} -phosphate transfection. Human iPSC-derived neurons 10 days after differentiation were transfected with tdTomato plasmid only in a 24-well plate (see protocol for details). Chart shows the outcome of a typical experiment using single transfection of tdTomato (1 ug of DNA/24 well, see protocol for details). Measurements of normalized tdTomato intensity are per transfected cell

transfection efficiency. Store at $-20\text{ }^{\circ}\text{C}$ in 10 mL aliquots (*see Note 1*).

5. 1X phosphate-buffered saline (PBS) solution (*see Note 2*).
6. 2.5 M CaCl_2 : Weigh 183.7 g $\text{CaCl}_2 \cdot 2\text{H}_2\text{O}$ (powder for cell culture), and add H_2O to 500 mL; filter-sterilize through a $0.45\text{ }\mu\text{m}$ nitrocellulose filter. Store at $-20\text{ }^{\circ}\text{C}$ in 10 mL aliquots. This solution can be frozen and thawed repeatedly.
7. Solution A: 1 μg plasmid DNA (optimal concentration), 2.48 μL 2.5 M CaCl_2 , and sterile water to 25 μL ; add water first, and then the DNA, mix well, and finally the CaCl_2 solution and mix again.
8. Solution B: 25 μL 2X HBS.
9. Vector DNA (plasmids): Check DNA concentration and purity before use. Plasmids used here are pShuttleCMV/td-Tomato, pDendra2c-hTau40, and pShuttleCMV/Dendra2c/ht40/P301L.

3 Methods

This protocol is optimized for human iPSC-derived neurons and for a 24-well plate (WP). We have experienced that upscaling (e.g., to standard 12 or 24 well plates) results in improved viability and transfection efficiency.

3.1 Day 0: Prepare Cultured Cells for Transfection

1. Seed cells in a 24WP with coverslips (approximately 50,000 cells per well).
2. Incubate with appropriate media (0.5 mL) at $37\text{ }^{\circ}\text{C}$, 5% CO_2 incubator for at least 10 days (for details on how to cultivate and differentiate these cells, refer to [12]). There is no need for adaptation of the iPSC culture nor the differentiation procedure (see also chapter in this book, Bachmann et al. (2022)).

3.2 Day 10 After Differentiation: Transfection

Transfection is optimal between day 8 and day 15 for the study of axodendritic proteins [3]:

1. Transfer selected coverslips to be transfected containing cultured neurons from their original well to a new 24-well plate with 0.5 mL pre-warmed transfection medium. Return both the original and the new plate to the incubator with 5% CO_2 [3]; time is 3–5 min.
2. Prepare DNA for transfection (make sure it is pure and clean).
3. Prepare DNA- CaCl_2 Solution A in a tube, in the final volume of 1:20 (25 μL) of total growth medium volume in which cells are plated.

4. Prepare 2X HBS Solution B in another tube, in the final volume of 1:20 (25 μ L) of total growth medium volume in which cells are plated; time (**steps 2–4**) is 5–30 min (depending on number of wells to be transfected).
5. Add gently 1:8 volume at a time of solution A to solution B while quickly pipetting several times or very brief intermittent vortexing for around 1 s. Repeat until solution A is completely added to solution B (*see Notes 3 and 4*); time is 3–15 min (depending on number of wells to be transfected).
6. Allow the precipitate to sit at room temperature for 20–30 min without any vortexing (*see Note 3*); time is 20–30 min.
7. Add the complete mixture/precipitate (50 μ L) dropwise to the coverslip to be transfected (now in transfection medium). Shake gently to make sure the precipitate is evenly spread out over the whole well/coverslip; time is 2 min.
8. Incubate in a cell culture incubator at 37 °C with 5% CO₂ for 1–3 h (*see Notes 5 and 6*); time is 1–3 h. Note that longer time of incubation results in higher efficiency/number of cells transfected and expression/amount of protein expressed (*see Note 7*), but in particular if increased more than 3 h also, it decreased cell viability.
9. After 1–3 h of incubation, dissolve the precipitate by incubating for 20 min in a 5% CO₂ incubator with transfection medium that has been pre-equilibrated in a 10% CO₂ incubator at 37 °C (*see Note 8*). For the pre-equilibration, incubate the medium separately in a 10% CO₂ incubator for about 40–60 min, before adding to the wells [3] (*see Note 9*); time is 25–30 min.
10. Transfer the transfected coverslips back to their original wells containing the original neuronal culture medium (*see Note 10*). Note that the original culture medium will minimize the cell toxicity, with 50% conditioned medium being the preferred choice over fresh medium [3]; time is 3 min.
11. Check the next day for protein expression. Protein expression can peak between days 3 and 6, depending on neuronal cell type, neuronal age, and type of inserted DNA (*see Notes 11 and 12*); time is 10–15 min (without overnight incubation).

4 Notes

1. Critical considerations for the optimization of transfection efficiency include the pH of the transfection buffer which is important for generating even and small precipitates. The pH of the HBS should be between 7.05 and 7.12. The pH of the solution may change with prolonged storage. Always use a

HBS solution that has been properly stored. If the pH is low, no precipitate will form, and if too high, large aggregates tend to form [3, 8, 10, 13].

2. This sodium phosphate solution is prepared to accurately control the phosphate concentration in the 2× HBS solution. The phosphate concentration is critical for obtaining small and even calcium phosphate precipitation [8].
3. Transfection solution A should be added dropwise into solution B, with 1:8 volume of solution A each time and gentle, intermittent vortexing. Intensive and continuous vortexing may result in large and unevenly distributed particles. No further vortexing is necessary after mixing A and B [3]. Note that the formation of the appropriate size of DNA-Ca²⁺-phosphate precipitate is critical to achieve adequate transfection efficiency.
4. Dropwise addition of the transfection mix plus HBS is critical for forming uniform precipitates. When doing this, the pipette tip should be about 2–3 cm above the liquid surface, so that the mixture is added in droplets [3, 8, 13].
5. Incubation time of **step 8** lower than 60 min might result in decreased transfection efficiency, but it can be extended up to 3 h to improve transfection efficiency. However, neuronal toxicity tends to increase after that point. We recommend to test several time points between 1 and 3 h; even small changes in cell number or cell age can change outcomes significantly.
6. Longer incubation time increases the transfection efficiency with minimal effect on cell survival, because the precipitate is subsequently dissolved. After 20–60 min of incubation, if examined under the microscope, the precipitate should be homogeneous and resemble a cover of snow all over the field [3].
7. Inefficient expression due to the profile of the plasmid requires a well-designed expression vector that includes a strong promoter that is helpful to improve the transfection efficiency [3].
8. Incubating neurons in a 10% CO₂ incubator will result in increased cell death. After adding transfection medium pre-equilibrated in a 10% CO₂ incubator, place the plate in a 5% CO₂ incubator [3].
9. The 10% CO₂ will make the medium more acidic, and Ca²⁺-phosphate will dissolve in acidic solution. It is essential to dissolve the precipitate after incubation to reduce cell toxicity. After microscopic examination, at the end of a 20-min incubation, the precipitate should largely disappear. If neurons normally cultured in a 5% CO₂ incubator are exposed to 10% CO₂ for more than 15–20 min, cells will start dying. Thus, media

should be pre-equilibrated and the plate to be returned to the 5% CO₂ incubator rather than the 10% CO₂ incubator [3].

10. The culture media at this point may contain important trophic factors released by cells (“conditioned medium”) and therefore is kept for reuse after transfection. In our experience, reusing conditioned medium provides better neuronal viability and reduces markers of stress, for example, missorting of Tau into the somatodendritic compartment.
11. The exogenous protein expression using this transfection method is very rapid. tdTomato expression in cultured neurons can be observed as early as 4 h after the transfection, but in our experience, cells that express, for example, Tau within a few hours after transfection usually show reduced viability/signs of stress within 1–2 days and die within 3–4 days, likely simply due to overexpression stress. We have not done side-to-side experiments but feel that this is also true for supposedly non-toxic fluorescent proteins, indicating that this kind of toxicity may simply be due to too much exogenous expression.
12. Younger neurons (D8–D12) are more efficiently transfected and show higher resistance to transfection-based toxicity. However, further experiments with the transfected neurons (e.g., immunostaining) are advised to be performed within 3–5 days following transfection; for Tau protein at least this appears to be the time when there is sufficient expression that can easily be detected and expected to influence the cellular phenotype but not as much that expression alone is already toxic. While especially with this protocol it is easily possible to achieve transfection levels sufficient for detection after even half a day or so, these cells usually succumb to expression stress independent of the protein function (e.g., also the case for fluorescent proteins), which makes interpretation of the functional consequences of the transfected protein difficult.

References

1. Sun M, Bernard LP, DiBona VL, Wu Q, Zhang H (2013) Calcium phosphate transfection of primary hippocampal neurons. *JoVE* 50808. <https://doi.org/10.3791/50808>
2. Karra D, Dahm R (2010) Transfection techniques for neuronal cells. *J Neurosci* 30:6171–6177. <https://doi.org/10.1523/JNEUROSCI.0183-10.2010>
3. Jiang M, Chen G (2006) High Ca²⁺-phosphate transfection efficiency in low-density neuronal cultures. *Nat Protoc* 1: 695–700. <https://doi.org/10.1038/nprot.2006.86>
4. Dudek H, Ghosh A, Greenberg ME (1998) Calcium phosphate transfection of DNA into neurons in primary culture. *Curr Protoc Neurosci* 3. <https://doi.org/10.1002/0471142301.ns0311s03>
5. Jiang M, Deng L, Chen G (2004) High Ca²⁺-phosphate transfection efficiency enables single neuron gene analysis. *Gene Ther* 11:1303–1311. <https://doi.org/10.1038/sj.gt.3302305>
6. Graham FL, van der Eb AJ (1973) A new technique for the assay of infectivity of human adenovirus 5 DNA. *Virology* 52:456–467.

- [https://doi.org/10.1016/0042-6822\(73\)90341-3](https://doi.org/10.1016/0042-6822(73)90341-3)
7. Banker G, Goslin K (1998) *Culturing nerve cells*, 2nd edn. MIT Press, Cambridge, MA
 8. Wang S, Cho YK (2016) An optimized calcium-phosphate transfection method for characterizing genetically encoded tools in primary neurons. In: Kianianmomeni A (ed) *Optogenetics*. Springer, New York, pp 243–249
 9. Eguchi M, Yamaguchi S (2007) Double transfection into primary dissociated neurons. *J Biosci Bioeng* 103:497–499. <https://doi.org/10.1263/jbb.103.497>
 10. Kwon M, Firestein BL (2013) DNA transfection: calcium phosphate method. In: Zhou R, Mei L (eds) *Neural development*. Humana Press, Totowa, pp 107–110
 11. Dahm R, Zeitelhofer M, Götze B, Kiebler MA, Macchi P (2008) Visualizing mRNA localization and local protein translation in neurons. In: *Methods in cell biology*. Elsevier, pp 293–327
 12. Bachmann S, Bell M, Kabbani MAA, Klimek J, Zempel H (2021) Investigating isoform-specific functions of tau under healthy and pathological conditions using Tau-deficient hiPSC-derived cortical neurons. *Alzheimers Dement* 17. <https://doi.org/10.1002/alz.058005>
 13. Kumar P, Nagarajan A, Uchil PD (2019) Transfection of mammalian cells with calcium phosphate–DNA coprecipitates. *Cold Spring Harb Protoc* 2019:pdb.top096255. <https://doi.org/10.1101/pdb.top096255>

6.3 Article 3

Al Kabbani, M. A., Köhler, C., Zempel, H. (2024) Effects of P301L-TAU on post-translational modifications of microtubules in human iPSC-derived cortical neurons and TAU transgenic mice. *Neural Regen Res.* 20(8): 2348-2360. doi: 10.4103/NRR.NRR-D-23-01742.

Effects of P301L-TAU on post-translational modifications of microtubules in human iPSC-derived cortical neurons and TAU transgenic mice

Mohamed Aghyad Al Kabbani^{1,2}, Christoph Köhler³, Hans Zempel^{1,2,*}

<https://doi.org/10.4103/NRR.NRR-D-23-01742>

Date of submission: October 23, 2023

Date of decision: December 19, 2023

Date of acceptance: April 16, 2024

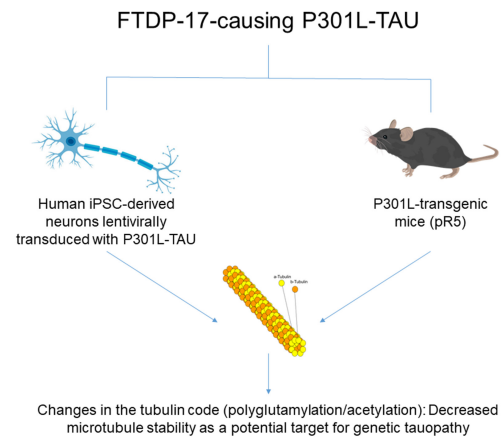
Date of web publication: June 26, 2024

From the Contents

Introduction	1
Methods	3
Results	4
Discussion	8

Graphical Abstract

P301L mutation of TAU affects essential post-translational modifications of neuronal microtubules in human neurons and transgenic mice



Abstract

TAU is a microtubule-associated protein that promotes microtubule assembly and stability in the axon. TAU is missorted and aggregated in an array of diseases known as tauopathies. Microtubules are essential for neuronal function and regulated via a complex set of post-translational modifications (PTMs), changes of which affect microtubule stability and dynamics, microtubule interaction with other proteins and cellular structures, and mediate recruitment of microtubule-severing enzymes. As impairment of microtubule dynamics causes neuronal dysfunction, we hypothesize cognitive impairment in human disease to be impacted by impairment of microtubule dynamics. We therefore aimed to study the effects of a disease-causing mutation of TAU (P301L) on the levels and localization of microtubule PTMs indicative of microtubule stability and dynamics, to assess whether P301L-TAU causes stability-changing modifications to microtubules. To investigate TAU localization, phosphorylation, and effects on tubulin PTMs, we expressed wild-type or P301L-TAU in human *MAPT*-KO induced pluripotent stem cell-derived neurons (iNeurons) and studied TAU in neurons in the hippocampus of mice transgenic for human P301L-TAU (pR5 mice). Human neurons expressing the longest TAU isoform (2N4R) with the P301L mutation showed increased TAU phosphorylation at the AT8, but not the p-Ser-262 epitope, and increased polyglutamylation and acetylation of microtubules compared with endogenous TAU-expressing neurons. P301L-TAU showed pronounced somatodendritic presence, but also successful axonal enrichment and a similar axodendritic distribution comparable to exogenously expressed 2N4R-wildtype-TAU. P301L-TAU-expressing hippocampal neurons in transgenic mice showed prominent missorting and tauopathy-typical AT8-phosphorylation of TAU and increased polyglutamylation, but reduced acetylation, of microtubules compared with non-transgenic littermates. In sum, P301L-TAU results in changes in microtubule PTMs, suggestive of impairment of microtubule stability. This is accompanied by missorting and aggregation of TAU in mice but not in iNeurons. Microtubule PTMs/impairment may be of key importance in tauopathies.

Key Words: human induced pluripotent stem cell; microtubules; P301L; pR5 mice; TAU; tauopathy; tubulin code

Introduction

Microtubules are instrumental in structuring and maintaining the cytoskeleton, which in turn contributes to the structure and shape of the cells. Dimers of α - and β -tubulin are polymerized into protofilaments that associate to form

hollow cylindrical tubes, the microtubules. Microtubules are essential for cell division and intracellular transport, and serve as tracks for cellular cargos, such as vesicles, organelles, and other substances (Nogales, 2000). This is especially important in neurons, where axonal transport is mediated

¹Institute of Human Genetics, Faculty of Medicine and University Hospital Cologne, University of Cologne, Cologne, Germany; ²Center for Molecular Medicine Cologne (CMMC), University of Cologne, Cologne, Germany; ³Center Anatomy, Department II, Medical Faculty, University of Cologne, Cologne, Germany

*Correspondence to: Hans Zempel, PhD, MD, hans.zempel@uk-koeln.de.

<https://orcid.org/0000-0002-7510-3077> (Hans Zempel)

Funding: This study was supported by the Koeln Fortune Program/Faculty of Medicine, University of Cologne, the Alzheimer Forschung Initiative e.V. (grant #22039, to HZ); open-access funding from the DFG/GRC issued to the University of Cologne; and Alzheimer Forschung Initiative e.V. for Open Access Publishing (a publication grant #P2401, to MAAK).

How to cite this article: Al Kabbani MA, Köhler C, Zempel H (2025) Effects of P301L-TAU on post-translational modifications of microtubules in human iPSC-derived cortical neurons and TAU transgenic mice. *Neural Regen Res* 20(0):000-000.

by the interaction of motor proteins with microtubules. Microtubules undergo a complex set of post-translational modifications (PTMs) known as the tubulin code, such as acetylation, polyglutamylation, and tyrosination, all of which regulate their dynamics and functions (Janke and Kneussel, 2010). Interestingly, PTMs of microtubules are highly enriched in neurons.

Acetylated microtubules are resistant, stable microtubules that show higher flexibility and are less prone to breakage (Xu et al., 2017). Acetylation of microtubules is carried out by several acetyltransferases, and the major site of acetylation is the lysine 40 residue of α -tubulin, although several additional acetylation sites have been identified on both α - and β -tubulin (Choudhary et al., 2009).

Polyglutamylation is the addition of a glutamate side chain to a glutamate residue on the C-terminal tail of either α - or β -tubulin (Lacroix et al., 2010). Initial glutamylation and subsequent polyglutamylation are carried out by several members of a class of enzymes known as tubulin-tyrosine-ligase-like proteins (TTLs). The increased length of the polyglutamate side chain leads to the recruitment of SPASTIN, a microtubule-severing enzyme, and subsequent fragmentation of microtubules (Magiera et al., 2018a), which was also associated with oligomeric Amyloid-beta induced TAU missorting-mediated loss of microtubules (Zempel et al., 2013; Zempel and Mandelkow, 2015)

Detyrosination is the reversible removal of the C-terminal tyrosine residue of α -tubulin. Tyrosinated microtubules are highly dynamic, while detyrosinated ones are long-lived. This cycle of tyrosination/detyrosination is suggested to play an important role in establishing neuronal polarity (Erck et al., 2005).

Besides PTMs, microtubule-associated proteins (MAPs), such as TAU, also regulate the functions and properties of microtubules. TAU, also known as microtubule-associated protein TAU, is a microtubule-binding protein encoded in humans by the gene *MAPT*, which is alternatively spliced to produce six isoforms expressed in the human central nervous system (Andreadis et al., 1992). Under normal conditions, TAU is sorted into axons, where it promotes microtubule assembly and stability (Zempel and Mandelkow, 2015). However, disease conditions are associated with TAU dissociation from microtubules, leading to depolymerization of microtubules and subsequent phosphorylation of unbound TAU, and TAU mislocalization ('TAU missorting') or ectopic appearance in the somatodendritic compartments. Hyperphosphorylated and missorted TAU tends to form insoluble aggregates, which are the hallmarks of several neurodegenerative diseases known collectively as tauopathies (Arendt et al., 2016). In Alzheimer's disease and some other tauopathies, TAU aggregates appear in the form of neurofibrillary tangles. A fraction of tauopathies are caused by mutations in the *MAPT* gene, of which the P301L mutation has been identified in familial cases of frontotemporal dementia with parkinsonism linked to chromosome 17 (FTDP-17/*MAPT*-associated FTD). P301L mutation of TAU is the most common *MAPT* mutation (Lewis et al., 2000), and FTDP-17 is in turn one of the major degenerative dementia syndromes (Boeve et al., 2008).

FTDP-17 patients exhibit behavioral and personality changes, cognitive impairment, and motor symptoms, with current treatments being only supportive and symptomatic (Wszolek et al., 2006). The P301L mutation decreases TAU affinity to microtubules (Hasegawa et al., 1998) and promotes aberrant TAU phosphorylation (Alonso et al., 2004).

Therefore, it is essential to investigate P301L-TAU-related pathology in a human-relevant model, such as the expression of mutant TAU in human neurons on TAU knockout (KO) background. This can be achieved in the newly-established *MAPT* KO human induced pluripotent stem cells (iPSCs), which can be easily differentiated into layer 2/3 glutamatergic cortical neurons via doxycycline-induced expression of the transcription factor neurogenin 2. This method yields pure (more than 90%) cultures of fully polarized and synaptically active cortical neurons (Wang et al., 2017). These cells have already served as a human model to study neuronal activity, TAU isoform-specific functions, and TAU-related pathology (Sohn et al., 2019; Bachmann et al., 2021b; Bichmann et al., 2021; Tjiang and Zempel, 2022; Tracy et al., 2022; Bell-Simons et al., 2023).

Neurofibrillary tangle formation associated with tauopathies has been modeled in the transgenic pR5 mouse strain, which expresses the longest human TAU isoform (2N4R) carrying the P301L mutation. pR5 mice show TAU hyperphosphorylation and neurofibrillary tangle formation in different areas of the brain, predominantly in the hippocampus, amygdala, and cerebral cortex, around 8 months of age (Götz et al., 2001; Deters et al., 2008; Köhler et al., 2013), and display impaired spatial reference memory (Pennanen et al., 2006).

Potential changes in the PTMs of neuronal microtubules, which could alter their dynamics and stability, namely acetylation, tyrosination, and polyglutamylation, have not yet been investigated in iPSC-derived human neurons (iNeurons) or in the transgenic pR5 mice. To do so, we used lentiviral transduction to express P301L-TAU or the longest WT isoform (2N4R-TAU) in iNeurons on a TAU KO background and examined their axonal and dendritic sorting capacities and changes in the above-mentioned PTMs of microtubules in the transduced iNeurons. In addition, we performed immunofluorescence labeling of brain sections and western blotting of hippocampal lysates from transgenic pR5 mice and non-transgenic littermates. We aimed to investigate the effects of P301L mutation of TAU on the PTMs of microtubules using a human disease-relevant cellular model (human iNeurons, without endogenous TAU, expressing P301L-(2N4R-) TAU or WT-(2N4R-)TAU as a control, also in comparison with iNeurons still carrying endogenous TAU), and an animal model (pR5 mice transgenic for P301L-TAU and non-transgenic littermates as a control). Hence, we investigated the same disease-causing TAU mutation in both our human cellular model and humanized TAU animal model. This enabled us to compare and evaluate findings in human neuronal cultures and mouse brains.

We found that P301L-TAU results in changes in tubulin PTMs, most prominently acetylation and polyglutamylation, indicative of impairment of microtubule stability and dynamics. P301L-TAU missorts into the neuronal somatodendritic

compartments in mice, but while P301L-TAU prominently appears also in the dendritic compartment in iNeurons, this missorting is similar to 2N4R-TAU. P301L-TAU aggregates in mice around 8 months of age, but we did not find evidence for aggregation in iNeurons. In sum, we here show evidence that tubulin PTMs and microtubule stability may be instrumental in tauopathies, and subtle changes in tubulin PTMs could be an early event of the disease. Hence, targeting tubulin-modifying enzymes may be a therapeutic option for tauopathies.

Methods

iPSC maintenance

WTC11 cells with a doxycycline-inducible Ngn2 transgene (Miyaoaka et al., 2014; Wang et al., 2017) were obtained from Prof. Li Gan laboratory (Weill Cornell Medicine, New York, NY, USA) and cultured as described before (Bachmann et al., 2021b; Buchholz et al., 2024). The WTC11 line is widely used and commercially available in many variations. This cell line is an established cell line that is registered (<https://hpscereg.eu/cell-line/UCSFi001-A>), and commercially available (e.g., www.coriell.org/0/Sections/Search/Sample_Detail.aspx?Ref=GM25256). Briefly, cells were cultured on Geltrex-coated plates (Thermo Fisher Scientific, Waltham, MA, USA, Cat# A1413302) at 37°C, 5% CO₂, and regularly passaged when 80%–90% confluent using Versene (Thermo Fisher Scientific, Cat# 15040066) and thiazovivin-supplemented StemMACS iPS-Brew X.F. (Axon Medchem, Groningen, Netherlands, Cat# Axon 1535 and Miltenyi Biotec, Bergisch Gladbach, Germany, Cat# 130-104-368) for the first 24 hours.

Differentiation of hiPSCs into cortical neurons (iNeurons)

Differentiation into cortical neurons was performed as described before with slight modifications (Wang et al., 2017; Bachmann et al., 2021b; Buchholz et al., 2024). At the start of differentiation, iPS cells were harvested using Accutase (Sigma, St. Louis, MO, USA, Cat# A6964-100ML) and seeded onto Geltrex-coated plates using pre-differentiation medium (Thermo Fisher Scientific, Cat# 12660012) supplemented with thiazovivin (day before differentiation (d) –3). The medium was changed daily for 2 days to fresh pre-differentiation medium without thiazovivin. On day 0, 50,000 cells were seeded onto Poly-D-Lysine (Sigma, #P7886-50MG)/Laminin (Trevigen, Minneapolis, MN, USA, Cat# 3446-005-01)-coated 24-well-plates using maturation medium supplemented with 1:100 GelTrex. Half of the media was exchanged once per week until analysis.

Lentiviral-based expression of TAU species

The longest human TAU isoform 2N4R or 2N4R-TAU with the P301L mutation were cloned into the lentiviral expression plasmid pUltra (Addgene, Watertown, MA USA, Cat# 24129), resulting in a multi-cistronic lentiviral construct expressing green fluorescent protein (GFP) and the corresponding HA-tagged TAU. To produce lentiviral particles, HEK293T cells (standard cell line used here for virus production purposes only, refer to CVCL_0063) were co-transfected with the corresponding pUltra plasmid alongside the packaging plasmid psPAX (Addgene, Cat# 12259) and the envelope plasmid pMD2.G (Addgene, Cat# 12260). Four and five days after

transfection, the lentivirus-containing culture supernatant was collected, filtered, and stored at –80°C. TAU knockout (KO) iNeurons were transduced with the lentiviral particles on day 21 with 5000–10,000 transduction units to obtain a transduction efficiency of 10%–20%, to avoid overexpression by multiplicity of infection and to easier select the transduced cells. iNeurons were analyzed 10 days following transduction (day 31). More details on the lentiviral transduction of iNeurons are described in Buchholz et al. (2024).

Immunofluorescence labeling of iNeurons

iPSC-derived neuronal cultures were fixed with 3.7% Formaldehyde in PBS containing 4% sucrose at room temperature for 30 minutes. Afterwards, cells were permeabilized and blocked for 10 minutes in 5% BSA (Carl Roth, Karlsruhe, Germany, Cat# 8076.4) and 0.2% Triton X-100 (Carl Roth, Cat# 3051.2) in PBS. Fixed neurons were then stained with the corresponding primary antibody dilution at 4°C overnight. On the next day, coverslips were washed three times with PBS and stained with the corresponding secondary antibodies coupled to an AlexaFluor dye for 2 hours at room temperature. Following washing with PBS and staining with NucBlue (Thermo Fisher Scientific, #R37605) for 20 minutes at room temperature, coverslips were mounted onto glass slides using Aqua-Poly/Mount (Polysciences, Warrington, PA, USA #18606-20) and left to dry for 24 hours at room temperature. The primary and secondary antibodies used are shown in

Table 1.

Sorting of TAU species in TAU KO iNeurons

TAU KO iNeurons were transduced with the corresponding lentiviral particles as described above and stained for HA-tag and microtubule-associated protein 2 (MAP2). Axonal and dendritic sorting were analyzed as described before (Bachmann et al., 2021a; Bell et al., 2021) by measuring mean fluorescence intensities of GFP and TAU in the axon or dendrite, and soma.

Animals

Transgenic TAU mice (pR5 mice) have been previously generated on a B6D2F2 background followed by backcrossing with C57BL/6 mice for more than ten generations. They express the longest human TAU isoform, htau40, together with the pathogenic mutation P301L that has been previously identified in frontotemporal dementia and parkinsonism (FTDP). Transgene expression is driven by a modified version of the mThy1.2 promoter that confers neuronal expression (Götz et al., 2001; Köhler et al., 2013). Up to five animals were housed per cage. Paraffin sections from pR5 mouse brains available from a previous study (Köhler et al., 2013) were used for immunolabelling. For transcardial perfusion (used for histology) mice were deeply anesthetized with ketamine (100 mg/kg)/xylazine (5 mg/kg) i.p. and perfused via the left ventricle with 0.1 M phosphate-buffered saline, pH 7.4 for 3 minutes, followed by 4% paraformaldehyde for 15 minutes. To obtain material for biochemical analysis, mice were deeply anesthetized with 3.5% isoflurane in an anesthesia chamber and then subjected to cervical dislocation. For the generation of primary neurons, postnatal animals (day

1–2 pups) were subjected to rapid scissor cut decapitation, which is the method of choice according to the EU-guideline 2010/63. Apart from acute sacrificing, no potentially painful experiments were performed, no surgery was performed, and no drugs were administered. A total of 31 animals were used for this study; for histology, previously available brain sections from 20 animals were studied (ten pR5 mice and ten non-transgenic littermates); for western blotting, 11 animals were used (five pR5 mice and six non-transgenic littermates). Animal experiments (e.g., the methods of sacrifice and anesthesia were chosen in consultation with the veterinarians) were approved by the State Agency for Nature, Environment and Consumer Protection (LANUV), North Rhine-Westphalia, Recklinghausen, Germany (Ethics protocol Nos. AZ 84-02.05.40.14.028, AZ 8.87-51.05.20.10.260, AZ §4.21.004, AZ §4.21.006).

Primary neuronal cultures from the hippocampus of postnatal pR5 mice

Primary mouse neurons were isolated and cultured as described before (Zempel et al., 2017). Briefly, the brains of postnatal mice (p0) were dissected. The cerebellum, midbrain, thalamic tissue, and meninges were removed, and the hippocampi were separated and digested with trypsin (PAN-Biotech, Aidenbach, Germany, Cat# P10-024100). The cell suspension was diluted in neuronal plating medium [DMEM/F12+GlutaMax (Thermo Fisher Scientific, Cat# 10565-018), 10% FBS, 1% antibiotic/antimycotic solution (Sigma, #A5955-100ml)], and seeded onto coated plates. After 4 hours, the media was exchanged to neuronal maintenance medium [Neurobasal media (Thermo Fisher Scientific, Cat# 21103-049), 1× GlutaMax (Thermo Fisher Scientific, Cat# 35050061), 1× NS21 (PAN-Biotech, Cat# P07-20001), 1% antibiotic/antimycotic solution]. Two days after plating, cells were treated with 0.5 µg/mL AraC (Sigma, Cat# C6645), and half the media was exchanged twice a week.

Immunofluorescence labeling of mouse brain sections

Staining of five µm-thick paraffin mouse brain sections was performed as described before (Puladi et al., 2021). The number of animals used for each experiment is indicated in the figure legends. Briefly, sections were deparaffinized in xylene and rehydrated. Afterwards, sections were pre-treated by boiling three times for 5 minutes in citrate buffer (pH 6.0) in a microwave oven to retrieve the antigens. After three washes in TBS and blocking in 5% horse serum (Vector Laboratories, Newark, CA, USA, Cat# S-2000-20) for 45 minutes at room temperature, the primary antibodies, diluted in TBS, were applied, and the sections were incubated overnight at 4°C. After washing with TBS, the sections were incubated with the corresponding secondary antibody coupled to an AlexaFluor dye for 30 minutes at room temperature. Following washing with TBS, autofluorescence was quenched with Sudan Black B solution (Carl Roth, Cat# 0292.1) for 20 minutes, and nuclei were stained with Hoechst solution (Invitrogen, Waltham, MA, USA, Cat# H3570). Sections were mounted on glass slides and left to dry at 4°C overnight. The primary and secondary antibodies used are shown in **Table 1**.

Imaging

Immunostained iNeurons and mouse brain sections were imaged using a wide-field fluorescence microscope (Axioscope 5, Zeiss, Oberkochen, Germany) with the help of ZenBlue Pro imaging software (V2.5, Zeiss). Images were later analyzed using ImageJ software (version 2.14.0/1.54f, National Institutes of Health and the Laboratory for Optical and Computational Instrumentation (LOCI), University of Wisconsin, USA). In general, the absolute somatic or dendritic levels of the signal of interest were measured as mean fluorescence intensity for each channel in the CA1, CA3, and subiculum regions of the hippocampus. For each neuron, the region of interest (ROI) was manually delineated as a profile of the soma or the dendrite where no other somas or processes overlapped, and the mean fluorescence intensity signal was measured.

Western blot analysis

For Western blot analysis, mice hippocampal lysates were diluted in 5× Laemmli sample buffer, boiled for 10 minutes at 95°C, and separated on 10% Sodium dodecyl sulfate (SDS)-polyacrylamide gels. Afterwards, proteins were transferred to polyvinylidene fluoride (PVDF) membranes overnight at 4°C and blocked in 5% bovine serum albumin (BSA) in Tris-buffered saline with 0.1% Tween (TBS-T). Membranes were incubated with the primary antibody overnight at 4°C, washed three times with TBS-T, and incubated with the corresponding secondary horseradish peroxidase (HRP)-coupled antibody for 1 hour at room temperature. Following washing with TBS-T, the immunoreactions were detected by applying the SuperSignal West Pico Chemiluminescent Substrate (Thermo Fisher Scientific) using a ChemiDoc XRS + system (Bio-Rad, Hercules, CA, USA). The primary and secondary antibodies used are shown in **Table 1**.

Statistical analysis

The GraphPad Prism (v9.5.1, GraphPad Software, Boston, MA, USA, www.graphpad.com) was used for statistical analysis. Shapiro-Wilk test was performed to test for normal distribution of the data. In case of normal distribution, statistical analysis was performed by unpaired *t*-test to compare the means of two groups, or one-way analysis of variance with correction for multiple comparisons (Tukey's test) to compare three or more groups. Otherwise, the Mann-Whitney *U* test or Kruskal-Wallis test with correction for multiple comparisons (Dunn's test) were carried out, respectively. Statistical significance was denoted by a significance level of *P* < 0.05.

Results

pR5 mice exhibit changes in acetylation and polyglutamylation of neuronal microtubules

Microtubule stability is of key importance for proper neuronal function. We thus aimed to investigate the hallmarks and progress of TAU pathology in an *in vivo* model of tauopathy and its potential downstream effects on major PTMs of microtubules indicative of their stability and dynamics. We first stained brain sections of pR5 mice (transgenic for P301L-TAU) and age-matched non-transgenic littermates for TAU localization and phosphorylation. TAU was hyperphosphorylated (more than 20-fold increase in



Table 1 | Primary and secondary antibodies used in this study

Antibody	Animal species	Clonality	Cat#	Supplier	RRID	Use and dilution
Total TAU (K9JA)	Rabbit	Polyclonal	A0024	Agilent, Santa Clara, CA, USA	AB_10013724	ICC (1:1000) IHC (1:500)
Phospho-TAU (Ser202, Thr205) antibody (AT8)	Mouse	Monoclonal	MN1020	Thermo Fisher Scientific, Waltham, MA, USA	AB_223647	ICC (1:500) IHC (1:400)
Anti-TAU Alzheimer's disease antibody (GT-38)	Mouse	Monoclonal	ab246808	Abcam, Cambridge, UK	AB_2864300	ICC (1:500)
TAU (phospho-Ser262) antibody	Rabbit	Polyclonal	11111	Signalway Antibody, College Park, MD, USA	AB_896045	ICC (1:500)
Acetylated tubulin (Lys40) (D20G3)	Rabbit	Monoclonal	5335	Cell Signaling Technology, Danvers, MA, USA	AB_10544694	ICC (1:500) IHC (1:400) WB (1:1000)
Anti-polyglutamylated tubulin antibody	Mouse	Monoclonal	T9822	Sigma, St. Louis, MO, USA	AB_477598	ICC (1:500) IHC (1:1000) WB (1:1000)
Anti-tyrosinated tubulin antibody	Rat	Monoclonal	MAB1864-I	Sigma	AB_2890657	ICC (1:500) WB (1:1000)
Anti-tubulin antibody clone DM1A	Mouse	Monoclonal	T6199	Sigma	AB_477583	WB (1:1000)
βIII-Tubulin antibody	Rabbit	Polyclonal	A17074	ABClonal, Woburn, Massachusetts, USA	AB_2772760	WB (1:1000)
GAPDH antibody	Mouse	Monoclonal	sc-365062	Santa Cruz Biotechnology, Dallas, Texas, USA	AB_10847862	WB (1:1000)
Anti-HA.11 Epitope Tag antibody	Mouse	Monoclonal	MMS-101P	BioLegend, San Diego, California, USA	AB_2314672	ICC (1:1000)
Anti-MAP2 antibody	Chicken	Polyclonal	ab5392	Abcam	AB_2138153	ICC (1:2000)
Anti-mouse secondary antibody, Alexa Fluor™ 488	Goat	Polyclonal	A-10680	Thermo Fisher Scientific	AB_2534062	ICC (1:1000) IHC (1:500)
Anti-rabbit secondary antibody, Alexa Fluor™ 488	Donkey	Polyclonal	A-21206	Thermo Fisher Scientific	AB_2535792	ICC (1:1000)
Anti-Mouse Secondary Antibody, Alexa Fluor™ 568	Goat	Polyclonal	A-11031	Thermo Fisher Scientific	AB_144696	ICC (1:1000)
Anti-rabbit secondary antibody, Alexa Fluor™ 568	Donkey	Polyclonal	A10042	Thermo Fisher Scientific	AB_2534017	ICC (1:1000) IHC (1:400)
Anti-rat secondary antibody, Alexa Fluor™ 568	Goat	Polyclonal	A-11077	Thermo Fisher Scientific	AB_2534121	ICC (1:1000)
Anti-chicken secondary antibody, Alexa Fluor™ 647	Goat	Polyclonal	A21449	Thermo Fisher Scientific	AB_2535866	ICC (1:1000)
Anti-mouse secondary antibody, HRP	Goat	Polyclonal	115-035-003	Jackson ImmunoResearch Labs, Baltimore Park, PA, USA	AB_10015289	WB (1:1000)
Anti-rabbit secondary antibody, HRP	Goat	Polyclonal	7074	Cell Signaling Technology	AB_2099233	WB (1:1000)
Anti-rat secondary antibody, HRP	Goat	Polyclonal	31470	Invitrogen	AB_228356	WB (1:1000)

GAPDH: Glyceraldehyde 3-phosphate dehydrogenase; HRP: horseradish peroxidase; ICC: immunocytochemistry; IHC: immunohistochemistry; WB: western blot.

tauopathy-typical AT8 phosphorylation, **Figure 1A**), and markedly missorted to the somatodendritic compartments of neurons in the hippocampi of pR5 mice as early as 8 months of age (**Figure 1B–D**). As aggregation of TAU in this mouse model only starts to occur at around 8 months of age (Köhler et al., 2013), this means that TAU missorting likely precedes the appearance of the first mature neurofibrillary tangles.

Next, we stained for acetylation and polyglutamylation of microtubules. Intensely AT8-positive neurons in 24-month-old pR5 mice exhibited a statistically significant decrease (~30%) of acetylated tubulin compared with neighboring, AT8-negative neurons (**Figure 2A and C**). Additionally, we observed morphological changes in the dendrites positive for polyglutamylated tubulin of 2-year-old pR5 mice, but the pattern of polyglutamylation did not show changes in the brains of the group of younger mice (**Figure 2B and D**). Dendrites were shorter and stubbier compared with longer and thinner dendrites abundant in the brains of non-transgenic littermates, and there was an obvious decrease (~45%) in the number of polyglutamylation-positive long dendrites (**Figure 2B and E**). In addition, the remaining long thin dendrites in 2-year-old pR5 mice showed a slight, but

statistically significant increase in the fluorescence intensity of polyglutamylated tubulin (**Figure 2B and E**).

Next, we wanted to further compare the potential changes of PTMs of microtubules in the brains of pR5 mice and non-transgenic littermates. For this, hippocampal lysates of pR5 mice and non-transgenic littermates at the age of 40 weeks were probed via immunoblotting to assess PTMs of microtubules. The levels of acetylated tubulin showed a robust decrease in the hippocampal lysates from pR5 mice, while the levels of polyglutamylated tubulin were statistically significantly increased when normalized to β-III-tubulin, which is a neuron-specific isoform of tubulin, but showed only a trend when normalized to glyceraldehyde 3-phosphate dehydrogenase (GAPDH) or total α-tubulin. Tyrosinated tubulin showed a trend to decrease in pR5 mice but this was only significant when normalized to GAPDH. The same recurrent tendency to decrease was observed for β-III-tubulin, while the levels of α-tubulin remained constant between the two groups (**Figure 3A–D**). Taken together, these results show a global and prominent decrease in acetylated microtubules (and thus in their stability) in the hippocampi of pR5 mice, while the increase in polyglutamylated tubulin was

Downloaded from http://journals.lww.com/nrronline by BNDMSEPHKav1zEoum1tQINd4+kLLHEZgbsIH04XMI0hCw CX1AWNvQpIIGHDB33D00dRy7TVSFI4C3VC1y0abgQZXdg9j2mWZLei= on 07/10/2024

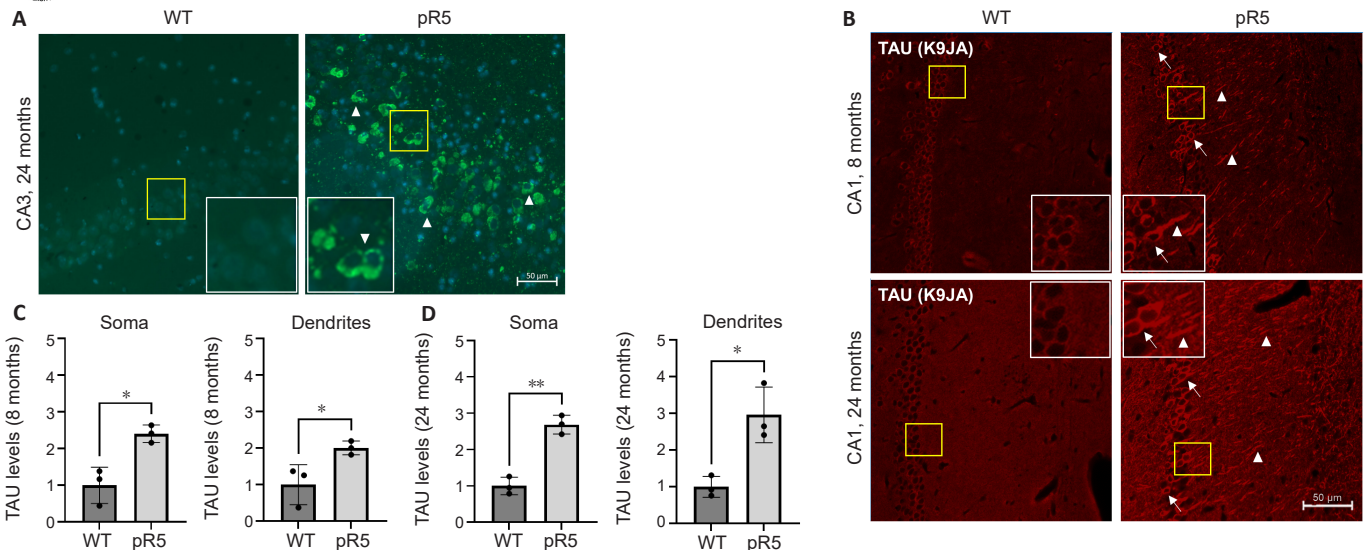


Figure 1 | Several neurons in the CA1 and CA3 regions of the hippocampus of pR5 mice exhibit strong AT8 immunoreactivity and TAU missorting.

Paraffin brain sections from pR5 mice and non-transgenic littermates were immunolabelled with antibodies against pan-TAU and phospho-TAU as described in the Methods section. (A) Immunofluorescence labeling of pR5 mice hippocampal sections shows abundance of (green) AT8-positive neurons, while similar immunoreactivity is absent in mouse brain sections from non-transgenic littermates. Arrowheads indicate AT8-positive neurons. Insets show 2.5-fold magnification of the areas in the yellow frames. (B) Immunofluorescence labeling with a pan-TAU antibody (K9JA, red) shows that TAU is missorted (i.e., present in the soma and dendrites, as shown in insets displaying 3-fold magnification of the areas in the yellow frames) in pR5 mice neurons. Arrows indicate somas positive for TAU, while arrowheads indicate dendrites. Scale bars: 50 μ m in A and B. (C, D) Quantification of Tau mean immunofluorescence intensity in somas and dendrites of 8- (C) and 24-month-old (D) pR5 mice and non-transgenic littermates show a significant increase of TAU signal in somatodendritic compartments of pR5 mice neurons of both age groups. $n = 3$ animals per group. Unpaired t -test was performed for the determination of significant differences. * $P < 0.05$, ** $P < 0.01$. pR5: Mice transgenic for human P301L-TAU; WT: wild-type.

subtler and only significant when normalized to a neuronal subtype of tubulin, β -III-tubulin. Of note, β -III-tubulin itself exhibited a slight, albeit statistically insignificant, decrease in pR5 mice as well (Figure 3E). This could be due to SPASTIN-mediated severing because of elevated polyglutamylation, and consequent loss of microtubule mass/neuronal volume.

Sorting and phosphorylation of 2N4R- and P301L-TAU in iNeurons

Next, we aimed to study P301L-TAU in neuronal cell culture, to gain an in-depth understanding of its axodendritic sorting and effect on microtubule PTMs. Primary neuronal cultures from the hippocampus of postnatal pR5 mice did not show specific human TAU immunolabelling using a human TAU-specific antibody in a significant number of cells (HT7, $< 1/1000$ cells, data not shown, while the antibody worked well in human neurons, Figure 4D). This is likely due to promoter incompatibility with immediate postnatal preparations of primary neurons. This renders primary neurons from the pR5 mice unsuitable as a cell model to study the consequences of human P301L-TAU expression. Therefore, the next step was to validate the previous findings regarding the effect of P301L-TAU on TAU sorting and phosphorylation, and on the PTMs of microtubules, in a human-relevant cell model. For this, we used human induced pluripotent stem cells-derived neurons (iNeurons). WTC11 cells with an additional transgene, Neurogenin2, were differentiated into excitatory cortical neurons with extremely high efficiency ($> 90\%$), and within 3 weeks, via a differentiation protocol that provides minimal neuronal survival factors (N2, BDNF, NT3 in standard neuronal

differentiation medium) but with the addition of doxycycline (Wang et al., 2017). In addition, our lab established MAPT-KO iPSC lines, which can also be differentiated into the same neuronal subtype without effects on neuronal activity or properties (Bachmann et al., 2023). To introduce P301L-TAU into the cells, we cloned the coding sequence of the MAPT gene, carrying the mutation P301L associated with FTDP-17 and marked with an HA-tag, into a lentiviral vector (pUltra, which contains an eGFP marker, separated by a 2A peptide), on the basis of the longest TAU isoform, 2N4R-TAU. As a control, WT-MAPT cDNA coding for the longest TAU isoform 2N4R was also cloned in the same vector.

iNeurons on day 21 after the start of differentiation were transduced with the corresponding lentiviral particles (Figure 4A), and the neurons were fixed 10 days after transduction. The sorting of 2N4R-TAU and P301L-TAU was investigated and compared as described previously (Bell et al., 2021). Unexpectedly, P301L-TAU did not show less efficient axonal targeting compared with wild-type 2N4R-TAU. Both 2N4R- and P301L-TAU favored localization to axons more than somatodendritic compartments, as indicated by their high axonal enrichment factors (AEF), which is defined as the axon-to-soma ratio of TAU normalized to the axon-to-soma ratio of the randomly distributed volume/transduction marker GFP ($AEF_{2N4R-TAU} = 8.37 \pm 2.42$, $AEF_{P301L-TAU} = 9.12 \pm 2.97$) (Figure 4B and C). Dendritic enrichment factor (DEF) was also similar for both WT and mutant TAU, but less by around 40% than their AEFs, indicating an axonal preference for both expressed TAU, albeit with a prominent dendritic presence.

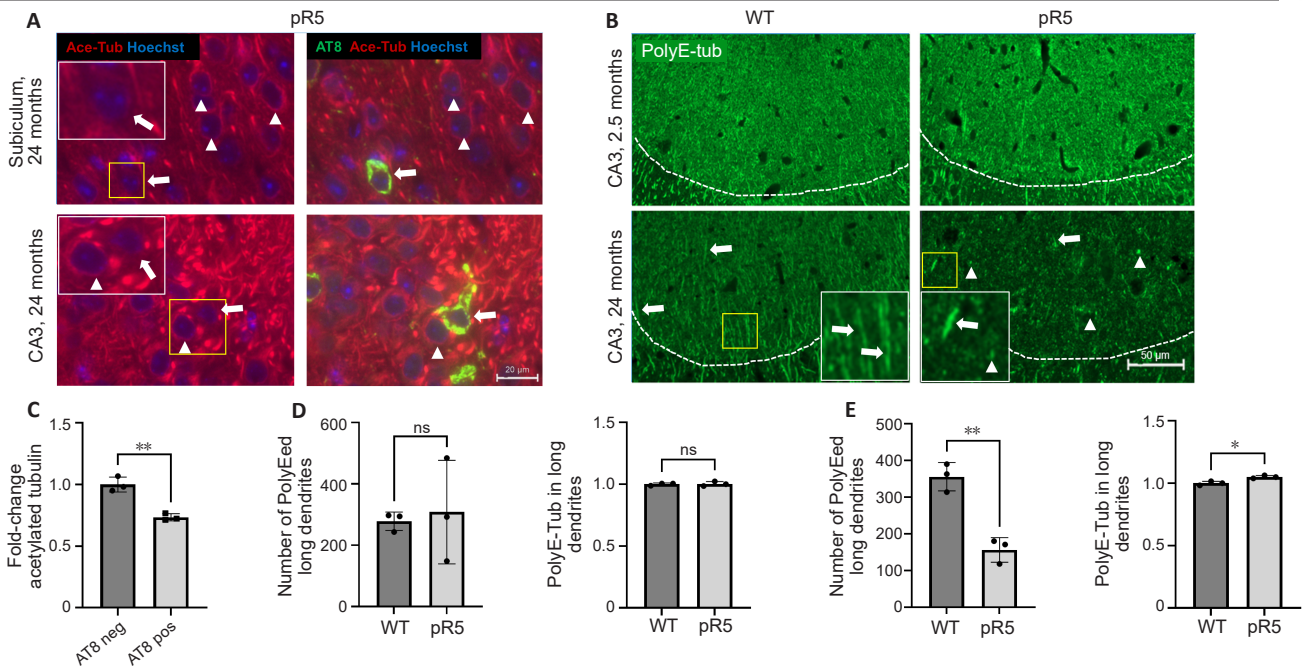


Figure 2 | Microtubules in neurons in the CA3 region of the hippocampus and subiculum of pR5 mice exhibit stability-decreasing changes in their essential post-translational modifications.

Paraffin brain sections from pR5 mice and non-transgenic littermates were immunolabelled with antibodies against ace-tub and polyE-tub as described in the Methods section. (A) Intensely AT8-positive neurons (green) have less tubulin acetylation (red) in comparison to neighbouring AT8-negative neurons in pR5 mice brain sections. The right panels represent merged images of both signals (AT8 and ace-tub), while the left panels show the same images only with the red signal. Insets show 2.5-fold magnifications of the areas in the yellow frames. Arrows indicate AT8-positive neurons lacking ace-tub, while arrowheads indicate neighboring AT8-negative neurons exhibiting normal tubulin acetylation. (B) Dendrites positive for polyE-tub (green) showed morphological changes in the CA3 field of the hippocampus of pR5 mice. The PolyE-tub antibody stained more intensely shorter, stubbier dendrites in the transgenic mice compared with longer, thinner ones in the non-transgenic littermates 24 months of age (lower panel), but not in the younger, 2.5-month-old mice (upper panel). Insets show 2.5-fold magnifications of the areas in the yellow frames. Arrows indicate long thin dendrites, while arrowheads indicate shorter, stubbier dendrites. The area below the dashed lines is an axon-rich area (Mossy fibers), which was not analyzed. Scale bars: 20 μ m in A and 50 μ m in B. (C) Quantification of the mean fluorescence intensity of ace-tub in A shows a significant decrease of tubulin acetylation in AT8-positive (pos) neurons compared with AT8-negative (neg) neurons. $n = 3$ animals per group. (D, E) Quantification of the number of dendrites which are larger than 20 μ m² and positive for PolyE-tub (left) and PolyE-tub mean fluorescence intensity (right) in brain sections of 2.5-month-old (D) or 24-month-old (E) pR5 mice and non-transgenic littermates. $n = 3$ animals per group. Unpaired *t*-test was performed for the determination of significant differences except for D, right, where a Mann–Whitney *U* test was carried out. * $P < 0.05$, ** $P < 0.01$. Ace-tub: Acetylated tubulin; ns: not significant; PolyE-tub: polyglutamylated tubulin; pR5: mice transgenic for human P301L-Tau; WT: wild-type.

Similar to our finding in pR5 mice, overexpressed P301L-TAU showed a significant increase in AT8 reactivity compared with WT control. Interestingly, 2N4R-TAU also exhibited increased AT8 reactivity, albeit insignificant, compared with WT iNeurons (Figure 5). However, 2N4R-TAU showed a remarkable increase in the phosphorylation level on the Ser262 epitope (the first of KxGS motifs within the repeat domains), which was significantly higher than the level observed with P301L-TAU (Figure 5). On the other hand, both WT- and P301L-TAU did not show any specific reactivity towards the conformation-specific GT-38 antibody, indicating the lack of any TAU aggregation following the expression of either of them (Figure 5). This means that the expression of either 2N4R- or P301L-TAU on TAU KO background results in increases in their phosphorylation on different epitopes compared with endogenous WT levels, but does not lead to TAU aggregation.

PTMs of microtubules in iNeurons transduced with 2N4R- or P301L-TAU

Next, the potential changes in the levels of different PTMs of microtubules following the overexpression of 2N4R- or P301L-TAU were investigated and compared in both somas and

dendrites of transduced neurons. Firstly, acetylation levels were checked as a marker of stable microtubules. Expression of both TAU species significantly increased the levels of acetylated tubulin compared with control WT and TAU KO neurons transduced with empty vector (Figure 6). P301L-TAU-transduced neurons showed slightly less acetylation than their WT-TAU-transduced counterparts did, more prominently in the dendrites. Interestingly, although insignificant, TAU KO neurons in general showed slightly increased levels of tubulin acetylation.

When investigating the levels of tubulin polyglutamylation, P301L-TAU-transduced neurons exhibited increased polyglutamylation compared with WT and TAU KO control neurons. However, no significant changes in polyglutamylation were observed between P301L- and 2N4R-expressing neurons (Figure 6).

Finally, the expression of 2N4R-TAU led to an insignificant increase in the levels of tubulin tyrosination. Despite not crossing the traditional threshold of significance, it was still noteworthy that P301L-expressing neurons had less tyrosinated tubulin compared with 2N4R-expressing neurons (Figure 6).

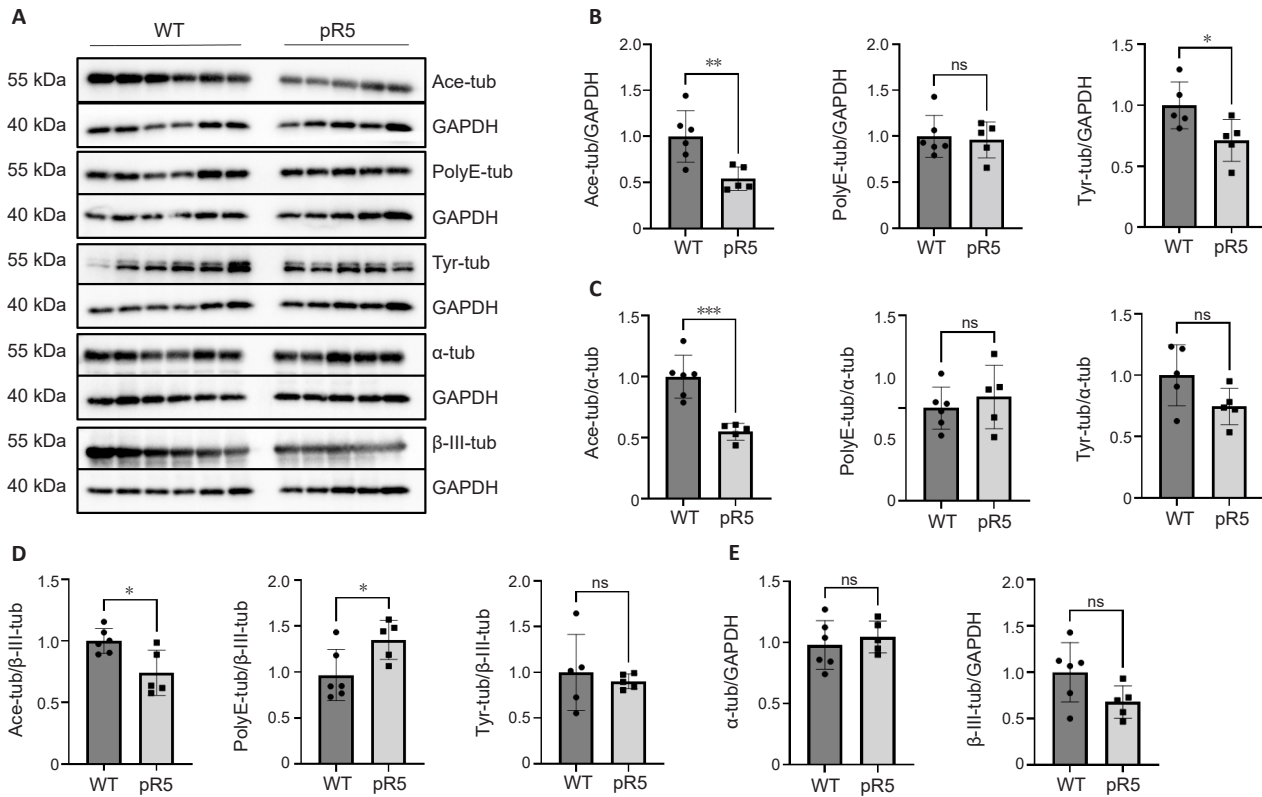


Figure 3 | Levels of tubulin and its post-translational modifications in hippocampal lysates from 40-week-old pR5 mice and non-transgenic littermates.

(A) Western blots of Ace-tub, PolyE-tub, and Tyr-tub, and loading controls α -tubulin, β -III-tubulin, and GAPDH. (B–D) Quantification of the levels of tubulin acetylation, polyglutamylation, and tyrosination normalized to GAPDH (B), α -tubulin (C), or β -III-tubulin (D). (E) Quantification of the levels of α -tubulin and β -III-tubulin normalized to GAPDH. $n = 5$ –6 animals per group. Unpaired t -test was performed for the determination of significant differences. * $P < 0.05$, ** $P < 0.01$. Ace-tub: acetylated tubulin; GAPDH: glyceraldehyde 3-phosphate dehydrogenase; ns: not significant; PolyE-tub: polyglutamylated tubulin; Tyr-tub: tyrosinated tubulin; WT: wild-type; β -III-tub: β -III-tubulin.

Discussion

Here we described the effect of P301L-TAU, a common *MAPT* mutation involved in frontotemporal dementia with parkinsonism linked to chromosome 17 (FTDP-17), on PTMs of microtubules indicative of their stability and dynamics. We carried out this study in pR5 mice, an established transgenic mouse model of tauopathy, and also in human iPSC-derived cortical neurons. Neurons in pR5 mouse brains showed typical TAU AT8 hyperphosphorylation and TAU mislocalization to the somatodendritic compartments. The presence of intensely AT8-positive neurons in old pR5 mice is tightly associated with the presence of neurofibrillary tangles (Deters et al., 2008; Köhler et al., 2014). The neuronal microtubules of pR5 mice exhibited a prominent decrease in acetylation both in stained hippocampal sections (mainly in the subiculum and field CA3 of the hippocampus) and in immunoblotted hippocampal lysates. Acetylated microtubules have long been associated with stable, long-lived microtubules (Maruta et al., 1986), and their significant decrease in intensely AT8-positive neurons compared with AT8-negative neurons in the same field of view indicates that this decrease in the acetylation of microtubules, and therefore in their stability, is a result of the presence of neurofibrillary tangles in these neurons. It is interesting to know whether tubulin acetylation is already reduced when TAU is only hyperphosphorylated but tangles have not yet formed. Our western blot results suggest this, because tangles

are rare or absent at the age of the mice investigated by western blot.

Changes in polyglutamylation were subtler but still statistically significant. In the hippocampus of pR5 mice, dendrites positive for polyglutamylated tubulin in CA3 showed stubby morphology unlike the long slender dendrites in the same brain region of the non-transgenic littermates. This observation was true for the 2-year-old mice with advanced TAU pathology. It has been reported that aged transgenic pR5 mice showed decreased dendritic length of hippocampal CA1 neurons, as well as an increase in stubby spines and filopodia, which is thought to be a consequence of hyperphosphorylated P301L-TAU (Müller-Thomsen et al., 2020). Polyglutamylation is a unique modification that adds glutamate residues on the C-terminal tail of tubulin, and results in the recruitment of SPASTIN, a microtubule-severing enzyme. Polyglutamylation is carried out by members of the TLL family, a member of which, TLL6, is thought to recruit SPASTIN upon $A\beta$ -induced TAU misorting in primary rat neurons (Zempel et al., 2013), while TLL1 and 4 were recently shown to drive neurodegeneration in Purkinje cell degeneration (pcd) mice (Wu et al., 2022). Our western blot data also showed increased polyglutamylation in the brain lysate of 40-week-old pR5 mice when normalized to neuronal β -III-tubulin. Taken together, we think that P301L-TAU expression results in polyglutamylation of microtubules,

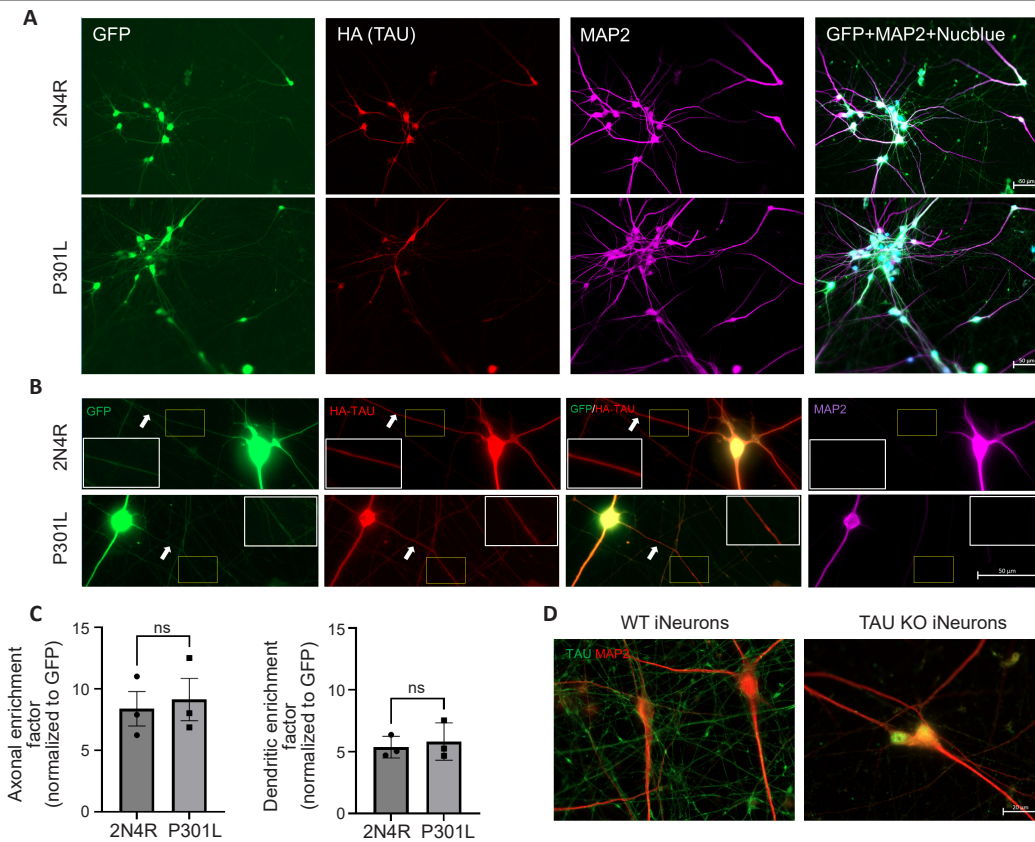


Figure 4 | 2N4R- and P301L-Tau exhibit similar sorting behavior when overexpressed in iNeurons.

Tau KO neurons on day 21 were lentivirally transduced with the corresponding TAU construct for 10 days, followed by fixation and immunostaining as described in the Methods section. (A) Exemplary staining of lentivirally expressed 2N4R- or P301L-TAU in iNeurons. TAU (red) is visualized via staining with an anti-HA tag antibody, while MAP2 (magenta) serves as a dendritic marker. GFP (green) is a marker for volume distribution as well as transduction efficiency. Scale bars: 50 μ m. (B) Co-staining of HA-TAU and MAP2 in iNeurons lentivirally expressing 2N4R- or P301L-TAU. GFP was used as a volume marker. Arrows indicate axons. Insets show 2-fold magnifications of axonal segments within the yellow frames. Scale bars: 50 μ m. (C) Quantification of the axonal and dendritic enrichment factors of both TAU species. $n = 3$ biological replicates, $n = 15$ neurons of each replicate. Unpaired t -test was performed for the determination of significant differences. (D) Immunostaining of iNeurons reveals typical axonal sorting of endogenous TAU (anti-human TAU clone HT7, green) and somatodendritic localization of MAP2 (red) in WT iNeurons (left) and lack of TAU immunoreactivity in Tau KO iNeurons (right). Scale bar: 20 μ m. 2N4R: TAU isoform; GFP: green fluorescent protein; HA-tag: human influenza hemagglutinin tag; iNeurons: induced pluripotent stem cell-derived neurons; KO: knockout; MAP2: microtubule associated protein 2; ns: not significant; WT: wild-type.

labeling them for SPASTIN severing, which may lead to the morphological changes of dendrites observed in our immunofluorescence labeling data.

We also managed to express P301L-TAU and WT 2N4R-TAU in our iPSC-derived neurons on a *MAPT* KO background as a human tauopathy-relevant neuronal model. Interestingly, P301L-TAU here showed similar axonal sorting efficiency as 2N4R-TAU did. Both WT and mutant TAU showed comparable dendritic targeting, and while their dendritic enrichment factors were significantly lower than their axonal enrichment factors, TAU still showed considerable presence in the dendrites, unlike endogenous TAU in this cell model, which indicates that the axonal targeting of overexpressed WT and mutant TAU was partially reduced. Moreover, it was also interesting to investigate the patterns of TAU phosphorylation on different epitopes, such as AT8 and p-Ser262, in addition to the conformation-specific GT-38 epitope associated with TAU aggregates. GT-38 antibody detects a conformation-specific epitope within tangles containing both 3R and 4R isoforms of TAU in a phosphorylation-independent manner, making it able

to detect Alzheimer's disease-specific TAU pathology, and also TAU pathology in Frontotemporal Lobar Degeneration-TAU (FTLD-TAU) (Gibbons et al., 2019). We used GT-38 antibody in our study to investigate whether the expression of P301L-TAU or 2N4R-TAU promotes the aggregation of TAU in our model, and to distinguish this potential aggregation from total hyperphosphorylated TAU detected by the AT8 antibody. As could be expected due to the absence of 3R-TAU in our model, we did not find AD-typical aggregation in our human neurons. However, it was of note that both TAU species exhibited different phosphorylation patterns, with 2N4R-TAU being more phosphorylated at the Ser262 epitope, and P301L-TAU at the AT8 epitope. Phosphorylation of TAU at Ser262 regulates TAU binding to microtubules, and its elevated phosphorylation level on 2N4R-TAU could be an important regulation mechanism that is lacking in P301L-TAU. Interestingly, a previous study showed that 12E8 staining (which includes p-Ser262 epitope) did not discriminate wild type from pR5 mice (Götz et al., 2001). We think that the overexpression of WT 2N4R-TAU overloads the microtubules, which results in a feedback mechanism that phosphorylates

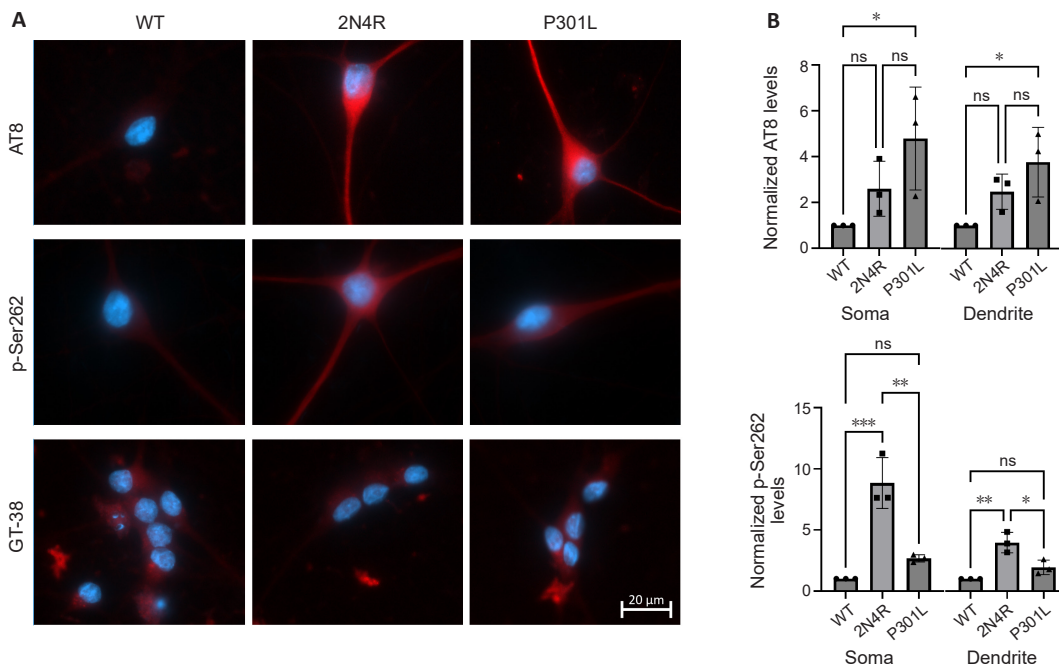


Figure 5 | 2N4R- and P301L-Tau exhibit different phosphorylation patterns when expressed in iNeurons.

iNeurons on day 21 were lentivirally transduced with the corresponding Tau construct for 10 days, followed by fixation and immunostaining as described in the Methods section. (A) TAU KO iNeurons transduced with 2N4R- or P301L-TAU, and WT iNeurons transduced with empty vector were immunostained for two different TAU phosphorylation epitopes (AT8, red, p-Ser262, red), and one TAU aggregation epitope (GT-38, red). Blue color corresponds to 4',6-diamidino-2-phenylindole (DAPI) staining (nuclei). Scale bar: 20 μ m. (B) Quantification of the mean fluorescence intensities of AT8 and p-Ser262 shows a significant increase of AT8 signal in neurons expressing P301L-TAU and a significant increase of p-Ser262 signal in neurons expressing 2N4R-TAU. $N = 3$ biological replicates, $n = 15$ neurons of each replicate. Ordinary one-way analysis of variance with Tukey's multiple comparison test was performed for the determination of significant differences. * $P < 0.05$, ** $P < 0.01$, *** $P < 0.001$. 2N4R: Tau isoform; iNeurons: induced pluripotent stem cell (iPSC)-derived neurons; KO: knockout; ns: not significant; WT: wild-type.

TAU on Ser262 inducing TAU dissociation from microtubules. This phosphorylation was not significantly increased in P301L-TAU, probably since P301L-TAU already has a reduced affinity to microtubules (Hasegawa et al., 1998).

Furthermore, we investigated the effects of the expression of 2N4R- and P301L-TAU on the PTMs of neuronal microtubules via immunolabelling and fluorescent microscopy. We aimed to compare the levels of PTMs in a compartment-specific manner, which is only doable via fluorescence microscopy allowing distinguishing between different neuronal compartments. In addition, it was important to compare the PTMs in the transduced cells only, which are easily distinguishable via the GFP signal, and which allows the exclusion of the effects of the baseline levels of PTMs in non-transduced cells. The efficiency we aimed to achieve was between 10%–20%. Higher transduction rates would go along with marked overexpression of (mutant) TAU (which is after all a microtubule-stabilizing protein) which would introduce confounding effects that are to be avoided to maintain a physiologically relevant model.

Interestingly, expression of both 2N4R- and P301L-TAU resulted in increased tubulin acetylation compared with TAU KO iNeurons or iNeurons expressing endogenous levels of TAU. This could indicate that the overexpression of 2N4R-TAU leads to more microtubule stabilization, evidenced by the elevated acetylation levels. However, although insignificant, it is noteworthy that P301L-TAU expression induced less tubulin

acetylation levels than 2N4R-TAU did. It has been shown that TAU interacts with histone deacetylase 6 (HDAC6), which is a major α -tubulin deacetylase (Ding et al., 2008), and that inhibition of HDAC6 rescues microtubules defects induced by TAU overexpression (Mao et al., 2017). As prolonged expression of P301L-TAU at least in our mice results in decreased acetylation, this increase in acetylation observed in our iNeurons could simply be due to the canonical function of TAU, stabilization of microtubules, and may not be of pathological relevance.

Polyglutamylated tubulin increased following expression of both WT and mutant TAU, but this was statistically significant only when iNeurons expressing P301L-TAU were compared with TAU KO iNeurons. Previous studies showed that increased tubulin polyglutamylation leads to neurodegeneration (Magiera et al., 2018b), and that TAU may recruit TLL6 to the somatodendritic compartments under pathological conditions, causing elevated polyglutamylation of dendritic microtubules and subsequent recruitment of SPASTIN, a microtubule-severing enzyme (Zempel et al., 2013). Hence, polyglutamylation may be a pathologically relevant microtubule PTM in tauopathy.

Detyrosination is a unique tubulin PTM where the C-terminal tyrosine residue is removed by the recently identified VASH1 and VASH2 (Aillaud et al., 2017). Detyrosination is reversible and tyrosination is carried out by Tubulin-Tyrosine-Ligase (TTL). Typically, tyrosinated microtubules are very dynamic,

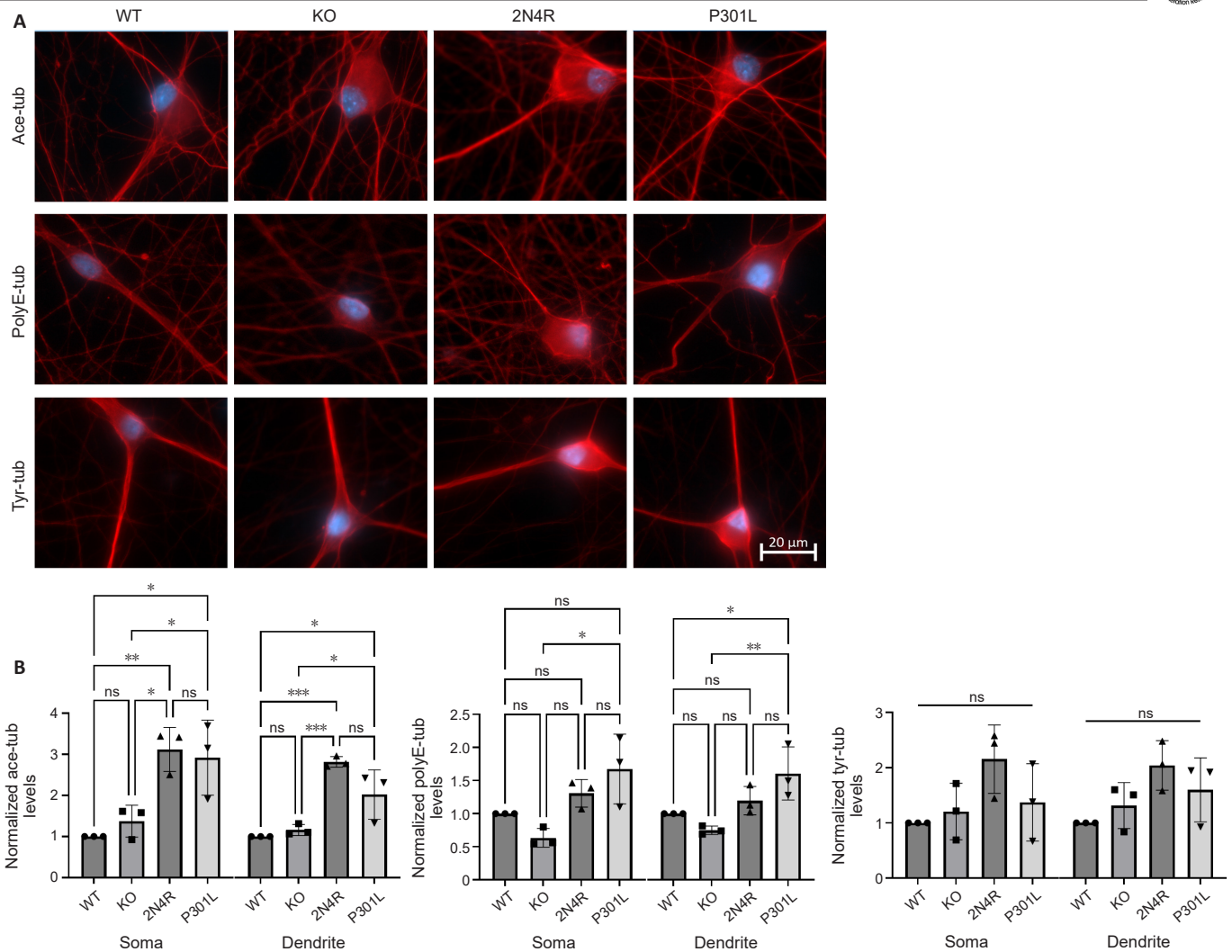


Figure 6 | Expression of 2N4R- or P301L-TAU alters some PTMs of microtubules in iNeurons.

iNeurons on day 21 were lentivirally transduced with the corresponding TAU construct for 10 days, followed by fixation and immunostaining as described in the Methods section. (A) TAU KO iNeurons transduced with 2N4R- or P301L-Tau, and WT or TAU KO iNeurons transduced with empty vector were immunostained for tubulin acetylation (Ace-tub), polyglutamylation (PolyE-tub) and tyrosination (Tyr-tub). Blue color corresponds to 4',6'-diamidino-2-phenylindole (DAPI) staining (nuclei). Scale bar: 20 μ m. (B) Quantification of the levels of the three PTMs of microtubules along different cell lines, transduction conditions, and neuronal compartments. Significant increases in ace-tub were observed in neurons expressing 2N4R- or P301L-TAU compared with control groups, while a significant increase in PolyE-tub was detected only in P301L-Tau-expressing neurons. $N = 3$ biological replicates, $n = 15$ neurons of each replicate. Ordinary one-way analysis of variance with Tukey's multiple comparison test was performed for the determination of significant differences, except for Tyr-tub levels in the dendrites (represented in B, graph on the right) where a Kruskal–Wallis with Dunn's multiple comparison test was carried out. * $P < 0.05$, ** $P < 0.01$, *** $P < 0.001$. 2N4R: Tau isoform; iNeurons: induced pluripotent stem cell (iPSC)-derived neurons; KO: knockout; ns: not significant; WT: wild-type.

while detyrosinated microtubules are more stable (Webster et al., 1987). In our study, tyrosinated tubulin was decreased (when normalized to GAPDH) in hippocampal lysates of pR5 mice compared with WT mice. The same trend was also observed in iNeurons expressing P301L-TAU compared with their 2N4R-TAU-expressing counterparts. Previous studies have highlighted the potential regulatory role of tubulin detyrosination in neuronal polarisation (Erck et al., 2005; Peris et al., 2009), and a recent study reported a significant accumulation of detyrosinated tubulin in the brains of advanced AD patients (Peris et al., 2022). Removal of the tyrosine residue at the end of C-terminal tails of tubulin, coupled with increased TAU phosphorylation, could lead to electrostatic repulsion and subsequent dissociation of TAU from microtubules (Rogowski et al., 2021), but whether this is of pathological relevance is to be determined.

This study has also some limitations. 2N4R- and P301L-TAU were exogenously expressed in iNeurons which may induce effects that differ from those observed at endogenous biological levels, in particular as we are focusing on the longest isoform here. Western blot experiments to investigate the levels of PTMs of microtubules were only carried out on hippocampal lysates from 40-week-old mice. Similar experiments on lysates from older (or younger) mice could reveal important information on the changes in PTMs induced via ageing and disease progression. PTMs investigated in this study are indirect indicators of microtubule stability and dynamics. More direct parameters to measure microtubule mass and dynamics should be performed in future studies to support the conclusions reflected by changes in PTMs.

In conclusion, our paper shed light on some of the subtle

changes in tubulin PTMs associated with the FTDP-17-causing P301L mutation of TAU. The tubulin code is essential for the regulation of microtubules, and changes in these PTMs are linked to human diseases affecting neurological functions and processes. Targeting tubulin-modifying enzymes could be a promising alternative therapeutic approach for tauopathies (Rogowski et al., 2021). This can be achieved via identifying the specific glutamylases and detyrosinases responsible for these pathological changes, and the development of specific inhibitors thereof, in order to prevent microtubule loss and restore neuronal polarity and microtubule-based axonal transport.

Acknowledgments: We thank Prof. Li Gan (Weill Cornell Medicine, NY, USA) for providing Ngn2-WTC11 iPSCs. We thank Prof. Florian Klein (Institute of Virology, University Hospital Cologne) for providing lentiviral vectors. We thank Jennifer Klimek (Institute of Human Genetics, University Hospital of Cologne) and Dr. Stefan Wagner (Center Anatomy, University of Cologne) for their essential technical help. We thank Dr. Sarah Buchholz and Michael Bell-Simons (current address: Max Planck Institute for Biology of Ageing, Cologne, Germany) for the stimulating discussions and helpful insights. Stem cell work was performed at the iPSC-lab of the CMMC (Cologne, Germany).

Author contributions: Material preparation, data collection and analysis were performed and the first draft of the manuscript was written by MAAK. All authors contributed to the study conception and design, commented on previous versions of the manuscript, read and approved the final manuscript.

Conflicts of interest: The authors have no relevant financial or non-financial interests to disclose.

Data availability statement: No additional data are available.

Open access statement: This is an open access journal, and articles are distributed under the terms of the Creative Commons Attribution-NonCommercial-ShareAlike 4.0 License, which allows others to remix, tweak, and build upon the work non-commercially, as long as appropriate credit is given and the new creations are licensed under the identical terms.

References

Aillaud C, Bosc C, Peris L, Bosson A, Heemeryck P, Van Dijk J, Le Fric J, Boulan B, Vossier F, Sanman LE, Syed S, Amara N, Couté Y, Lafanechère L, Denarier E, Delphin C, Pelletier L, Humbert S, Bogoy M, Andrieux A, Rogowski K, Moutin MJ (2017) Vasohibins/SVBP are tubulin carboxypeptidases (TCPs) that regulate neuron differentiation. *Science* 358:1448-1453.

Alonso Adel C, Mederlyova A, Novak M, Grundke-Iqbal I, Iqbal K (2004) Promotion of hyperphosphorylation by frontotemporal dementia tau mutations. *J Biol Chem* 279:34873-34881.

Andreadis A, Brown W M, Kosik KS (1992) Structure and novel exons of the human tau gene. *Biochemistry* 31:10626-10633.

Arendt T, Stieler JT, Holzer M (2016) Tau and tauopathies. *Brain Res Bull* 126:238-292.

Bachmann S, Bell M, Klimek J, Zempel H (2021a) Differential effects of the six human TAU isoforms: somatic retention of 2N-TAU and increased microtubule number induced by 4R-TAU. *Front Neurosci* 15:643115.

Bachmann S, Linde J, Bell M, Spehr M, Zempel H, Zimmer-Bensch G (2021b) DNA methyltransferase 1 (DNMT1) shapes neuronal activity of human iPSC-derived glutamatergic cortical neurons. *Int J Mol Sci* 22:2034.

Bachmann S, Al Kabbani MA, Bell M, Kluge L, Klimek J, Zempel H (2023) Tau deficiency protects human neurons from Abeta-induced reduction of network activity. *Alzheimers Dement* 19:e063601.

Bell M, Bachmann S, Klimek J, Langerscheidt F, Zempel H (2021) Axonal TAU sorting requires the C-terminus of TAU but is independent of ANKG and TRIM46 enrichment at the AIS. *Neuroscience* 461:155-171.

Bell-Simons M, Buchholz S, Klimek J, Zempel H (2023) Laser-induced axotomy of human iPSC-derived and murine primary neurons decreases somatic Tau and AT8 Tau phosphorylation: a single-cell approach to study effects of acute axonal damage. *Cell Mol Neurobiol* 43:3497-3510.

Bichmann M, Prat Oriol N, Ercan-Herbst E, Schöndorf DC, Gomez Ramos B, Schwärzler V, Neu M, Schlüter A, Wang X, Jin L, Hu C, Tian Y, Ried JS, Haberkant P, Gasparini L, Ehrnhoefer DE (2021) SETD7-mediated monomethylation is enriched on soluble Tau in Alzheimer's disease. *Mol Neurodegener* 16:46.

Bovee BF, Hutton M (2008) Refining frontotemporal dementia with parkinsonism linked to chromosome 17: introducing FTDP-17 (MAPT) and FTDP-17 (PGRN). *Arch Neurol* 65:460-464.

Buchholz S, Bell-Simons M, Cakmak C, Klimek J, Gan L, Zempel H (2024) Cultivation, differentiation, and lentiviral transduction of human-induced pluripotent stem cell (hiPSC)-derived glutamatergic neurons for studying human Tau. *Methods Mol Biol* 2754:533-549.

Choudhary C, Kumar C, Gnäd F, Nielsen ML, Rehman M, Walther TC, Olsen JV, Mann M (2009) Lysine acetylation targets protein complexes and co-regulates major cellular functions. *Science* 325:834-840.

Deters N, Ittner LM, Götz J (2008) Divergent phosphorylation pattern of tau in P301L tau transgenic mice. *Eur J Neurosci* 28:137-147.

Ding H, Dolan PJ, Johnson GV (2008) Histone deacetylase 6 interacts with the microtubule-associated protein tau. *J Neurochem* 106:2119-2130.

Erck C, Peris L, Andrieux A, Meissirel C, Gruber AD, Vernet M, Wehland J (2005). A vital role of tubulin-tyrosine-ligase for neuronal organization. *Proc Natl Acad Sci U S A* 102:7853-7858.

Gibbons GS, Kim SJ, Robinson JL, Changolkar L, Irwin DJ, Shaw LM, Lee VM, Trojanowski JQ (2019) Detection of Alzheimer's disease (AD) specific tau pathology with conformation-selective anti-tau monoclonal antibody in co-morbid frontotemporal lobar degeneration-tau (FTLD-tau). *Acta Neuropathol Commun* 7:34.

Götz J, Chen F, Barmettler R, Nitsch RM (2001) Tau filament formation in transgenic mice expressing P301L tau. *J Biol Chem* 276:529-534.

Hasegawa M, Smith MJ, Goedert M (1998) Tau proteins with FTDP-17 mutations have a reduced ability to promote microtubule assembly. *FEBS Lett* 437:207-210.

Janke C, Kneussel M (2010) Tubulin post-translational modifications: encoding functions on the neuronal microtubule cytoskeleton. *Trends Neurosci* 33:362-372.

Köhler C, Dinekov M, Götz J (2013) Active glycogen synthase kinase-3 and tau pathology-related tyrosine phosphorylation in pR5 human tau transgenic mice. *Neurobiol Aging* 34:1369-1379.

Köhler C, Dinekov M, Götz J (2014) Granulovacuolar degeneration and unfolded protein response in mouse models of tauopathy and A β amyloidosis. *Neurobiol Dis* 71:169-179.

Lacroix B, van Dijk J, Gold ND, Guizzetti J, Aldrian-Herrada G, Rogowski K, Gerlich DW, Janke C (2010) Tubulin polyglutamylation stimulates spastin-mediated microtubule severing. *J Cell Biol* 189:945-954.

Lewis J, McGowan E, Rockwood J, Melrose H, Nacharaju P, Van Slegtenhorst M, Gwinn-Hardy K, Paul Murphy M, Baker M, Yu X, Duff K, Hardy J, Corral A, Lin WL, Yen SH, Dickson DW, Davies P, Hutton M (2000) Neurofibrillary tangles, amyotrophy and progressive motor disturbance in mice expressing mutant (P301L) tau protein. *Nat Genet* 25:402-405.

- Magiera MM, Singh P, Gadadhar S, Janke C (2018a) Tubulin posttranslational modifications and emerging links to human disease. *Cell* 173:1323-1327.
- Magiera MM, Bodakuntla S, Žiak J, Lacomme S, Marques Sousa P, Leboucher S, Hausrat TJ, Bosc C, Andrieux A, Kneussel M, Landry M, Calas A, Balastik M, Janke C (2018b) Excessive tubulin polyglutamylation causes neurodegeneration and perturbs neuronal transport. *EMBO J* 37:e100440.
- Mao CX, Wen X, Jin S, Zhang YQ (2017) Increased acetylation of microtubules rescues human tau-induced microtubule defects and neuromuscular junction abnormalities in *Drosophila*. *Dis Model Mech* 10:1245-1252.
- Maruta H, Greer K, Rosenbaum JL (1986) The acetylation of alpha-tubulin and its relationship to the assembly and disassembly of microtubules. *J Cell Biol* 103:571-579.
- Miyaoka Y, Chan AH, Judge LM, Yoo J, Huang M, Nguyen TD, Lizarraga PP, So PL, Conklin BR (2014). Isolation of single-base genome-edited human iPSC cells without antibiotic selection. *Nat Methods* 11:291-293.
- Müller-Thomsen L, Borgmann D, Morcinek K, Schröder S, Dengler B, Moser N, Neumaier F, Schneider T, Schröder H, Huggenberger S (2020) Consequences of hyperphosphorylated tau on the morphology and excitability of hippocampal neurons in aged tau transgenic mice. *Neurobiol Aging* 93:109-123.
- Nogales E (2000) Structural insights into microtubule function. *Annu Rev Biochem* 69:277-302.
- Pennanen L, Wolfer DP, Nitsch RM, Götz J (2006) Impaired spatial reference memory and increased exploratory behavior in P301L tau transgenic mice. *Genes Brain Behav* 5:369-379.
- Peris L, Wagenbach M, Lafanechère L, Brocard J, Moore AT, Kozielski F, Job D, Wordeman L, Andrieux A (2009) Motor-dependent microtubule disassembly driven by tubulin tyrosination. *J Cell Biol* 185:1159-1166.
- Peris L, et al. (2022) Tubulin tyrosination regulates synaptic function and is disrupted in Alzheimer's disease. *Brain* 145:2486-2506.
- Puladi B, Dinekov M, Arzberger T, Taubert M, Köhler C (2021) The relation between tau pathology and granulovacuolar degeneration of neurons. *Neurobiol Dis* 147:105138.
- Rogowski K, Hached K, Crozet C, van der Laan S (2021) Tubulin modifying enzymes as target for the treatment of tau-related diseases. *Pharmacol Ther* 218:107681.
- Sohn PD, Huang CT, Yan R, Fan L, Tracy TE, Camargo CM, Montgomery KM, Arhar T, Mok SA, Freilich R, Baik J, He M, Gong S, Roberson ED, Karch CM, Gestwicki JE, Xu K, Kosik KS, Gan L (2019) Pathogenic Tau impairs axon initial segment plasticity and excitability homeostasis. *Neuron* 104:458-470.
- Tjiang N, Zempel H (2022) A mitochondria cluster at the proximal axon initial segment controls axodendritic TAU trafficking in rodent primary and human iPSC-derived neurons. *Cell Mol Life Sci* 79:120.
- Tracy TE, et al. (2022) Tau interactome maps synaptic and mitochondrial processes associated with neurodegeneration. *Cell* 185:712-728
- Wang C, Ward ME, Chen R, Liu K, Tracy TE, Chen X, Xie M, Sohn PD, Ludwig C, Meyer-Franke A, Karch CM, Ding S, Gan L (2017) Scalable production of iPSC-derived human neurons to identify Tau-lowering compounds by high-content screening. *Stem Cell Reports* 9:1221-1233.
- Webster DR, Gundersen GG, Bulinski JC, Borisy GG (1987) Differential turnover of tyrosinated and detyrosinated microtubules. *Proc Natl Acad Sci U S A* 84:9040-9044.
- Wu HY, Rong Y, Bansal PK, Wei P, Guo H, Morgan JI (2022) TLL1 and TLL4 polyglutamylases are required for the neurodegenerative phenotypes in pcd mice. *PLoS Genet* 18:e1010144.
- Wszolek ZK, Tsuboi Y, Ghetti B, Pickering-Brown S, Baba Y, Cheshire WP (2006) Frontotemporal dementia and parkinsonism linked to chromosome 17 (FTDP-17). *Orphanet J Rare Dis* 9:30.
- Xu Z, Schaedel L, Portran D, Aguilar A, Gaillard J, Marinkovich MP, Théry M, Nachury MV (2017) Microtubules acquire resistance from mechanical breakage through intraluminal acetylation. *Science* 356:328-332.
- Zempel H, Luedtke J, Kumar Y, Biernat J, Dawson H, Mandelkow E, Mandelkow EM (2013) Amyloid- β oligomers induce synaptic damage via Tau-dependent microtubule severing by TLL6 and spastin. *EMBO J* 32:2920-2937.
- Zempel H, Mandelkow EM (2015) Tau missorting and spastin-induced microtubule disruption in neurodegeneration: Alzheimer disease and hereditary spastic paraplegia. *Mol Neurodegener* 10:68.
- Zempel H, Luedtke J, Mandelkow EM (2017) Tracking Tau in neurons: how to transfect and track exogenous tau into primary neurons. *Methods Mol Biol* 1523:335-340.

C-Editor: Zhao M; S-Editor: Li CH; L-Editors: Li CH, Song LP; T-Editor: Jia Y

6.4 Article 4

Al Kabbani, M. A., Wied, T., Adam, D., Klimek, J., Zempel, H. (2024) Knockdown of TLL1 reduces A β -induced TAU pathology in human iPSC-derived cortical neurons. *bioRxiv*. doi: 10.1101/2024.11.19.624324.

Knockdown of TTLL1 reduces A β -induced TAU pathology in human iPSC-derived cortical neurons

Mohamed Aghyad Al Kabbani^{1,2}, Tamara Wied³, Daniel Adam^{1,2}, Jennifer Klimek^{1,2}, Hans Zempel^{1,2,*}

1 Institute of Human Genetics, Faculty of Medicine and University Hospital Cologne, University of Cologne, Cologne, Germany

2 Center for Molecular Medicine Cologne (CMMC), Faculty of Medicine and University Hospital Cologne, University of Cologne, Cologne, Germany

3 Current affiliation: Max Planck Institute for the Biology of Ageing, Cologne, Germany

* Correspondence to: Dr. Dr. Hans Zempel, hans.zempel@uk-koeln.de

Abstract

Microtubules play a crucial role in neuronal structure and function, with their stability and dynamics regulated by post-translational modifications (PTMs) such as polyglutamylation. In Alzheimer disease (AD), the microtubule-associated protein TAU becomes mislocalized into the somatodendritic compartment (TAU missorting), dissociates from microtubules, aggregates into neurofibrillary tangles, and contributes to microtubule destabilization and neuronal death. Here, we investigated the role of Tubulin-Tyrosine-Ligase-Like proteins (TTLLs) in TAU missorting and microtubule dysregulation using human induced pluripotent stem cell (hiPSC)-derived cortical neurons treated with oligomeric amyloid-beta ($\text{oA}\beta$) to replicate AD-like conditions. TTLL1, TTLL4, TTLL6 were selectively knocked down (KD) to assess their impact on TAU missorting and microtubule stability. Fluorescence resonance energy transfer (FRET) microscopy was used to examine interactions between TAU and TTLL proteins. We observed TAU missorting, increased tubulin polyglutamylation, decreased microtubule stability, and synaptic declustering in $\text{oA}\beta$ -treated neurons. TTLL1 KD significantly reduced TAU missorting, tubulin polyglutamylation, and synaptic disintegration, while TTLL4 KD showed moderate effects, and

TTLL6 KD restored microtubule acetylation. Importantly, TTLL KD did not impair neuritic networks, dendritic complexity, or neuronal activity. FRET microscopy revealed a potential interaction between TAU and TTLL1, but not other TTLLs, suggesting a direct role of TTLL1 in TAU-mediated toxicity. Our findings indicate that targeting TTLL1, either alone or in combination with other TTLLs, may be a promising therapeutic strategy to counteract microtubule and synaptic dysfunction in AD and related neurodegenerative disorders.

Keywords: TAU, TTLL, Alzheimer disease, hiPSCs, microtubules, synapses

Introduction

Microtubules are cylindrical filamentous heterodimers of α - and β -tubulin that form an essential part of the cytoskeleton. Microtubules play an important role in maintaining neuronal shape and facilitating the transportation of organelles and vesicles across neuronal networks (Sakakibara et al., 2013). Microtubule dynamics and functions are tightly regulated by a complex set of post-translational modifications (PTMs) (Janke and Kneussel, 2010), as well as binding to and interacting with proteins like microtubule-associated proteins (MAPs) and microtubule-severing enzymes such as spastin (Goodson and Jonasson, 2018). In Alzheimer disease (AD), microtubules are significantly depleted in affected brains, though the underlying causes remain unclear (Cash et al., 2003; Jean and Bass, 2013).

TAU, a microtubule-associated protein encoded by the *MAPT* gene, is an axonal-enriched protein that binds microtubules and promotes their assembly and stability. However, in tauopathies like AD, TAU dissociates from microtubules, missorts to the somatodendritic compartments, and aggregates into hyperphosphorylated neurofibrillary tangles, leading to microtubule fragmentation and neuronal death (Zempel and Mandelkow, 2015). Spastin, an ATP-dependent enzyme encoded by the *SPAST* gene, mediates microtubule severing, and its activity is catalyzed by a specific PTM of microtubules called polyglutamylation, which

comprises the addition of a glutamate side chain to a glutamate residue, usually on the C-terminal tail of tubulin (Lacroix et al., 2010). This modification is carried out by several members of a class of enzymes known as Tubulin-Tyrosine-Ligase-Like proteins (TTLLs), mainly TTLL 1, 4, 5, 6, 7 and 11 (Magiera et al., 2018).

Polyglutamylation is reversible, with cytosolic carboxypeptidases (CCPs) removing glutamate side chains (Rogowski et al., 2010). The balance between adding and removing glutamate chains is essential for health, with hyperglutamylation linked to neurodegeneration. For instance, Purkinje cell degeneration (*pcd*) mice, in which CCP1 is deficient, exhibit severe neurodegeneration, which is attenuated by knocking out TTLL1 and TTLL4, but not TTLL5 or TTLL7 (Li et al., 2020; Wu et al., 2022). Another hint towards potential involvement of TTLLs in neurodegeneration came from primary rat neurons treated with oligomeric amyloid-beta ($\text{oA}\beta$), where missorted TAU appeared to recruit TTLL6 to the somatodendritic compartments, inducing polyglutamylation and spastin-mediated microtubule severing, leading to extensive microtubule loss (Zempel et al., 2010, 2013). However, the underlying and potentially druggable disease mechanisms by which TAU missorting triggers microtubule dysfunction, and the specific TTLLs involved, remain unclear in human disease-relevant models.

In this study, we first aimed to establish a human tauopathy-relevant model using human induced pluripotent stem cell (hiPSC)-derived cortical neurons (iNeurons). We treated these neurons with $\text{oA}\beta$ and observed TAU missorting, increased tubulin polyglutamylation, and synaptic declustering. We then aimed to identify the TTLL(s) responsible for mediating the pathological effects of missorted TAU via individually knocking down TTLL1, TTLL4, or TTLL6. We show that decreased expression of TTLL1, and to some extent TTLL4, alleviate the pathological effects of $\text{oA}\beta$ without disturbing neuritic network, dendritic morphology, or neuronal function. We provide first evidence that targeting TTLL1 alone or in combination with another

TTLL is a potential therapeutic target in AD and other tauopathies, and should be further validated and investigated.

Methods

hiPSC maintenance

WTC11 cells with a doxycycline-inducible Ngn2 transgene (Miyaoaka et al., 2014; Wang et al., 2017) were cultured on Geltrex-coated plates (Thermofisher Scientific #A1413302) at 37°C, 5% CO₂ and regularly passaged when almost fully confluent using Versene (Thermofisher Scientific #15040066) and thiazovivin-supplemented StemMACS iPS-Brew X.F. (Axon Medchem #1535, Miltenyi Biotec #130-104-368) for the first 24 hours (Buchholz et al., 2024).

Differentiation of hiPSCs into cortical neurons (iNeurons)

Differentiation of hiPSCs into cortical neurons was carried out as described before (Buchholz et al., 2024; Bachmann et al., 2021; Wang et al., 2017). At the start of differentiation, iPSCs were harvested using Accutase (Sigma-Aldrich #A6964-100ML) and seeded onto Geltrex-coated plates pre-differentiation medium (Thermofisher Scientific #12660012) supplemented with thiazovivin (Day before differentiation: D-3). The medium was changed every day for 2 days to fresh pre-differentiation medium without supplementation. On Day 0, 50,000 or 300,000 cells were seeded onto Poly-D-Lysine- (Sigma-Aldrich #P7886-50MG) and Laminin- (Trevigen #3446-005-01) coated 24-well-plates or 6-well plates respectively using maturation medium supplemented with 1:100 GelTrex. Half of the media was exchanged once per week until analysis.

oA β preparation and treatment

A β was prepared and reconstituted into oligomers as described before (Zempel et al., 2013). Briefly, A β 40 and A β 42 powder (rPeptide #A-1153-1 and #A-1163-2) were completely dissolved

in Hexafluoro-2-propanol (HFIP) to a final concentration of 1 mM. Following aliquotation, HFIP was evaporated completely using a vacuum concentrator, and the lyophilized powder was stored at -80°C. On the day of treatment of iNeurons, lyophilized A β 40 and A β 42 were redissolved in 50 mM NaOH and mixed to produce a A β 40/A β 42 ratio of 7:3, and then diluted with PBS and 50 mM HCl to a final concentration of 100 μ M. To induce oligomerization, A β mixture was incubated at 37°C for one hour. Subsequently, iNeurons at Day 21 were treated with 1 μ M oA β for 3 hours and analyzed.

Short hairpin RNA sequences

For the knockdown of human *TLLs* in iNeurons, short hairpin RNA (shRNA) oligonucleotides were inserted into pLKO.3G vector (Addgene #14748) resulting in a multi-cistronic lentiviral construct expressing green fluorescent protein (GFP) and the corresponding shRNA. The following shRNA sequences were used to target human *TLLs* or as a control:

Scrambled shRNA (control): 5'-TTGTCTTGCATTCGACTAA-3'

sh*TLL1*: 5'-GTTTGTGTCTCAATCTAATAA-3'

sh*TLL4*: 5'-GAGCCTTGGCAATAAGTTC-3'

sh*TLL6*: 5'-CGGACUCATGAUUUCCAGGATT-3', 5'-AACAAUCUCCUCUCCAGAAU-3'

Lentiviral-based knockdown of TLLs

Lentivirus particle production and subsequent lentiviral transduction of iNeurons are described in detail in Buchholz et al., 2024. Briefly, HEK293T cells were co-transfected with the corresponding pLKO.3G plasmid, the packaging plasmid psPAX, and the envelope plasmid pMD2.G (Addgene #12259 and #12260). Four and five days after transfection, the culture supernatant containing lentivirus was collected, filtered and stored at -80°C. iNeurons were

transduced with the lentiviral particles on Day 10 and analyzed 11 days after transduction (Day 21).

Western blot analysis

For Western blot analysis, iNeurons were lysed in RIPA buffer (Sigma Aldrich #R0278), centrifuged at 16,000 \times g for 20 minutes at 4°C, diluted in 5 \times Laemmli buffer, boiled for 10 minutes at 95°C, and then separated on 10% Sodium dodecyl sulfate (SDS)-polyacrylamide gels. Afterwards, proteins were transferred to polyvinylidene fluoride (PVDF) membranes overnight at 4°C, and blocked in 5% bovine serum albumin (BSA) in Tris-buffered saline with 0.1% Tween (TBS-T). Membranes were incubated with the primary antibody overnight at 4°C, washed three times with TBS-T, and incubated with the corresponding secondary horseradish peroxidase (HRP)-coupled antibody for 1 hour at room temperature. After three washing rounds with TBS-T, the immunoreactions were detected by applying the SuperSignal West Pico Chemiluminescent Substrate (Thermofisher Scientific #34580) using a ChemiDoc XRS + system (Bio-Rad).

Immunofluorescence labeling of iNeurons

For immunocytochemistry, iNeurons were fixed with 3.7% Formaldehyde in PBS containing 4% sucrose at room temperature for 30 minutes. Afterwards, cells were permeabilized and blocked in 5% BSA (Carl Roth #8076.4) and 0.2% Triton X-100 (Carl Roth #3051.2) in PBS for 10 minutes. After fixation, iNeurons were stained with primary antibodies at 4°C overnight. The following day, coverslips were washed three times with PBS and stained with the corresponding secondary antibodies coupled to an AlexaFluor dye (Thermofisher Scientific) for two hours at room temperature. Coverslips were then washed with PBS and stained with NucBlue (Thermofisher Scientific #R37605) for 20 min at room temperature, followed by mounting onto

glass slides using Aqua-Poly/Mount (Polysciences #18606-20). The slides were dried 24 hours at room temperature and then imaged.

Imaging

Immunostained iNeurons were imaged using a wide-field fluorescence microscope (Axioscope 5, Zeiss) with ZenBlue Pro imaging software (V2.5, Zeiss). Images were analyzed using ImageJ software (Version 2.14.0/1.54f, National Institutes of Health and the Laboratory for Optical and Computational Instrumentation (LOCI), University of Wisconsin, USA). To measure the levels of TAU or tubulin PTMs in neurons, regions of interest (ROIs) were manually delineated as profiles of the soma or the dendrite where no other somas or processes overlapped, and the mean fluorescence intensity (MFI) of each ROI was measured.

Neuronal network analysis

Fields of iNeurons cultures were imaged at 10x magnification after immunolabeling of the axon-enriched neurofilament light chain (NF-L) and the somatodendritic marker microtubule-associated protein 2 (MAP2). The area of NF-L- or MAP2- positive neurites was calculated using ImageJ software and normalized to the number of transduced nuclei in each field, identified via GFP fluorescence.

Sholl analysis

Sholl analysis (Sholl, 1953) was used to investigate the complexity of dendritic arbouring in iNeurons immunostained for MAP2. The center of the soma was designated as the center of concentric circles, and the number of intersections was analyzed via the Neuroanatomy plugin in ImageJ software. Sholl profiles were created by plotting the number of intersections against the distance from the soma (μm). For statistical comparison, either the area under the curve (AUC) or the full-width at half maximum of the Sholl profiles were compared. Data was tested

for normality by Shapiro-Wilk test and compared using a pairwise t-test. Analysis was performed using R (R Core Team, 2024), AUC was calculated using the DescTools package (Signorell, 2024).

Microelectrode array measurements

For microelectrode array (MEA) measurements, iPSCs were seeded on MEA 24-well plates and differentiated into cortical neurons as described above. At Day 10, iNeurons were transduced with lentiviral particles carrying the corresponding shRNA. Spontaneous activity was recorded for 2 minutes at Day 21 at 37°C.

Fluorescence Resonance Energy Transfer (FRET) assay

Live-cell imaging-based FRET assay was carried out to assess interactions between TAU and different TTLLs. HEK293T cells were co-transfected for 24 hours with teal fluorescent protein (TFP)-TAU construct (FRET donor) and yellow fluorescent protein (YFP)-TTLL1, TTLL4, or TTLL6 constructs (FRET acceptor). HEK293T cells were also transfected for 24 hours with empty vectors expressing TFP or YFP as controls. Live-cell imaging was performed with an inverted Leica DMI8 microscope with the help of Leica LAS X software (v3.7.3). FRET efficiency was analyzed via FRET and Colocalization Analyzer plugin (Hachet-Hass et al., 2006) on ImageJ software.

Statistical analysis

The GraphPad Prism (v9.5.1, GraphPad Software, Boston, Massachusetts, USA) was used for statistical analysis. Shapiro-Wilk test was performed to test for normal distribution of the data. In case of normal distribution, statistical analysis was performed by unpaired t-test to compare the means of two groups, or one-way ANOVA with correction for multiple comparisons (Tukey's test) to compare three or more groups. When the data were not normally distributed, Mann–

Whitney U test or Kruskal-Wallis test with correction for multiple comparisons (Dunn's test) were carried out, respectively. Statistical significance was denoted by a significance level of $P < 0.05$.

Antibodies

The antibodies used in this study are listed in Table 1.

Table 1. List of the primary and secondary antibodies used in the study.

Antibody	Animal species	Clonality	Cat#	Supplier	RRID	Use and dilution
Total TAU (K9JA)	rabbit	polyclonal	A0024	Agilent, USA	AB_100137 24	ICC (1:1000)
Acetyl- α -Tubulin (Lys40) (D20G3)	rabbit	monoclonal	5335	Cell Signaling, USA	AB_105446 94	ICC (1:500)
Anti-Tubulin Polyglutamylated antibody	mouse	monoclonal	T9822	Sigma-Aldrich, USA	AB_477598	ICC (1:500)
Anti-tyrosinated- α -Tubulin Antibody	rat	monoclonal	MAB1864-I	Sigma-Aldrich, USA	AB_289065 7	ICC (1:500)
GAPDH Antibody	mouse	monoclonal	sc-365062	Santa Cruz Biotechnology, USA	AB_108478 62	WB (1:1000)
Anti-MAP2 Antibody	chicken	polyclonal	ab5392	Abcam, UK	AB_213815 3	ICC (1:2000)

Anti-NF-L antibody	rabbit	polyclonal	12998-1-AP	Proteintech, USA	AB_105973 88	ICC (1:500)
Anti-Homer1 antibody	rabbit	polyclonal	12433-1-AP	Proteintech, USA	AB_229557 3	ICC (1:200)
Anti-synaptophysin antibody	mouse	monoclonal	67864-1-Ig	Proteintech, USA	AB_291862 2	ICC (1:200)
Anti-TTLL1 antibody	rabbit	polyclonal	PA5-27285	Thermofisher Scientific, USA	AB_254476 1	WB (1:500)
Anti-TTLL4 antibody	rabbit	polyclonal	HPA027091	Sigma Aldrich, USA	AB_106018 28	WB (1:500)
Anti-TTLL6 antibody	rabbit	polyclonal	PA5-100050	Thermofisher Scientific, USA	AB_281558 0	WB (1:500)
Anti-Chicken Secondary Antibody, DyLight™ 350	goat	polyclonal	SA5-10069	Thermofisher Scientific, USA	AB_255664 9	ICC (1:1000)
Anti-Rabbit Secondary Antibody, Alexa Fluor™ 488	donkey	polyclonal	A-21206	Thermofisher Scientific, USA	AB_253579 2	ICC (1:1000)
Anti-Mouse Secondary	goat	polyclonal	A-11031	Thermofisher Scientific, USA	AB_144696	ICC (1:1000)

Antibody, Alexa Fluor™ 568						
Anti-Rabbit Secondary Antibody, Alexa Fluor™ 568	donkey	polyclonal	A10042	Thermofisher Scientific, USA	AB_2534017	ICC (1:1000) IHC (1:400)
Anti-Rat Secondary Antibody, Alexa Fluor™ 568	goat	polyclonal	A-11077	Thermofisher Scientific, USA	AB_2534121	ICC (1:1000)
Anti-Chicken Secondary Antibody, Alexa Fluor™ 647	goat	polyclonal	A21449	Thermofisher Scientific, USA	AB_2535866	ICC (1:1000)
Anti-Mouse Secondary Antibody, Alexa Fluor™ 647	donkey	polyclonal	A-31571	Thermofisher Scientific, USA	AB_162542	ICC (1:1000)
anti-Mouse Secondary Antibody, HRP	goat	polyclonal	115-035-003	Jackson ImmunoResearch Labs, USA	AB_10015289	WB (1:1000)
Anti-Rabbit Secondary	goat	polyclonal	7074	Cell Signaling, USA	AB_2099233	WB (1:1000)

Antibody, HRP						
---------------	--	--	--	--	--	--

Results

Establishment of A β -induced TAU pathology in iNeurons

Previous insights into the potential connection between TAU missorting, microtubule instability, and TTLs were obtained from rodent-derived models, while a representative human neuronal model was lacking. In order to establish a human tauopathy-relevant model to study TAU-based effects on microtubules, human iPSCs were differentiated into cortical neurons. Briefly, genetically modified WTC11 iPSC line harboring a doxycycline-inducible neurogenin-2 (Ngn2) transgene were induced to differentiate into pure glutamatergic neuronal cultures (See: Methods in this paper; Wang et al., 2017; Buchholz et al., 2024).

Day 21 iNeurons treated with 1 μ M oA β showed increased levels of somatic TAU indicative of TAU missorting (Fig. 1A, E). This was accompanied by a marked increase in the levels of tubulin polyglutamylation (Fig. 1B, F). To further evaluate the stability of microtubules in oA β -treated iNeurons, we investigated the levels of acetylated and tyrosinated tubulin, and observed reduced acetylation in the dendrites and decreased tyrosination in the somatic compartments (Fig. 1C, G, H), indicating that microtubule stability and dynamics were further compromised.

We also wanted to test the effects of oA β on the synaptic integrity in our iNeurons. To this end, we triple stained Homer1, synaptophysin, and MAP2 to identify dendritic synapses and quantified the size and mean fluorescence intensity of synaptophysin-colocalized Homer1. While the fluorescence intensity of synaptic Homer1 clusters did not change, the size of these clusters was reduced upon oA β treatment, indicating synaptic destabilization (Fig. 1D, I). Hence,

$\alpha\beta$ treatment in iNeurons causes TAU missorting, microtubule instability, and synaptic instability, making these neurons a suitable human model for our study.

Reduction of TTLL1 and TTLL4 expression attenuates $\alpha\beta$ toxicity and TAU missorting

To identify the specific TTLL(s) driving pathological microtubule polyglutamylation upon TAU missorting, we aimed to knock down three polyglutamylating TTLLs and then to observe the effects of subsequent $\alpha\beta$ insult on the levels of polyglutamylated tubulin, and on the other toxicity read-outs established above.

TTLL1, TTLL4, and TTLL6 were individually knocked down using shRNA-lentiviral transduction of Day 10 iNeurons. Effective knockdown was confirmed via Western blotting at Day 21, with residual expression of targeted TTLLs reduced to 20-50% of the control (iNeurons transduced with viruses carrying scrambled shRNA) (Fig. 2B).

Following the establishment of efficient lentiviral-based knockdown of TTLL1, TTLL4, and TTLL6, the effects of each of these knockdowns on $\alpha\beta$ -induced toxicity was investigated. Day10 iNeurons were transduced with the knockdown viruses or scrambled control. At Day 21, transduced iNeurons were treated with either $\alpha\beta$ or a vehicle control for 3 hours, followed by fixation and staining as above (Fig. 2A). Interestingly, $\alpha\beta$ -induced TAU missorting and tubulin polyglutamylated tubulin were significantly reduced by TTLL1 knockdown to near normal levels, with TTLL4 knockdown showing a similar effect on polyglutamylation but only a partial effect on TAU missorting. On the other hand, TTLL6 knockdown significantly restored acetylated tubulin levels but did not impact TAU missorting or tubulin polyglutamylation. However, the knockdown of none of these TTLLs was sufficient to counteract the decrease of tyrosinated tubulin induced by $\alpha\beta$ treatment (Fig. 2C-D).

While neither TTLL1 nor TTLL4 knockdowns fully restored synaptic Homer1 cluster size, they both prevented significant cluster disassembly by 15-30 % upon $\alpha\beta$ insult, a protective effect

not observed with TTLL6 knockdown (Fig. 3A-B). This indicates that knocking down TTLL1 and TTLL4 in iNeurons reduced $\alpha\beta$ -induced TAU missorting, tubulin polyglutamylation, and partially protected synapses, while TTLL6 restored acetylated tubulin but did not affect TAU missorting or synaptic protection, with none preventing tyrosinated tubulin loss.

Knockdown of TTLLs does not impair neuritic networks or neuronal function

To assess the broader impact of TTLL knockdown on neuronal networks, morphology, and function, TTLL1, TTLL4, or TTLL6 were knocked down at Day 10 and the effects on neuritic networks and dendritic branching were investigated at Day 21. Axonal and dendritic networks were studied via staining of NF-L and MAP2, respectively.

No significant changes were observed in the overall axonal (NF-L staining) or dendritic (MAP2 staining) networks across TTLL knockdown conditions compared to control (Fig. 4A-D). Sholl analysis revealed no significant differences in dendritic complexity although we noted a trend towards longer dendrites in iNeurons with TTLL1 and TTLL6 knockdowns (Fig. 4E-H). Additionally, neuronal activity, measured by microelectrode array (MEA) recordings, showed no significant alterations in spike rate or burst count across the different knockdown conditions (Fig. 4I). This indicates that iNeurons tolerate individual knockdown of the TTLLs studied here without obvious impairments in neuronal morphology and function.

TTLL1 and TAU interact in HEK293T cells

To investigate the mechanistic basis behind the ameliorating effects of TTLL knockdowns against $\alpha\beta$ -induced toxicity and test molecular interaction and proximity, we applied Fluorescence Resonance Energy Transfer (FRET) live-cell imaging to explore potential interactions between TAU and TTLLs. TFP-TAU and YFP-TTLL1, YFP-TTLL4, or YFP-TTLL6

were co-expressed in HEK293T cells. Co-expression of TFP-TAU and YFP alone, or YFP-TTLL1, YFP-TTLL4, or YFP-TTLL6 and TFP alone, served as negative controls.

Cells co-transfected with TFP-TAU and YFP-TTLL1 showed significantly higher FRET efficiency compared to the corresponding negative controls, suggesting direct interaction between TAU and TTLL1. In contrast, no significant FRET signal was observed for TTLL4 or TTLL6 compared to their controls (Fig. 5).

Discussion

This study presents a novel in vitro model of A β -induced tauopathy and microtubule impairments using human iPSC-derived cortical neurons. The model effectively recapitulates key features of TAU pathology seen in AD, including TAU missorting, microtubule destabilization, and synaptic defects. By exploring the role of TTLL proteins in this context, we provide new insights into the molecular mechanisms underlying A β -induced tauopathy and identify potential therapeutic targets.

oA β are thought to be the upstream disease-causing agent in AD (Cline et al., 2018). Previously, acute oA β treatment of rat-derived primary neurons led to TAU missorting, decreased acetylation and increased polyglutamylation of tubulin (Zempel et al., 2013). In this study, we showed oA β -induced TAU missorting to the soma in our human iNeurons, a hallmark of early tauopathy (Thies and Mandelkow, 2007). This pathological shift in TAU localization was accompanied by decreased tubulin acetylation and tyrosination, and increased polyglutamylation. Microtubules are regulated by a complex set of PTMs that govern their dynamics and stability. Decreased acetylation for instance is a well-established marker of unstable microtubules (Maruta et al., 1986), while decreased tyrosination negatively affects neuronal polarity and neurite outgrowth (Erck et al., 2005). Polyglutamylation on the other hand recruits the microtubule-severing enzyme spastin (Lacroix et al., 2010), with hyperglutamylation

linked to neurodegeneration and neuronal death (Berezniuk et al., 2012). In addition, we observed a significant decrease in the size of synaptophysin-juxtaposing Homer1 clusters following oA β treatment. Homer1 is a post-synaptic density scaffold protein that is classified as an immediate early gene and which is induced by neuronal activity (Clifton et al., 2019). Synaptic Homer1 cluster disassembly was shown before to be driven by A β in primary rat neurons, which leads to the loss of synaptic structure and function (Roselli et al., 2009). Taken together, oA β -insulted iNeurons exhibit detrimental changes in the PTMs of their microtubules, alongside TAU missorting and synaptic declustering, all of which is reminiscent of AD and related tauopathies.

We decided to knock down several glutamylating TTLLs in order to pinpoint the one responsible for pathological polyglutamylation, and to observe whether abolishing it would mitigate the harmful effects of oA β . We opted to focus on TTLL1, TTLL4, and TTLL6 because of their expression levels and previously described pathological relevance: TTLL1 is the major polyglutamylating TTLL in the brain (Janke et al., 2005); TTLL1 and TTLL4 depletion mitigated neurodegeneration in *pcd* mice, a model that mainly exhibits adult-onset degeneration of cerebellar Purkinje neurons and selected thalamic neurons (Wu et al., 2022); and TTLL6 translocated to dendrites of primary neurons exposed to oA β where it mediated polyglutamylation, spastin recruitment, and microtubule loss (Zempel et al., 2013). In our study, TTLL1 knockdown significantly protected iNeurons against oA β -induced TAU missorting, reduced elevated levels of tubulin polyglutamylation, and partially alleviated the dissociation of synaptic clusters, suggesting that TTLL1 plays a critical role in the early stages of A β -induced tauopathy. TTLL4 knockdown managed to decrease polyglutamylation levels but its effect on TAU missorting were less pronounced, indicating a rather secondary role for TTLL4. Interestingly, TTLL6 knockdown did not significantly affect TAU missorting but was the only

knockdown that restored microtubule acetylation, hinting at a potential compensatory mechanism that stabilizes microtubules independently of TAU.

Polyglutamylating TTLLs are important enzymes that regulate neuronal microtubule organization, dynamics, and interactions with other proteins (Lacroix et al., 2010; Bodakuntla et al., 2020; Genova et al., 2023). Therefore, we speculated that knockdown of different TTLLs could impact neuronal morphology, networks, or activity, limiting the possibility of targeting TTLLs therapeutically. To investigate this further, we decided to study dendritic network and dendritic branching by staining for MAP2, a long-established dendritic marker (Caceres et al., 1984), and axonal network by staining for NF-L, an intermediate filament highly concentrated in axons and a biomarker of neuro-axonal damage (Khalil et al., 2024). However, neither neuritic networks nor dendritic branching were affected by knockdown of any of the three TTLLs investigated in this study. Additionally, burst count and spike rate of iNeurons measured by MEA recordings were also not impacted by TTLL depletion, indicating maintained neuronal activity and making TTLLs an attractive therapeutic target for reducing TAU pathology while preserving neuronal health.

In order to understand the mechanism through which TTLL1 could mediate the detrimental effects of $\text{oA}\beta$ insult and TAU missorting, we decided to investigate potential interactions between TFP-TAU and YFP-tagged constructs of the three TTLLs investigated in this study via FRET microscopy in HEK293T cells. It was reported before that TAU and TTLL6 overexpressed in HEK293T cells may interact directly (Zempel et al., 2013). In this study however, only cells expressing TFP-TAU and YFP-TTLL1 showed FRET efficiency values higher than negative controls. FRET phenomena can only occur when the distance between donor (TFP) and acceptor (YFP) is less than 10 nm, which indicates that TAU and TTLL1 are in close proximity and may interact directly with each other. This may explain why the most effective protection against $\text{oA}\beta$ was observed in iNeurons with TTLL1 knockdown. We think that missorted TAU

following $\text{oA}\beta$ insult transports TTLL1 to the somatodendritic compartments where it polyglutamylates microtubules, culminating in decreased microtubule stability and synaptic loss.

Conclusion

We showed that human iPSC-derived neurons subjected to $\text{oA}\beta$ suffer from TAU missorting, stability-decreasing changes of microtubule PTMs, and dissociation of synaptic clusters. These noxious effects are significantly reduced via TTLL1 knockdown, without affecting neuronal networks and activity. Our findings suggest that TTLL1, alone or with combination with another TTLL, could be a promising therapeutic target for preventing or slowing the progression of tauopathy in AD. Future studies should explore the therapeutic potential of genetic or pharmacological targeting of TTLL1 in vivo and investigate the broader implications of TTLL-mediated microtubule modifications in neurodegenerative diseases.

Declarations

Ethics approval and consent to participate: not applicable.

Consent for publication: not applicable

Availability of data and materials: The datasets used and/or analyzed during the current study are available from the corresponding author on reasonable request.

Competing interests: The authors have no relevant financial or non-financial interests to disclose.

Funding: This study was supported by the Alzheimer Forschung Initiative e.V. (grant #22039, to HZ).

Authors' contributions: Study design: MAAK, HZ. Experimental work: MAAK. Methodological support: TW, JK. Data analysis and interpretation: MAAK, DA, HZ. Manuscript writing: MAAK.

Manuscript commenting and proofreading: HZ, DA, TW, JK. All authors read and approved the final manuscript.

Acknowledgments: We thank Prof. Dr. Li Gan (Weill Cornell Medicine, NY, USA) for providing Ngn2-WTC11 iPSCs. We thank Prof. Dr. Florian Klein (Institute of Virology, University Hospital Cologne) for providing lentiviral vectors. We thank Dr. Sarah Buchholz (current address: Max Planck Institute for Biology of Ageing, Cologne, Germany) for the stimulating discussions and helpful insights. Stem cell work was performed at the iPSC-Lab core facility of the CMMC (Cologne, Germany).

References

Bachmann S, Linde J, Bell M, Spehr M, Zempel H, Zimmer-Bensch G. DNA Methyltransferase 1 (DNMT1) shapes neuronal activity of human iPSC-derived glutamatergic cortical neurons. *Int J Mol Sci.* 2021;22(4):2034. doi: 10.3390/ijms22042034.

Bachmann S, Al Kabbani MA, Bell M, Kluge L, Klimek J, Zempel H. TAU deficiency protects human neurons from Abeta-induced reduction of network activity. *Alzheimers Dement.* 2023;19. doi: 10.1002/alz.063601.

Berezniuk I, Vu HT, Lyons PJ, Sironi JJ, Xiao H, Burd B, et al. Cytosolic carboxypeptidase 1 is involved in processing α - and β -tubulin. *J Biol Chem.* 2012;287(9):6503-17. doi: 10.1074/jbc.M111.309138.

Bodakuntla S, Schnitzler A, Villablanca C, Gonzalez-Billault C, Bieche I, Janke C, et al. Tubulin polyglutamylation is a general traffic-control mechanism in hippocampal neurons. *J Cell Sci.* 2020;133(3). doi: 10.1242/jcs.241802.

Buchholz S, Bell-Simons M, Cagmak C, Klimek J, Gan L, Zempel H. Cultivation, differentiation, and lentiviral transduction of human induced pluripotent stem cell (hiPSC)-derived glutamatergic neurons for studying human TAU. In: TAU protein: Methods and Protocols. Springer; 2024.

Caceres A, Banker G, Steward O, Binder L, Payne M. MAP2 is localized to the dendrites of hippocampal neurons which develop in culture. *Brain Res.* 1984;315(2):314-8. doi: 10.1016/0165-3806(84)90167-6.

Cash AD, Aliev G, Siedlak SL, Nunomura A, Fujioka H, Zhu X, et al. Microtubule reduction in Alzheimer's disease and aging is independent of TAU filament formation. *Am J Pathol.* 2003;162(5):1623-7. doi: 10.1016/s0002-9440(10)64296-4.

Clifton NE, Trent S, Thomas KL, Hall J. Regulation and function of activity-dependent Homer in synaptic plasticity. *Mol Neuropsychiatry.* 2019;5(3):147-61. doi: 10.1159/000500267.

Cline EN, Bicca MA, Viola KL, Klein WL. The Amyloid- β oligomer hypothesis: Beginning of the third decade. *J Alzheimers Dis.* 2018;64(s1). doi: 10.3233/JAD-179941.

Erck C, Peris L, Andrieux A, Meissirel C, Gruber AD, Vernet M, et al. A vital role of tubulin-tyrosine-ligase for neuronal organization. *Proc Natl Acad Sci U S A.* 2005;102(22):7853-8. doi: 10.1073/pnas.0409626102.

Genova M, Grycova L, Puttrich V, Magiera MM, Lansky Z, Janke C, et al. Tubulin polyglutamylation differentially regulates microtubule-interacting proteins. *EMBO J.* 2023;42(5). doi: 10.15252/embj.2022112101.

Goodson HV, Jonasson EM. Microtubules and microtubule-associated proteins. *Cold Spring Harb Perspect Biol.* 2018;10(6). doi: 10.1101/cshperspect.a022608.

Hachet-Haas M, Converset N, Marchal O, Matthes H, Gioria S, Galzi JL, et al. FRET and colocalization analyzer--a method to validate measurements of sensitized emission FRET acquired by confocal microscopy and available as an ImageJ Plug-in. *Microsc Res Tech.* 2006;69(12):941-56. doi: 10.1002/jemt.20376.

Janke C, Rogowski K, Wloga D, Regnard C, Kajava AV, Strub JM, et al. Tubulin polyglutamylase enzymes are members of the TTL domain protein family. *Science.* 2005;308(5729):1758-62. doi: 10.1126/science.1113010.

Janke C, Kneussel M. Tubulin post-translational modifications: encoding functions on the neuronal microtubule cytoskeleton. *Trends Neurosci.* 2010;33(8):362-72. doi: 10.1016/j.tins.2010.05.001.

Jean DC, Baas PW. It cuts two ways: microtubule loss during Alzheimer disease. *EMBO J.* 2013;32(22):2900-2. doi: 10.1038/emboj.2013.219.

Khalil M, Teunissen CE, Lehmann S, Otto M, Piehl F, Ziemssen T, et al. Neurofilaments as biomarkers in neurological disorders - towards clinical application. *Nat Rev Neurol.* 2024;20(5):269-87. doi: 10.1038/s41582-024-00955-x.

Lacroix B, van Dijk J, Gold ND, Guizetti J, Aldrian-Herrada G, Rogowski K, et al. Tubulin polyglutamylation stimulates spastin-mediated microtubule severing. *J Cell Biol.* 2010;189(6):945-54. doi: 10.1083/jcb.201001024.

Li J, Snyder EY, Tang FH, Pasqualini R, Arap W, Sidman RL. Nna1 gene deficiency triggers Purkinje neuron death by tubulin hyperglutamylation and ER dysfunction. *JCI Insight.* 2020;5(19). doi: 10.1172/jci.insight.136078.

Magiera MM, Singh P, Gadadhar S, Janke C. Tubulin posttranslational modifications and emerging links to human disease. *Cell*. 2018;173(6):1323-7. doi: 10.1016/j.cell.2018.05.018.

Maruta H, Greer K, Rosenbaum JL. The acetylation of alpha-tubulin and its relationship to the assembly and disassembly of microtubules. *J Cell Biol*. 1986;103(2):571-9. doi: 10.1083/jcb.103.2.571.

Miyaoka Y, Chan AH, Judge LM, Yoo J, Huang M, Nguyen TD, et al. Isolation of single-base genome-edited human iPS cells without antibiotic selection. *Nat Methods*. 2014;11:291-3. doi: 10.1038/nmeth.2840.

R Core Team. R: A language and environment for statistical computing. Vienna, Austria: R Foundation for Statistical Computing; 2024. Available from: <https://www.R-project.org/>.

Rogowski K, van Dijk J, Magiera MM, Bosc C, Deloulme JC, Bosson A, et al. A family of protein-deglutamylating enzymes associated with neurodegeneration. *Cell*. 2010;143(4):564-78. doi: 10.1016/j.cell.2010.10.014.

Roselli F, Hutzler P, Wegerich Y, Livrea P, Almeida OF. Disassembly of shank and homer synaptic clusters is driven by soluble beta-amyloid(1-40) through divergent NMDAR-dependent signalling pathways. *PLoS One*. 2009;4(6). doi: 10.1371/journal.pone.0006011.

Sakakibara A, Ando R, Sapir T, Tanaka T. Microtubule dynamics in neuronal morphogenesis. *Open Biol*. 2013;3(7):130061. doi: 10.1098/rsob.130061.

Signorell A. DescTools: tools for descriptive statistics. R package version 0.99.54; 2024. Available from: <https://CRAN.R-project.org/package=DescTools>.

Sholl DA. Dendritic organization in the neurons of the visual and motor cortices of the cat. *J Anat.* 1953;87(4):387-406.

Thies E, Mandelkow EM. Missorting of TAU in neurons causes degeneration of synapses that can be rescued by the kinase MARK2/Par-1. *J Neurosci.* 2007;27(11):2896-907. doi: 10.1523/JNEUROSCI.4674-06.2007.

Wang C, Ward ME, Chen R, Liu K, Tracy TE, Chen X, et al. Scalable production of iPSC-derived human neurons to identify TAU-lowering compounds by high-content screening. *Stem Cell Reports.* 2017;9(4):1221-33. doi: 10.1016/j.stemcr.2017.08.019.

Wu HY, Rong Y, Bansal PK, Wei P, Guo H, Morgan JI. TTLL1 and TTLL4 polyglutamylases are required for the neurodegenerative phenotypes in *pcd* mice. *PLoS Genet.* 2022;18(4). doi: 10.1371/journal.pgen.1010144.

Zempel H, Thies E, Mandelkow E, Mandelkow EM. Abeta oligomers cause localized Ca(2+) elevation, missorting of endogenous TAU into dendrites, TAU phosphorylation, and destruction of microtubules and spines. *J Neurosci.* 2010;30(36):11938-50. doi: 10.1523/JNEUROSCI.2357-10.2010. Erratum in: *J Neurosci.* 32(17):6052.

Zempel H, Luedtke J, Kumar Y, Biernat J, Dawson H, Mandelkow E, et al. Amyloid- β oligomers induce synaptic damage via TAU-dependent microtubule severing by TTLL6 and spastin. *EMBO J.* 2013;32(22):2920-37. doi: 10.1038/emboj.2013.207.

Zempel H, Mandelkow EM. TAU missorting and spastin-induced microtubule disruption in neurodegeneration: Alzheimer disease and hereditary spastic paraplegia. *Mol Neurodegener.* 2015;10:68. doi: 10.1186/s13024-015-0064-1.

Figure Legends

Figure 1. oA β treatment induces TAU missorting, alters microtubule modifications, and disrupts synaptic clusters in iNeurons. **A)** Co-immunostaining of TAU and MAP2 in iNeurons treated with oA β for 3 hours or untreated control (Ctrl). Insets display 4-fold magnifications of areas framed with dashed lines, highlighting TAU missorting into the somatic compartment. Scale bar: 10 μ m. **B)** Co-staining of TAU and polyglutamylated tubulin (polyE-tub) in iNeurons treated with oA β for 3 hours or untreated control. Insets show 4-fold magnifications of areas framed with dashed lines, emphasizing increased polyglutamylation in oA β -treated neurons. Scale bar: 10 μ m. **C)** Immunostaining of acetylated tubulin (ace-tub) and tyrosinated tubulin (tyr-tub) in iNeurons treated with oA β for 3 hours or untreated control. Insets show 3-fold magnifications of areas framed with dashed lines, demonstrating reduced acetylation and tyrosination post-treatment. Scale bar: 10 μ m. **D)** Co-immunostaining of Homer1 and synaptophysin (SYP) in iNeurons treated with oA β for 3 hours or untreated control. Insets show 2-fold magnifications of the areas framed with dashed lines, illustrating the disassembly of synaptic clusters. Scale bar: 2 μ m. **E)** Quantification of somatic TAU levels in (A). (N=3, n=45 neurons). **F)** Quantification of somatic polyE-tub levels in (B). (N=3, n=45 neurons). **G)** Quantification of somatic and dendritic ace-tub levels in (C). (N=3, n=45 neurons). **H)** Quantification of somatic and dendritic tyr-tub levels in (C). (N=3, n=45 neurons). **I)** Quantification of SYP-colocalizing Homer1 cluster size and mean fluorescence intensity (MFI) in (D). (N=3, n=150 puncta). ^{ns} non-significance, * P \leq 0.05, ** P \leq 0.01.

Figure 2. Knockdown of TTLL1 and TTLL4 partially ameliorates oA β -induced pathological changes in iNeurons. **A)** Schematic representation of the experimental workflow, outlining the knockdown and treatment

procedures. Neurons were transduced at Day 10 with shRNA, and then treated and fixed as indicated. **B)** Immunoblotting confirmation of successful knockdown of TTLL1, TTLL4, and TTLL6 in iNeurons. **C)** Immunostaining for TAU, acetylated tubulin (Ace-tub), polyglutamylated tubulin (PolyE-tub), tyrosinated tubulin (Tyr-tub) in Day 21 iNeurons transduced with scrambled RNA (Scr.) or shRNAs targeting TTLL1, TTLL4, or TTLL6 for 11 days, and treated with oA β or vehicle control for 3 hours. Scale bar: 10 μ m. **D)** Quantification of somatic TAU, dendritic ace-tub, somatic polyE-tub, somatic tyr-tub levels of (C). (N=3, n=45 neurons). ^{ns} non-significance, * P \leq 0.05, ** P \leq 0.01.

Figure 3. Knockdown of TTLL1 and TTLL4 slightly attenuates oA β -induced synaptic declustering in iNeurons.

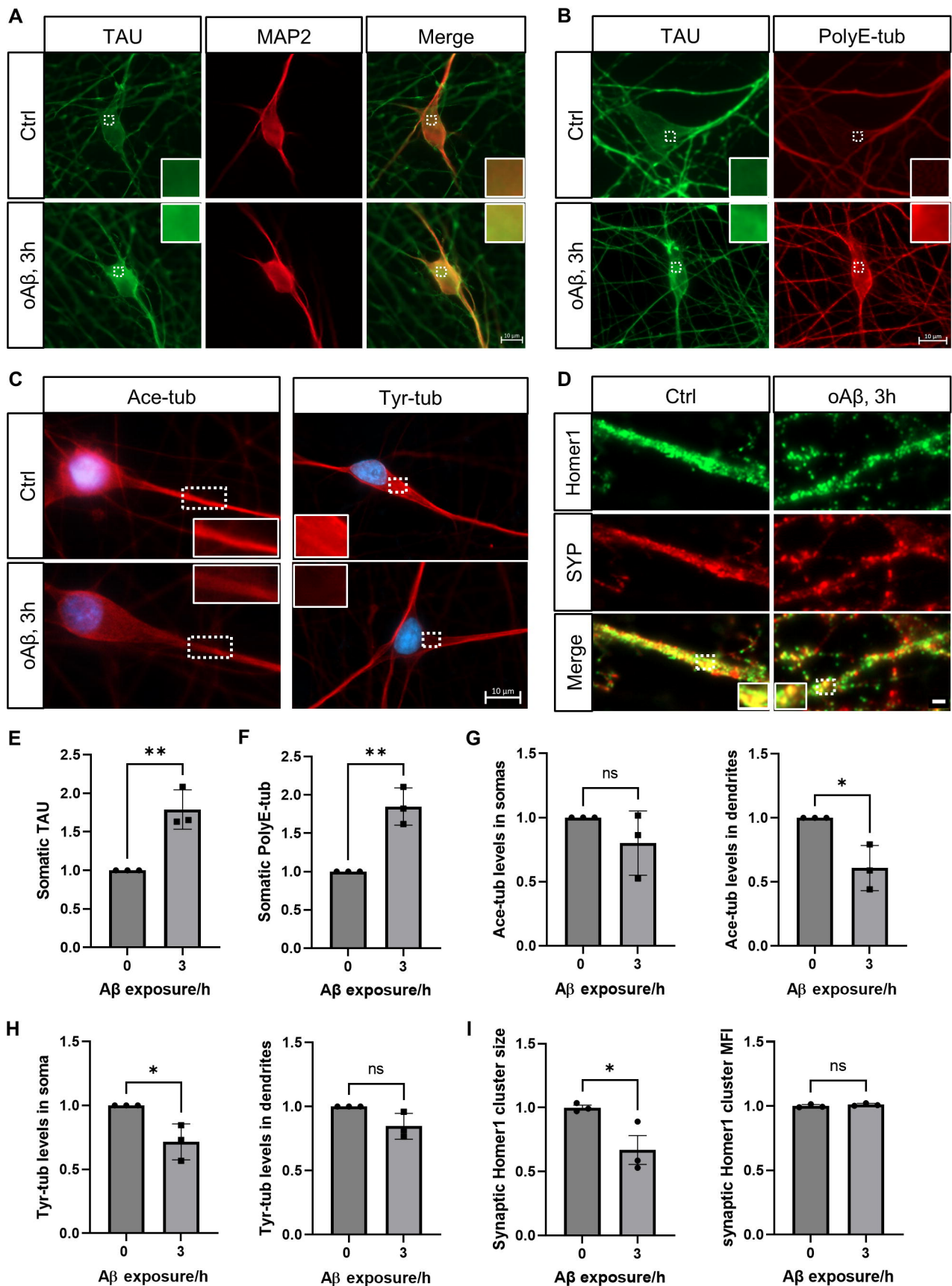
A) Co-immunostaining of Homer1 and synaptophysin (SYP) in Day 21 iNeurons transduced with scrambled RNA (Scr.) or shRNAs targeting TTLL1, TTLL4, or TTLL6 for 11 days, and treated with oA β or vehicle control for 3 hours. Insets show 2-fold magnifications of areas framed with dashed lines, highlighting changes in synaptic cluster size. Scale bar: 2 μ m. **B)** Quantification of SYP-colocalizing Homer1 cluster size and mean fluorescence intensity (MFI) in (A). (N=3, n \approx 300 puncta). ^{ns} non-significance, * P \leq 0.05.

Figure 4. TTLL Knockdown does not affect neuronal networks, morphology, or function. A-B)

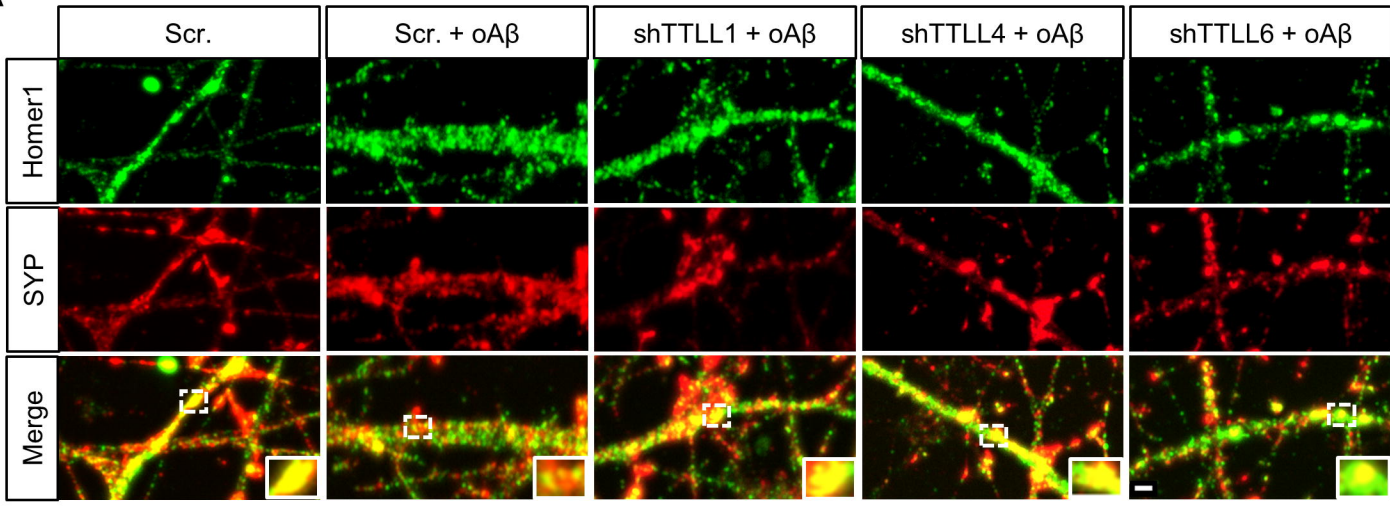
Immunostaining of neurofilament-L (NF-L) (A) or MAP2 (B) in Day 21 iNeurons transduced with scrambled RNA (Scr.) or shRNAs targeting TTLL1, TTLL4, or TTLL6 for 11 days. Scale bars: 200 μ m. **C)** Quantification of the area covered by the axonal network (NF-L) in (A). (N=3, n=15 fields). **D)** Quantification of the area covered by the dendritic network (MAP2) in (B). (N=3, n=15 fields). **E)** Quantification of the number of dendritic intersections obtained from Sholl analysis. (N=3, n=15 neurons). **F-H)** Sholl profiles showing dendritic branching complexity in Day 21 iNeurons transduced with scrambled RNA (Scr.) or shRNAs targeting TTLL1 (F), TTLL4 (G), or TTLL6 (H) for 11 days. (N=3, n=15 neurons). **I)** Quantification of spike rate and burst count from microelectrode array (MEA) recordings in Day 21 iNeurons transduced with scrambled RNA (Scr.) or shRNAs targeting TTLL1, TTLL4, or TTLL6 for 11 days. (N=3, n=12-15 wells). ^{ns} non-significance.

Figure 5. Fluorescence Resonance Energy Transfer (FRET) analysis reveals potential interaction between

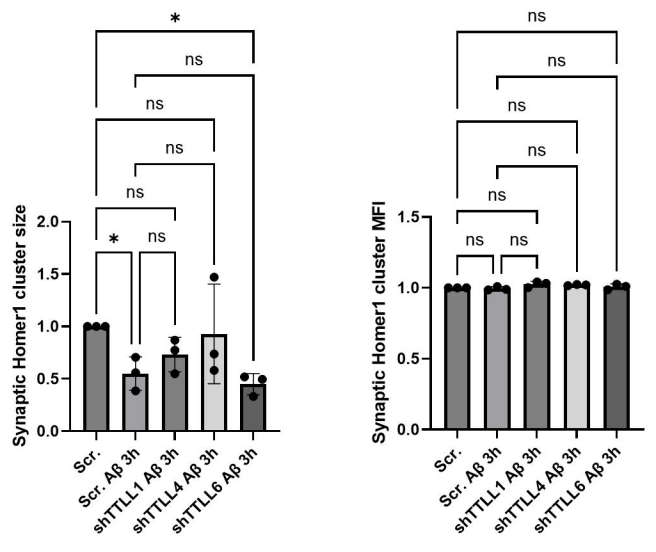
TAU and TTLL1. A) FRET microscopy images in HEK293T cells showing various controls (TFP-TAU+YFP, TFP+YFP-TTLL1, TFP+YFP-TTLL4, TFP+YFP-TTLL6) and experimental conditions (TFP-TAU+YFP-TTLL1, TFP-TAU+YFP-TTLL4, TFP-TAU+YFP-TTLL6). Images of the three detection channels: donor (TFP), acceptor (YFP), and FRET, as well as the spectral bleed-through (BT)-corrected FRET are depicted. Scale bar: 10 μ m. **B)** 7-fold magnification of the area framed by dashed lines in (A) showing enhanced FRET signal in low-expressing cells co-transfected with TFP-TAU and YFP-TTLL1. **C)** Quantification of FRET efficiency from the conditions shown in (A). (N=3, n=15 cells). ^{ns} non-significance, * P \leq 0.05, *** P \leq 0.001, **** P \leq 0.0001.

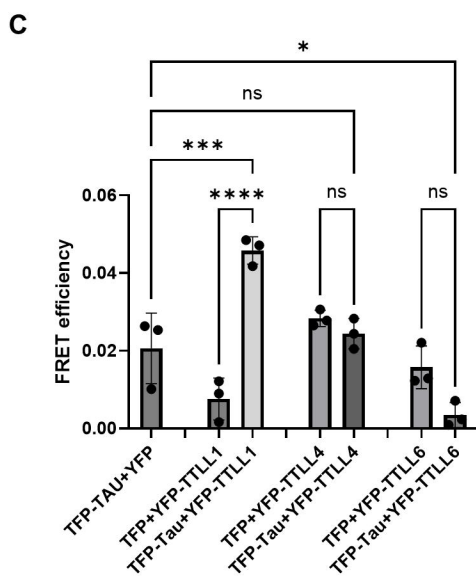
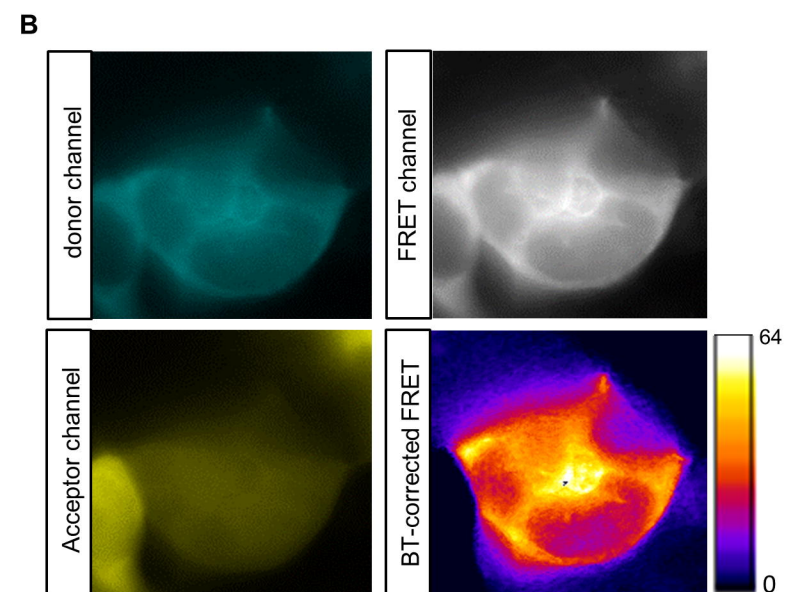
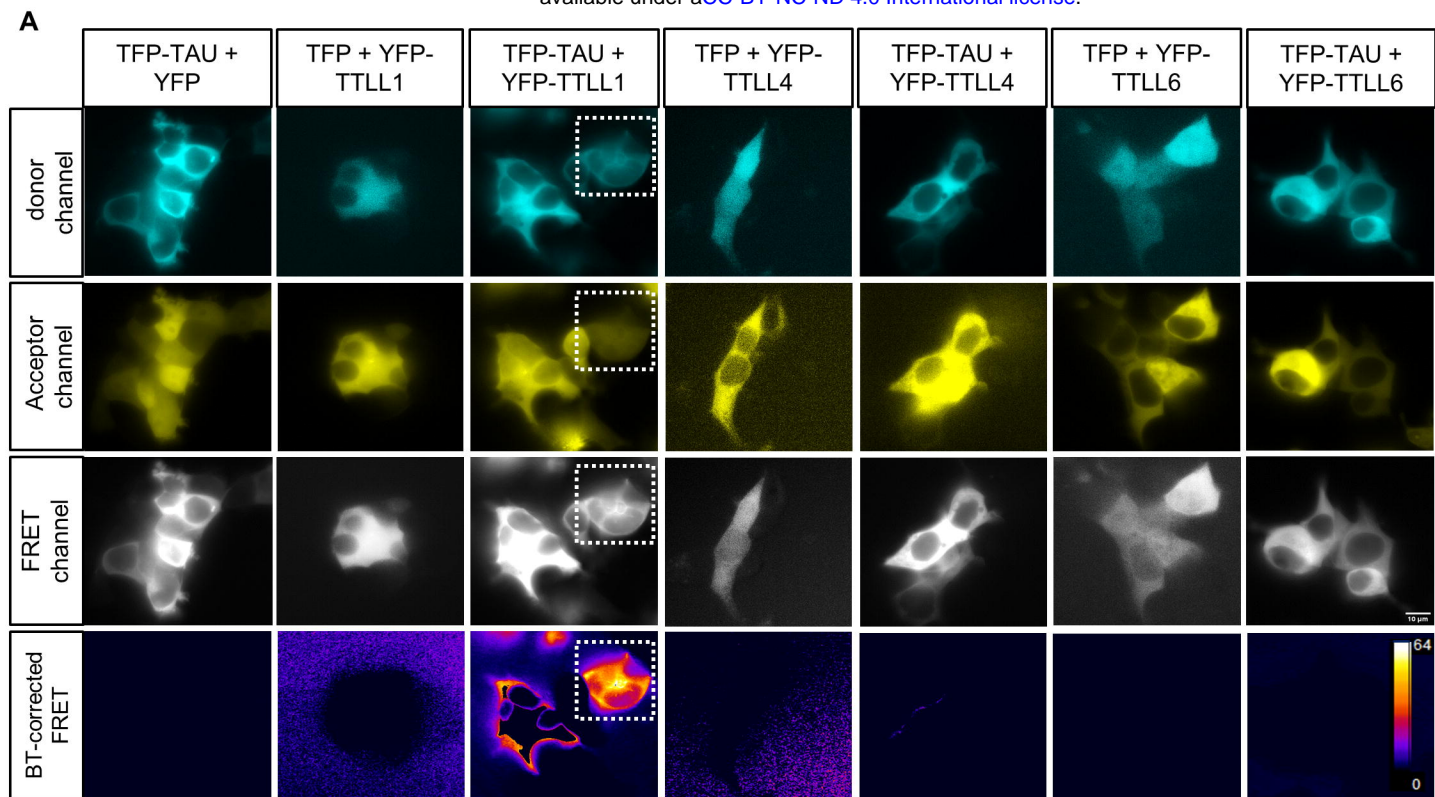


A



B





6.5 Article 5

Al Kabbani, M. A., Jatoo, P., Klebl, K., Klebl, B. M., Zempel, H. (2024) Expression of recombinant human glutamylating TLLs in human cells leads to differential tubulin glutamylation patterns, with only TLL6 disrupting microtubule dynamics. *bioRxiv*. doi: 10.1101/2024.11.25.624814.

Expression of recombinant human glutamylating TTLLs in human cells leads to differential tubulin glutamylation patterns, with only TTLL6 disrupting microtubule dynamics

Mohamed Aghyad Al Kabbani^{1,2}, Pragya Jatoo^{3,*}, Kathrin Klebl³, Bert M. Klebl³, Hans Zempel^{1,2,*}

1 Institute of Human Genetics, Faculty of Medicine and University Hospital Cologne, University of Cologne, Cologne, Germany

2 Center for Molecular Medicine Cologne (CMMC), Faculty of Medicine and University Hospital Cologne, University of Cologne, Cologne, Germany

3 Lead Discovery Center GmbH, Otto-Hahn-Str. 15, 44227 Dortmund, Germany

* Correspondence to: Dr. Dr. Hans Zempel, hans.zempel@uk-koeln.de

* Correspondence to: Dr. Pragya Jatoo, jatoo@lead-discovery.de

Abstract

Polyglutamylation, a post-translational modification (PTM) catalyzed by a subset of Tubulin Tyrosine Ligase-Like (TTLL) family enzymes, regulates microtubule dynamics through its influence on interactions with microtubule-associated, motor, and severing proteins, and has recently also been implicated in genetic and neurodegenerative diseases. In this study, we characterized the glutamylation activity of various glutamylating TTLLs in human embryonic kidney 293T (HEK293T) cells, revealing distinct patterns of mono- and polyglutamylation among TTLL family members, with TTLL4 and TTLL11 exhibiting the strongest chain initiation and elongation activities, respectively. We found that TTLL6 expression uniquely decreased microtubule stability, with live-cell imaging of end-binding protein (EB3) showing a TTLL6-induced decrease in microtubule stability. To explore therapeutic modulation of TTLL activity, we tested LDC10, a novel TTLL inhibitor, which successfully blocked glutamylation across all TTLLs investigated in this study, while also reversing the microtubule-destabilizing effects of TTLL6. These findings identify a potential pathogenic role of TTLL6 in microtubule dynamics and highlight LDC10 as a promising pharmacological tool to counteract TTLL-induced microtubule destabilization.

Introduction

Most members of the Tubulin Tyrosine Ligase-Like (TTLL) family are responsible for glutamylation, a post-translational modification (PTM) that adds a glutamate side chain to a glutamate residue within the C-terminal tail of α - and β -tubulin (Janke et al., 2005). Some TTLLs, such as TTLL4 and TTLL7, initiate the side chain by adding the first glutamate, while others, including TTLL1, TTLL6 and TTLL11, elongate this side chain by adding additional residues (van Dijk et al., 2007).

Polyglutamylation is an important microtubule PTM as it regulates microtubule binding to microtubule-associated proteins (MAPs), motor, and severing proteins (Genova et al., 2023). Long glutamate chains are known to recruit spastin and katanin, two microtubule severing enzymes, leading to microtubule severing (Lacroix et al., 2010). However, exceedingly long chains, above 8-9 glutamate residues, alter spastin's function from severing to stabilizing the microtubules (Valenstein & Roll-Mecak, 2016).

Disruption of tubulin polyglutamylation homeostasis has been implicated in several diseases. Notably, hyperglutamylation resulting from deficient cytosolic carboxypeptidase 1 (CCP1), a major deglutamylase responsible for removing glutamate residues from polyglutamate side chains (Rogowski et al., 2010), is associated with neurodegeneration in mice and humans (Magiera et al., 2018; Shashi et al., 2018). Other disorders linked to TTLL dysfunction include impaired ciliary structure and function, retinal dystrophy, and male infertility (Bedoni et al., 2016; Kolawole et al., 2023; Oh et al., 2022; Vogel et al., 2010). However, therapeutic approaches targeting TTLLs are still lacking.

Here, we expressed different recombinant human glutamylating TTLLs in human embryonic kidney 293T (HEK293T) cells and observed distinct patterns of mono- and polyglutamylation. TTLL6 expression also disrupted microtubule stability, as shown through live-cell imaging of microtubule plus-end tracking protein EB3 comets. Interestingly, a novel TTLL inhibitor, LDC10, successfully blocked the glutamylating activity of all TTLLs investigated in this study and mitigated the destabilizing effect of TTLL6 on microtubules. In summary, we have identified a potential pathological role of TTLL6-mediated polyglutamylation and described a new pharmacological intervention to counteract it.

Methods

HEK293T cell maintenance, transfection, and inhibitor treatment

HEK293T cells were cultured in high glucose DMEM (Thermofisher Scientific) supplemented with 10% FBS and 1x Antibiotic/Antimycotic solution (Thermofisher Scientific) at 37 °C in a humidified incubator with 5% CO₂. For EYFP-tagged TTLL expression, cells were seeded into 6-well plates and transfected with 3 µg DNA for 48 hours. For pharmacological treatments, cells were treated with 10 µM LDC10 or a vehicle control for 24 hours, beginning one day post-transfection.

Western Blot

For Western blot analysis, HEK293T cells were lysed in RIPA buffer containing 1x protease & phosphatase inhibitor cocktail (Thermofisher Scientific). Lysates were diluted in 5x Laemmli sample buffer, boiled at 95°C for 5 minutes, and separated on 10% SDS-polyacrylamide gels. Proteins were then transferred to PVDF membranes, which were blocked for one hour in TBS-T containing 5% milk. Following blocking, membranes were incubated with the primary antibody overnight at 4°C, washed three times with TBS-T, and incubated with the corresponding HRP-conjugated secondary antibody for one hour at room temperature. After three additional TBS-T washes, immunoreactions were detected using SuperSignal West Femto Chemiluminescent Substrate (Thermofisher Scientific) and a ChemiDoc XRS + system (Bio-Rad).

Live-cell imaging

For live-cell imaging, HEK293T cells were seeded into coated 6-well plates and co-transfected with 0.5 µg EB3-tdTomato and 1.5 µg EYFP-TTLL or empty EYFP vector. One day post-transfection, cells were transferred to a live-cell imaging chamber (ALA Scientific), and EB3 comets in single cells were imaged for 60 seconds (1 frame per 2 seconds) with a Leica DMI8 microscope (Leica). Only cells exhibiting both tdTomato and EYFP signals were included in the analysis. EB3 comet tracks were analyzed via ImageJ software using TrackMate plugin (Tinevez et al., 2017) as described in Allroggen et al., 2024. Microtubule dynamics were analyzed using LoG detector with an estimated object diameter of 1.5 µm, assessing parameters such as microtubule stability (s), microtubule run length (µm), and microtubule growth rate (µm/s).

Antibodies

The antibodies used in this study are listed in Table. 1

Table 1. List of the antibodies used in this study

Antibody	Species	Clonality	Cat#	Supplier	RRID	Dilution
Anti-Tubulin Polyglutamylated antibody (B3)	Mouse	Monoclonal	T9822	Sigma- Aldrich	AB_477598	1:500
Anti- polyglutamylation modification (GT335)	Mouse	Monoclonal	AG-20B- 0020	AdipoGen	AB_2490211	1:500
Anti-GFP antibody	Rabbit	Polyclonal	ab290	Abcam	AB_2313768	1:1000
Anti-GAPDH antibody (G-9)	Mouse	Monoclonal	sc-365062	Santa Cruz	AB_10847862	1:1000
Anti-beta actin antibody	Mouse	Monoclonal	HRP- 60008	Proteintech	AB_2819183	1:5000

Results

Expression of different TTLLs reveals distinct patterns of tubulin glutamylation

Differential analysis of individual TTLLs is challenging, due to low endogenous expression and potentially overlapping glutamylation activity. Hence, to investigate the effects of different glutamylating TTLLs on tubulin glutamylation and microtubule dynamics, we expressed EYFP-tagged constructs of TTLL1, TTLL4, TTLL6, TTLL7, and TTLL11 in HEK293T cells for 2 days and assessed their expression levels via Western blotting. All recombinant TTLLs exhibited very low expression levels compared to the EYFP control (despite using the same transfection protocol including DNA amount), with EYFP-TTLL11 showing the highest expression (Fig. 1A).

When analyzing the glutamylation patterns, the TTLLs grouped according to their established functional roles. Lysates of cells expressing the initiator TTLL4 showed stronger signal when probed with GT335 antibody, which detects the initial branching point of the glutamate chain. In contrast, lysates of cells expressing the elongators TTLL6 or TTLL11 displayed stronger bands when probed with B3 antibody, which specifically recognizes glutamate side chains with more

than two residues. Interestingly, TTLL7 showed both initiation and elongation activities, producing positive signals with both antibodies, whereas TTLL1 showed only barely detectable activity with B3, but not with GT335 antibody (Fig 1B). In sum, transfection of HEK293T cells with our constructs resulted in expression of TTLL enzymes with the expected size and the expected polyglutamylation activity.

TTLL6 expression decreases microtubule stability

Next, to assess whether expression of individual TTLLs affects microtubule dynamics besides glutamylation, we co-transfected HEK293T cells with EB3-tdTomato and the respective EYFP-TTLL for 2 days, and tracked EB3 comets in yellow fluorescent (i.e. co-transfected) cells (Fig. 1C). Analysis revealed that EYFP-TTLL6, but not any other expressed TTLL, led to decreased microtubule stability (in terms of duration of traceable comets) compared to cells expressing EYFP alone (Fig. 1D), while microtubule run length remained unchanged (Fig. 1E). Interestingly, this TTLL6-induced microtubule instability was associated with an increase in microtubule growth rate (Fig. 1F). Hence, while TTLL6 had one of the lowest impacts on microtubule glutamylation, it may be an important player for microtubule dynamics.

LDC10 inhibits TTLL-induced tubulin glutamylation and restores microtubule stability

A TTLL inhibitor identified through a high throughput screening (HTS) campaign at the Lead Discovery Center GmbH was further evaluated as a chemical tool to dissect glutamylation in cells. This hit compound is identified as LDC 10 (unpublished data). To this end, we treated HEK293T cells expressing various EYFP-TTLLs with 10 μ M LDC10 for 24 hours and assessed tubulin glutamylation using GT335 and B3 antibodies via Western blotting. Cells treated with LDC10 showed a significant reduction in both monoglutamylation or polyglutamylation compared to vehicle-treated control (Fig. 2A-B). Notably, LDC10 protected microtubules from the destabilizing effects of TTLL6, with LDC10-treated EYFP-TTLL6-expressing cells exhibiting microtubule stability and growth rate levels similar to those in cells expressing EYFP alone (Fig. 2C-E).

Discussion

In this study, we investigated the effects of several human recombinant glutamylating TTLLs by expressing them in HEK293T cells. Compared to EYFP control, EYFP-TTLLs showed low expression levels. Notably, TTLL11 exhibited relatively robust expression and strong polyglutamylation activity, while TTLL4 displayed prominent monoglutamylation activity despite

having the lowest expression among all investigated TTLLs. Glutamylation patterns probed at two different epitopes, one marking the branch starting point and the other marking long chains, corresponded with canonical TTLL initiation (TTLL4) and elongation (TTLL6 and TTLL11) functions, with the exception of TTLL7, which showed both activities despite being classified as an initiator. Remarkably, the initiator TTLL4 displayed some elongation activity, and the elongase TTLL11 exhibited minor initiation activity. TTLL1, in contrast, showed barely any detectable polyglutamylation activity, consistent with prior reports that it requires a five-subunit complex to be active (Garnham et al., 2015; Janke et al., 2005).

Glutamylation is known to regulate microtubule stability, dynamics, and function. Therefore, we investigated whether any TTLL would affect microtubule dynamics. Using live-cell imaging of fluorescently tagged EB3 protein, we observed that only TTLL6 negatively impacted microtubule stability while increasing microtubule growth rate. Long glutamate side chains are associated with spastin recruitment and subsequent microtubule destabilization due to microtubule severing (Brill et al., 2016; Lacroix et al., 2010; Roll-Mecak & Vale, 2005, 2008), which could explain decreased microtubule stability after the expression of the elongase TTLL6, and why the initiators TTLL4 and TTLL7 showed no such effect. However, this does not explain the apparent lack of impact on microtubule dynamics by the other elongase TTLL11, especially since it has remarkably higher expression and activity than TTLL6, as seen in our Western blot experiments. One possible explanation is that TTLL6 and TTLL11 modify different sites within the C-terminal tail of tubulin with different spastin recruitment capabilities. Another explanation is that while both TTLL6 and TTLL11 are elongators, the length of the side chain they generate is different. This could be linked to our Western blot results which showed a much stronger long chain band with TTLL11. Glutamate chains containing more than eight residues are known to inhibit spastin severing activity, switching its function to microtubule stabilization instead (Valenstein & Roll-Mecak, 2016). It could be that the strong polyglutamylation induced by TTLL11 in our model stabilizes microtubules, while modest polyglutamylation by TTLL6 is enough to recruit spastin and promote severing and destabilization. A third explanation would revolve around the severing enzyme recruited. Polyglutamylation does not only recruit spastin, but it is also able to recruit katanin, another microtubule severing enzyme (McNally & Vale, 1993; Szczesna et al., 2022). It has been shown before that TTLL6 induced a much stronger katanin activation compared to TTLL11 (Lacroix et al., 2010), suggesting that katanin, and not spastin, could be the primary downstream effector here.

Surprisingly, TTLL6-induced microtubule destabilization was associated with an increased microtubule growth rate. While this may seem contradictory at first, a simple explanation would rely on spastin recruitment. Spastin-mediated microtubule severing has been shown to increase the pool of free tubulin, making more tubulin available for the polymerization of new microtubules, and thus contributing to microtubule regrowth and organization (Aiken & Holzbaur, 2024; Kuo et al., 2019).

Given the therapeutic relevance of glutamylating TTLLs in cancer and neurodegenerative diseases (Das et al., 2014; Rogowski et al., 2021; Wu et al., 2022), finding new TTLL inhibitors is critical. We tested LDC10, a novel TTLL inhibitor, for its efficacy in reducing TTLL-induced glutamylation and reversing TTLL6-mediated microtubule instability. Our results show that LDC10 is able to inhibit TTLL4-induced monoglutamylation and, to a lower extent, TTLL7-induced monoglutamylation, as well as polyglutamylation generated by TTLL6 and TTLL11. Notably, LDC10 completely reversed the microtubule destabilizing effect of TTLL6, restoring stability and growth rate to control values. Although LDC10 shows initial promise in these microtubule stability assays as a tool compound, together with the remaining hits from the TTLL4 HTS, it is still under medicinal chemistry-based optimization to enhance specific potency against inhibition of TTLL4 and to improve its lead- and drug-likeness.

In conclusion, we showed direct detrimental effect of human TTLL6 on microtubule dynamics in HEK293T cells and presented LDC10 as a chemical tool compound that inhibits glutamylation and is capable of mitigating the associated negative effects.

Availability of data and materials: The datasets of the current study are available from the corresponding author on reasonable request.

Competing interests: MAAK, PJ, KKI, BKI, and HZ declare no conflict of interest.

Funding: MAAK and HZ: Our work is supported by the Alzheimer Forschung Initiative e.V. grant No. 22039. PJ, KKI, BKI: The identification of the tool compound LDC10 at the Lead Discovery Center GmbH was supported by the European Union's Horizon 2020 Research and Innovation Program under the Marie-Skłodowska-Curie grant agreement No. 675737.

Authors' contributions: Study design: MAAK, HZ. Experimental work, data acquisition and analysis, and manuscript writing: MAAK. Drug development: PJ, KKI. All authors proofread, commented on, and approved the final manuscript.

Acknowledgments: We thank Daniel Adam and Jennifer Klimek (CMMC and Institute of Human Genetics, University Hospital Cologne, Cologne, Germany), and Tamara Wied (current address: Max Planck Institute for Biology of Ageing, Cologne, Germany) for the technical help and stimulating discussions. We thank Carsten Janke (Institut Curie, Paris, France) for the provision of the plasmids.

References

- Aiken, J., & Holzbaur, E. L. F. (2024). Spastin locally amplifies microtubule dynamics to pattern the axon for presynaptic cargo delivery. *Current Biology*, *34*(8), 1687–1704.e8. <https://doi.org/10.1016/j.cub.2024.03.010>
- Allroggen, N., Breuer, H., Bachmann, S., Bell, M., & Zempel, H. (2024). Studying Microtubule Dynamics in Human Neurons: Two-Dimensional Microtubule Tracing and Kymographs in iPSC- and SH-SY5Y-Derived Neurons for Tau Research. In C. Smet-Nocca (Ed.), *Tau Protein: Methods and Protocols* (pp. 561–580). Springer US. https://doi.org/10.1007/978-1-0716-3629-9_33
- Bedoni, N., Haer-Wigman, L., Vaclavik, V., Tran, V. H., Farinelli, P., Balzano, S., Royer-Bertrand, B., El-Asrag, M. E., Bonny, O., Ikonomidis, C., Litzistorf, Y., Nikopoulos, K., Yioti, G. G., Stefaniotou, M. I., McKibbin, M., Booth, A. P., Ellingford, J. M., Black, G. C., Toomes, C., ... Rivolta, C. (2016). Mutations in the polyglutamylase gene TTLL5, expressed in photoreceptor cells and spermatozoa, are associated with cone-rod degeneration and reduced male fertility. *Human Molecular Genetics*, *25*(20), 4546–4555. <https://doi.org/10.1093/hmg/ddw282>
- Brill, M. S., Kleele, T., Ruschkies, L., Wang, M., Marahori, N. A., Reuter, M. S., Hausrat, T. J., Weigand, E., Fisher, M., Ahles, A., Engelhardt, S., Bishop, D. L., Kneussel, M., & Misgeld, T. (2016). Branch-Specific Microtubule Destabilization Mediates Axon Branch Loss during Neuromuscular Synapse Elimination. *Neuron*, *92*(4), 845–856.

<https://doi.org/10.1016/j.neuron.2016.09.049>

- Das, V., Kanakkanthara, A., Chan, A., & Miller, J. H. (2014). Potential role of tubulin tyrosine ligase-like enzymes in tumorigenesis and cancer cell resistance. *Cancer Letters*, *350*(1–2), 1–4. <https://doi.org/10.1016/j.canlet.2014.04.022>
- Garnham, C. P., Vemu, A., Wilson-Kubalek, E. M., Yu, I., Szyk, A., Lander, G. C., Milligan, R. A., & Roll-Mecak, A. (2015). Multivalent Microtubule Recognition by Tubulin Tyrosine Ligase-Like Family Glutamylases HHS Public Access molecular basis for specificity among the enzymes primarily responsible for chemically diversifying cellular microtubules. *Cell*, *161*(5), 1112–1123. <https://doi.org/10.1016/j.cell.2015.04.003>. Multivalent
- Genova, M., Grycova, L., Puttrich, V., Magiera, M. M., Lansky, Z., Janke, C., & Braun, M. (2023). Tubulin polyglutamylation differentially regulates microtubule-interacting proteins. *The EMBO Journal*, *42*(5), 1–17. <https://doi.org/10.15252/embj.2022112101>
- Janke, C., Rogowski, K., Wloga, D., Regnard, C., Kajava, A. V., Strub, J. M., Temurak, N., Van Dijk, J., Boucher, D., Van Dorsselaer, A., Suryavanshi, S., Gaertig, J., & Eddé, B. (2005). Biochemistry: Tubulin polyglutamylase enzymes are members of the TTL domain protein family. *Science*, *308*(5729), 1758–1762. <https://doi.org/10.1126/science.1113010>
- Kolawole, O. U., Gregory-Evans, C. Y., Bikoo, R., Huang, A. Z., & Gregory-Evans, K. (2023). Novel pathogenic variants in Tubulin Tyrosine Like 5 (TTLL5) associated with cone-dominant retinal dystrophies and an abnormal optical coherence tomography phenotype. *Molecular Vision*, *29*(December), 329–337.
- Kuo, Y. W., Trottier, O., Mahamdeh, M., & Howard, J. (2019). Spastin is a dual-function enzyme that severs microtubules and promotes their regrowth to increase the number and mass of microtubules. *Proceedings of the National Academy of Sciences of the United States of America*, *116*(12), 5533–5541. <https://doi.org/10.1073/pnas.1818824116>
- Lacroix, B., Van Dijk, J., Gold, N. D., Guizetti, J., Aldrian-Herrada, G., Rogowski, K., Gerlich, D. W., & Janke, C. (2010). Tubulin polyglutamylation stimulates spastin-mediated microtubule severing. *Journal of Cell Biology*, *189*(6), 945–954. <https://doi.org/10.1083/jcb.201001024>
- Magiera, M. M., Bodakuntla, S., Žiak, J., Lacomme, S., Marques Sousa, P., Leboucher, S., Hausrat, T. J., Bosc, C., Andrieux, A., Kneussel, M., Landry, M., Calas, A., Balastik, M., & Janke, C. (2018). Excessive tubulin polyglutamylation causes neurodegeneration and

perturbs neuronal transport. *The EMBO Journal*, 37(23), 1–14.

<https://doi.org/10.15252/embj.2018100440>

McNally, F. J., & Vale, R. D. (1993). Identification of katanin, an ATPase that severs and disassembles stable microtubules. *Cell*, 75(3), 419–429. [https://doi.org/10.1016/0092-8674\(93\)90377-3](https://doi.org/10.1016/0092-8674(93)90377-3)

Oh, J. K., Vargas Del Valle, J. G., Lima de Carvalho, J. R., Sun, Y. J., Levi, S. R., Ryu, J., Yang, J., Nagasaki, T., Emanuelli, A., Rasool, N., Allikmets, R., Sparrow, J. R., Izquierdo, N. J., Duncan, J. L., Mahajan, V. B., & Tsang, S. H. (2022). Expanding the phenotype of TTLL5-associated retinal dystrophy: a case series. *Orphanet Journal of Rare Diseases*, 17(1), 1–10. <https://doi.org/10.1186/s13023-022-02295-9>

Rogowski, K., Hached, K., Crozet, C., & van der Laan, S. (2021). Tubulin modifying enzymes as target for the treatment of tau-related diseases. *Pharmacology and Therapeutics*, 218, 107681. <https://doi.org/10.1016/j.pharmthera.2020.107681>

Rogowski, K., van Dijk, J., Magiera, M. M., Bosc, C., Deloulme, J. C., Bosson, A., Peris, L., Gold, N. D., Lacroix, B., Grau, M. B., Bec, N., Larroque, C., Desagher, S., Holzer, M., Andrieux, A., Moutin, M. J., & Janke, C. (2010). A family of protein-deglutamylating enzymes associated with neurodegeneration. *Cell*, 143(4), 564–578. <https://doi.org/10.1016/j.cell.2010.10.014>

Roll-Mecak, A., & Vale, R. D. (2005). The *Drosophila* homologue of the hereditary spastic paraplegia protein, spastin, severs and disassembles microtubules. *Current Biology*, 15(7), 650–655. <https://doi.org/10.1016/j.cub.2005.02.029>

Roll-Mecak, A., & Vale, R. D. (2008). Structural basis of microtubule severing by the hereditary spastic paraplegia protein spastin. *Nature*, 451(7176), 363–367. <https://doi.org/10.1038/nature06482>

Shashi, V., Magiera, M. M., Klein, D., Zaki, M., Schoch, K., Rudnik-Schöneborn, S., Norman, A., Lopes Abath Neto, O., Dusl, M., Yuan, X., Bartesaghi, L., De Marco, P., Alfares, A. A., Marom, R., Arold, S. T., Guzmán-Vega, F. J., Pena, L. D., Smith, E. C., Steinlin, M., ... Senderek, J. (2018). Loss of tubulin deglutamylase CCP 1 causes infantile-onset neurodegeneration. *The EMBO Journal*, 37(23), 1–12. <https://doi.org/10.15252/embj.2018100540>

Szczesna, E., Zehr, E. A., Cummings, S. W., Szyk, A., Mahalingan, K. K., Li, Y., & Roll-Mecak, A. (2022). Combinatorial and antagonistic effects of tubulin glutamylation and glycylation on katanin microtubule severing. *Developmental Cell*, *57*(21), 2497–2513.e6.

<https://doi.org/10.1016/j.devcel.2022.10.003>

Tinevez, J. Y., Perry, N., Schindelin, J., Hoopes, G. M., Reynolds, G. D., Laplantine, E., Bednarek, S. Y., Shorte, S. L., & Eliceiri, K. W. (2017). TrackMate: An open and extensible platform for single-particle tracking. *Methods*, *115*(2017), 80–90.

<https://doi.org/10.1016/j.ymeth.2016.09.016>

Valenstein, M. L., & Roll-Mecak, A. (2016). Graded Control of Microtubule Severing by Tubulin Glutamylation. *Cell*, *164*(5), 911–921. <https://doi.org/10.1016/j.cell.2016.01.019>

van Dijk, J., Rogowski, K., Miro, J., Lacroix, B., Eddé, B., & Janke, C. (2007). A Targeted Multienzyme Mechanism for Selective Microtubule Polyglutamylation. *Molecular Cell*, *26*(3), 437–448. <https://doi.org/10.1016/j.molcel.2007.04.012>

Vogel, P., Hansen, G., Fontenot, G., & Read, R. (2010). Tubulin tyrosine ligase-like 1 deficiency results in chronic rhinosinusitis and abnormal development of spermatid flagella in mice. *Veterinary Pathology*, *47*(4), 703–712. <https://doi.org/10.1177/0300985810363485>

Wu, H. Y., Rong, Y., Bansal, P. K., Wei, P., Guo, H., & Morgan, J. I. (2022). TTLL1 and TTLL4 polyglutamylases are required for the neurodegenerative phenotypes in pcd mice. *PLoS Genetics*, *18*(4), 1–25. <https://doi.org/10.1371/journal.pgen.1010144>

Figure 1:

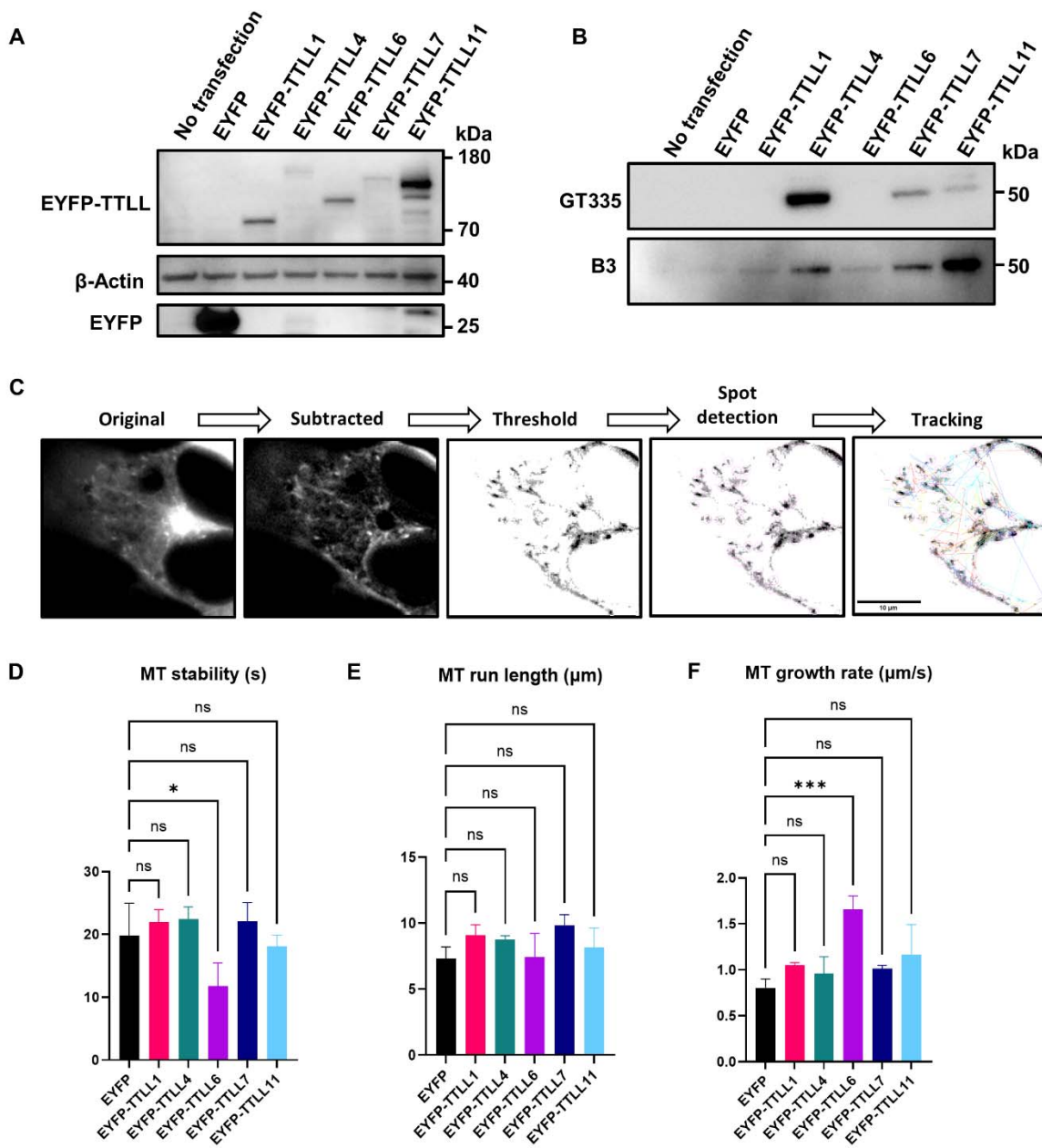


Figure 2:

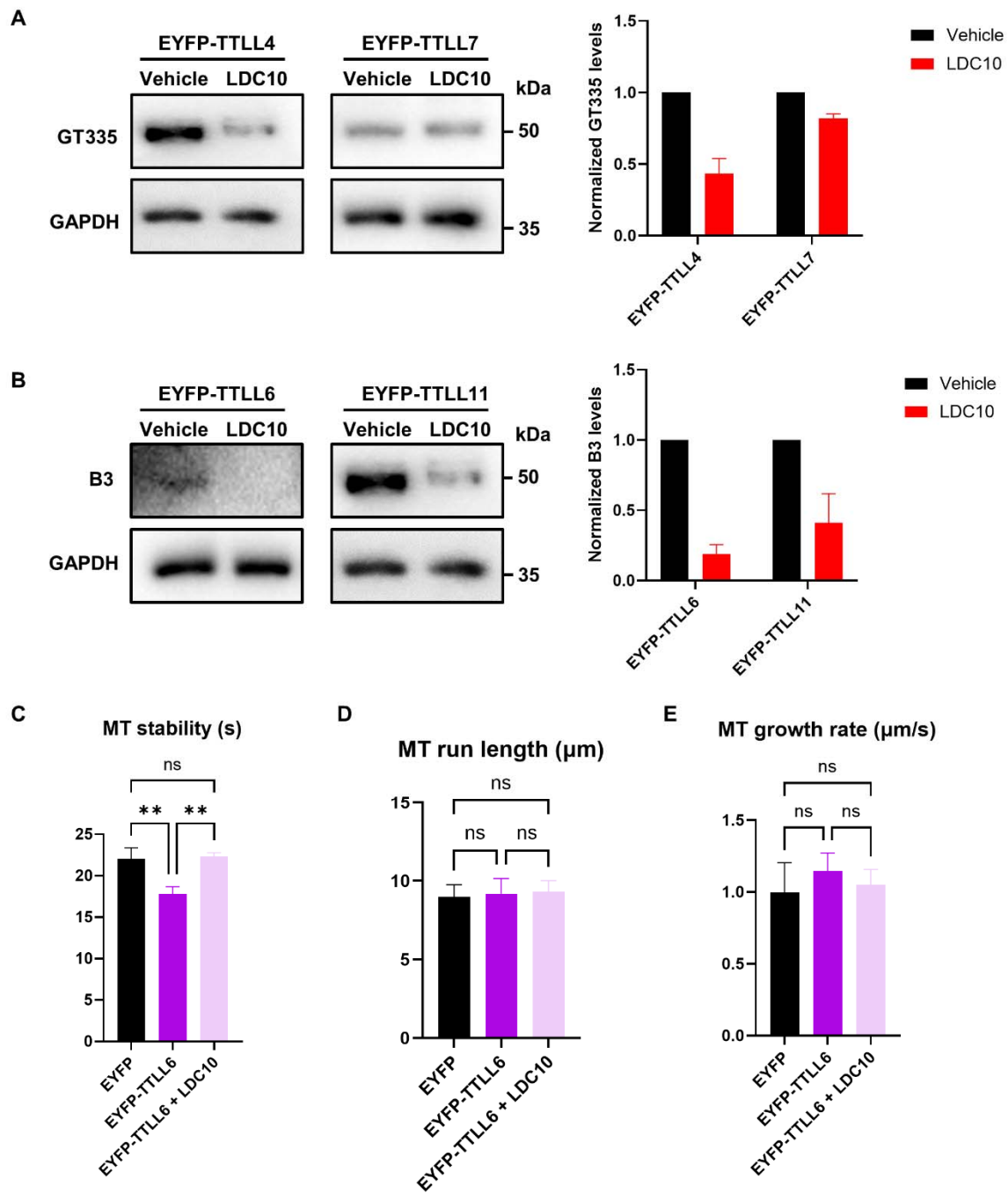


Figure Legends:

Figure 1. Expression of different TLLs induces distinct glutamylation patterns and alters microtubule dynamics. A) Western blotting of HEK293T cell lysates expressing EYFP-tagged TLLs or EYFP only shows variable TLL expression levels. **B)** Western blotting of HEK293T cell lysates expressing EYFP-tagged TLLs or EYFP only reveals various chain initiation or elongation functions by probing for two tubulin glutamylation epitopes: GT335 for branch point, and B3 for chains longer than two glutamate residues. **C)** Representation of image processing for the analysis of microtubule dynamics via live-cell EB3 imaging. Scale bar = 10 μ m. **D-F)** Microtubule dynamics of HEK293T cells co-transfected with EYFP-tagged TLLs and tdTomato-EB3. Growing microtubule plus-ends were monitored in living cells for 1 min (1 frame per 2s). Graphs show quantifications of microtubule (MT) stability (**D**), run length (**E**), and growth rate (**F**). N = 3, n = 9-11 cells per condition. Shapiro–Wilk test was performed to test for normal distribution of data; statistical analysis was performed by one-way ANOVA with Dunnett's test for correction of multiple comparisons. ^{ns} non-significance, * P \leq 0.05, *** P \leq 0.001.

Figure 2. LDC10 inhibits TLL-induced glutamylation and restores microtubule stability. A) Western blotting of HEK293T cell lysates expressing initiators TLL4 or TLL7 shows decreased monoglutamylation levels following LDC10 treatment for 24 hours. Images representative of 2-3 Western blots. **B)** Western blotting of HEK293T cell lysates expressing elongators TLL6 or TLL11 demonstrates decreased polyglutamylation levels following LDC10 treatment for 24 hours. Images representative of two Western blots. **C-E)** Microtubule dynamics of HEK293T cells co-transfected with EYFP-tagged TLLs and tdTomato-EB3. Growing microtubule plus-ends were monitored in living cells for 1 min (1 frame per 2s). Graphs show quantification of microtubule (MT) stability (**C**), run length (**D**), and growth rate (**E**). N = 3, n = 9-11 cells per condition. Shapiro–Wilk test was performed to test for normal distribution of data; statistical analysis was performed by one-way ANOVA with Tukey's test for correction of multiple comparisons. ^{ns} non-significance, ** P \leq 0.01.